UMTRI-84-14

# AN INFRARED DISTANCE SENSOR, ANALYSIS AND TEST RESULTS

J.D. Campbell

M.W. Sayers

The University of Michigan
Transportation Research Institute
Ann Arbor, Michigan 48109

March 1984

**Technical Report Documentation Page**

| 1. Report No. | 2. Government Accession No. | 3. Recipient's Catalog No. |
|---|---|---|
| | | |

**4. Title and Subtitle**

AN INFRARED DISTANCE SENSOR, ANALYSIS AND TEST RESULTS

**5. Report Date**

**6. Performing Organization Code**

**7. Author(s)**

J.D. Campbell and M.W. Sayers

**8. Performing Organization Report No.**

UMTRI-84-14

**9. Performing Organization Name and Address**

The University of Michigan
Transportation Research Institute
2901 Baxter Road
Ann Arbor, Michigan 48109

**10. Work Unit No.**

**11. Contract or Grant No.**

DTFH61-83-C-00123

**12. Sponsoring Agency Name and Address**

Federal Highway Administration
U.S. Department of Transportation
Washington, D.C. 20590

**13. Type of Report and Period Covered**

Special

**14. Sponsoring Agency Code**

**15. Supplementary Notes**

**16. Abstract**

An Infrared Sensor was developed for the FHWA as a noncontacting distance measuring device for the measurement of road topography. Tests of the sensor were conducted to quantify its performance for use in a road profilometer and rut depth measurement system. Detailed test results are presented, together with an analysis of the distance measurement concept employed. Statically, the sensor linearity is about 2% over a plus and minus one and one-half inch displacement range about its "zero" output reference height. On surfaces with constant reflectivity, its accuracy is about 2% at surface velocities up to 60 mph. However, test results agree with the theory which predicts short wavelength distance measurement errors when the sensor is operated over surfaces exhibiting reflectivity variations, while it is displaced from its "zero" output reference height. The results of quasi-static road tests demonstrate that common road features exhibit reflectivity variations which produce measurement errors on the order of one-quarter to one-half inch at wavelengths generally shorter than 12 inches, although longer error wavelengths are possible for certain conditions.

| 17. Key Words | 18. Distribution Statement |
|---|---|
| noncontact distance measurement, Infrared Sensor, road surface reflectivity, profilometer, rut depth | UNLIMITED |

| 19. Security Classif. (of this report) | 20. Security Classif. (of this page) | 21. No. of Pages | 22. Price |
|---|---|---|---|
| NONE | NONE | 121 | |

## TABLE OF CONTENTS

## LIST OF TABLES

LIST OF FIGURES

## LIST OF FIGURES (Cont.)

## LIST OF FIGURES (Cont.)

## LIST OF FIGURES (Cont.)

# 1.0 INTRODUCTION

## Background

This report describes the results of analysis and tests of an IR (infrared) distance sensor developed for the Federal Highway Administration, FHWA, by the Southwest Research Institute [1]. The sensor is being evaluated for possible use in a vehicle-based system for high-speed (up to 60 mph) measurement of road surface profile and rut depth. Figure 1 provides a schematic view of the proposed measurement system, which may employ up to five vehicle-to-ground height sensors for measurement of rut depth in both travelled wheel tracks, simultaneously. In order to measure rut depth, the height sensors must operate with a total error less than 0.10 inch for static and slowly changing (long wavelength) displacements. Additionally, the sensors must be capable of measuring to a point lying outboard of the vehicle, as shown in the figure ($h_1$ and $h_5$), to allow measurement of rut depth while the vehicle is driven over the travelled wheelpaths. For profile measurement, different requirements exist for the sensor accuracy and wavelength bandwidth. Measurement error should be no greater than 0.01 inch for wavelengths ranging from 0.5 - 5 ft, with larger errors permissible with longer wavelengths.

For the desired operation of the profile and rut depth measurement system at highway speeds, the sensors must operate consistently and accurately as the vehicle bounces, pitches, and rolls in response to road roughness and other disturbances. Hence, the accuracy of the height sensors must be maintained over variations in height of several inches, and variations in its vertical orientation of several degrees. The sensor must also yield good measures as it is passed over actual road surfaces, independently of road color, reflectivity, and texture.

The IR sensor is shown in Figure 2. The design provides voltage output proportional to height, relative to a zero-reference height of fourteen inches from the target surface. Displacement of the sensor from the zero reference height is detected by a triangulation technique, wherein an infrared

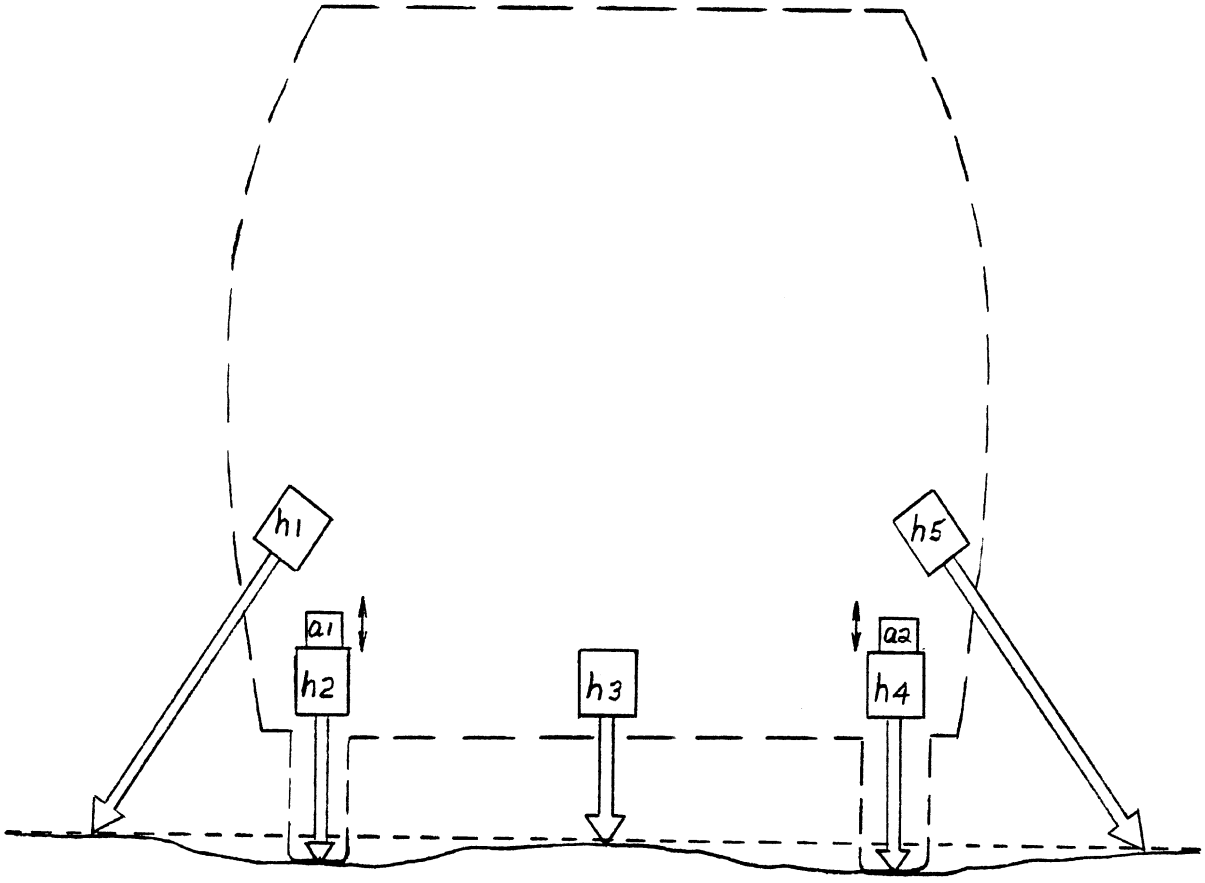


Figure 1. Schematic view of the proposed rut depth and road profile measurement system, employing 5 distance sensors.

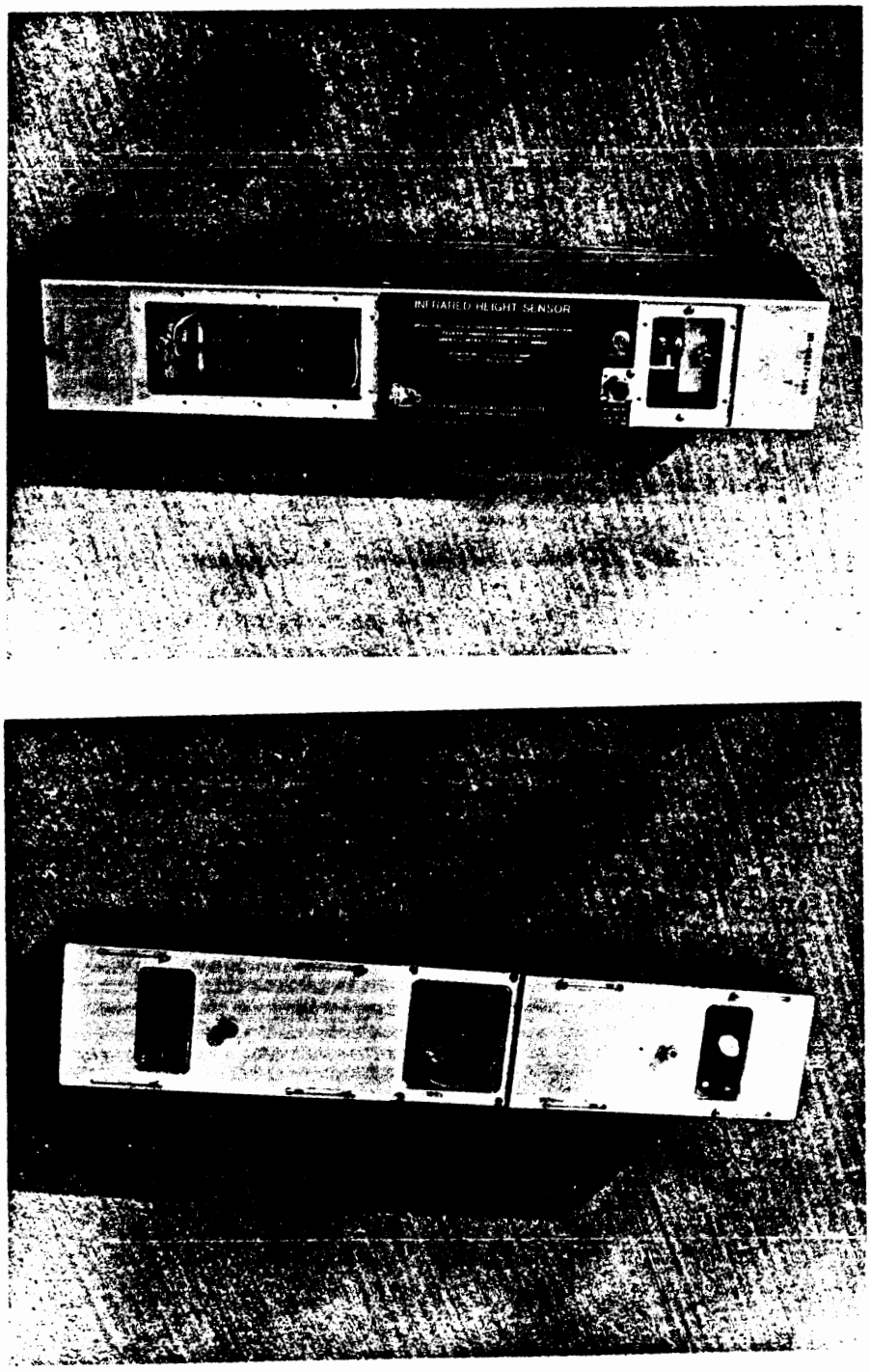


Figure 2. The FHWA Infrared Distance Sensor.

illuminated spot on the target surface is imaged on a pair of photocells viewing the spot from an angle of 35 degrees. When the sensor is displaced from the reference height, the spot image on the photocell pair moves so that the differential power between the individual cells varies, while the total power remains the same. The differential output is normalized by the total power, to remove the effect of the overall reflectivity of the road surface. Two pairs of photocells are used, viewing the illuminated spot from opposite sides, to cancel variations of surface reflectivity within the spot, when certain conditions are met.

In order to evaluate the suitability of the IR Sensor for the profile and rut depth measurement system, certain static and dynamic performance characteristics of the sensor were measured in the laboratory and on a variety of actual road surfaces, which have not been reported to date. Upon examining the test results, it became clear that the IR sensor did not perform nearly as well as had been expected. The analyses of the sensor concept that had been reported earlier [1] were studied, and were seen to contain assumptions that may be unrealistic, given the intended uses of the sensor.

The purpose of this report is to document the tests and analyses of the sensor that were performed over the period October 1983 through January 1984 at UMTRI.

**Report Summary**

Even though the IR sensor is designed to cancel erroneous indicated height changes due to variations in the reflectivity of the road surface, further analysis shows that complete cancellation of these effects is possible only when the sensor is at the reference height (when the spot is centered on the photocell pairs). With the sensor displaced from the reference height, a significant error occurs as the sensor passes over areas with changing reflectivity. This error is proportional to the magnitude of the reflectivity change and to the amount the sensor is displaced from the reference height. This result was derived theoretically and demonstrated in the laboratory, where a peak-to-peak output error of one inch was measured for a reflectivity change of 8:1.

Even with the sensor at the reference height, the theory predicts significant output errors if the surface exhibits unequal reflectivity in different directions. (In the Calibration Manual for the sensor (Appendix A), Southwest Research warns against using a surface with directional reflectivity, "such as sand paper," during calibration.)

In the laboratory tests, the IR sensor exhibited good performance in the measurement of surface height changes on the order of 0.25 inch, with a surface of uniform reflectivity , and at surface speeds from zero to sixty miles per hour. In static measurements, its linearity is about two percent for displacements of +1.5 inches from the reference height.

Dynamic testing of the IR sensor revealed a significant error resulting from nonuniform surface reflectivity, which was not predicted by the theory. When a change in the surface reflectivity passes across the IR spot, at surface speeds greater than about ten miles per hour, a transient signal appears on the sensor output, with a peak amplitude dependent on: 1) the change (ratio) in reflectivity, 2) the displacement of the sensor from the reference height, and 3) the surface velocity. While the results of the laboratory tests presented in this report provide some insight to the source of this problem, neither the underlying cause nor a solution has been determined. The solution of this problem has been given a low priority, until the more fundamental issues have been addressed.

Quasi-static tests on representative road surfaces have shown reflectivity variations producing significant sensor output errors, with wavelengths up to about 10 inches, when the sensor is displaced from its reference height.

This report is divided into sections describing the analytical work, results of the static testing, results of dynamic testing, results of test on actual road surfaces, and descriptions of some of the electronic circuit characteristics that are relevant to the performance observed. The Calibration Manual, from the Southwest Research Institute, is reproduced in Appendix A. The results of performing a recalibration of the sensor, and a

discussion of the calibration procedure and results, are given in Appendix B. A few minor circuit deficiencies, which were observed in the process of performing these tests, are discussed both in the report and, in more detail, in Appendix B.

## 2.0 SENSOR PERFORMANCE ANALYSIS

An analysis of the operation of the IR sensor using the same model employed by the Southwest Research Institute [1], but with the addition of directional reflection coefficients, shows that except for very special conditions, which are not necessarily satisfied by typical road surfaces, nonuniform surface reflectivity can result in significant sensor output errors.

### 2.1 Analytical Model

The IR Sensor model shown in figure 3, depicts a columnated IR (infrared) light source which provides a uniformly illuminated circular spot on a flat target surface with uniform reflectivity. This spot is imaged on two pairs of rectangular photocells (cells 1 through 4), located symmetrically at an angle, B, about a vertical axis passing through the center of the spot. When the target surface is at the reference distance, or reference height (nominally 14 inches), corresponding to "0" output from the sensor and indicated by solid lines in Figure 3, the spot image is centered on each photocell pair as shown. In this case the areas of the spot imaged on each photocell ($A_1$ through $A_4$) are equal. That is $A_1=A_2=A_3=A_4$. When the target surface moves closer to the sensor, the spot image moves toward photocells 2 and 4 as indicated by the dashed lines. Of course, when the surface moves away from the sensor, the spot image moves toward photocells 1 and 3. At all sensor heights, $A_1=A_3$ and $A_2=A_4$.

The image of the spot on the photocells is shown circular in figure 3. Actually, the spot image undergoes two distortions: 1) due to the viewing angle, B, the circle would appear as an ellipse, with its major axis parallel to the dividing line between the two photocells in each pair, and with a minor to major axis ratio equal to the cosine of the angle, B; 2) the ellipse is further distorted because one side is nearer to the photocells and therefore appears longer. For this analysis, the spot image is assumed to be circular in order to simplify the calculation of the spot area imaged on each

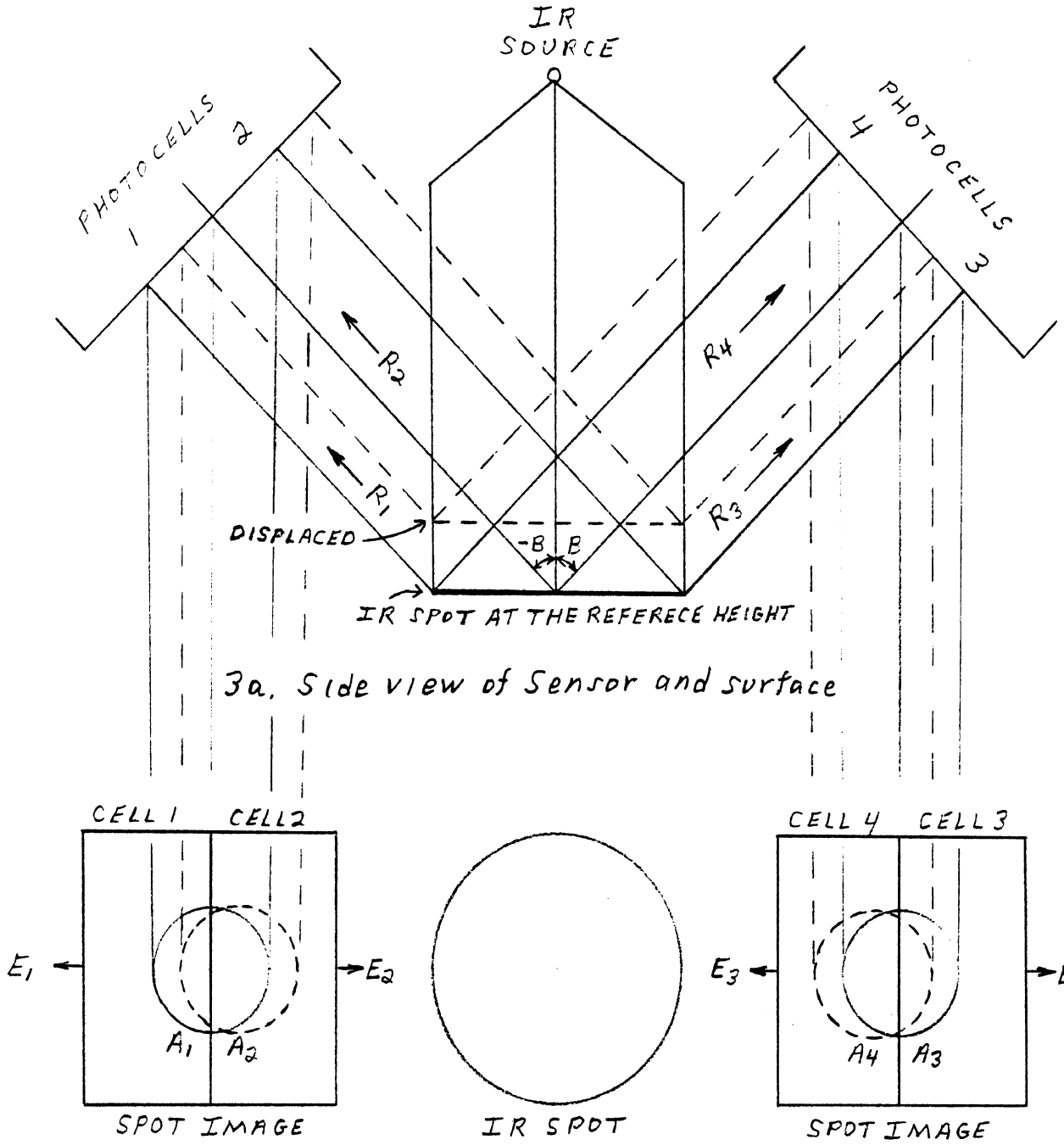


3a. Side view of Sensor and surface

3b. Schmatic view of the illuminated spot as seen by the four photocells.

$$\text{SENSOR OUTPUT} = E \doteq \frac{E_1 - E_2 + E_3 - E_4}{E_1 + E_2 + E_3 + E_4} \doteq \frac{A_1R_1 - A_2R_2 + A_3R_3 - A_4R_4}{A_1R_1 + A_2R_2 + A_3R_3 + A_4R_4}$$

$$\text{IF: } A_1 = A_3,\ A_2 = A_4,\ \& \ (R_1 + R_3) = (R_2 + R_4)$$

$$\text{THEN: } E = \frac{A_1 - A_2}{A_1 + A_2}$$

Figure 3. Schematic representation of the operation of the IR Sensor.

photocell, and also to follow the basic analysis presented by the Southwest Research Institute [1].

By design the sensor output, E, is defined by,

$$E = G\,(E_1 - E_2 + E_3 - E_4) \,/\, (E_1 + E_2 + E_3 + E_4), \qquad (1)$$

where $E_1$, $E_2$, $E_3$, and $E_4$ are the outputs of the photocells 1, 2, 3, and 4 respectively, and G is a scaling constant or gain. This design is intended to produce an output proportional to displacement distance, independent of changes in the overall surface reflectivity and also independent of nonuniform reflectivity over the illuminated surface.

The output of each photocell is proportional to the total power reaching the cell from the illuminated spot on the target surface. If the photocells have equal sensitivities and are linear over the range of power encountered, we have,

$$E1 = kP_1; \quad E2 = kP_2; \quad E3 = kP_3; \text{ and } E4 = kP_4, \qquad (2)$$

where $P_1$ through $P_4$ are the power reaching photocells 1 through 4, respectively, and k is the constant of proportionality between incident power and the cell output. (In the actual implementation of the sensor, electronic gains are adjusted to make the constant, k, effectively equal for all cells.) $P_1$ through $P_4$ can be expressed as:

$$P_1 = DA_1R_1, \quad P_2 = DA_2R_2, \quad P_3 = DA_3R_3, \text{ and } P_4 = DA_4R_4, \qquad (3)$$

where D is the IR power density over the illuminated spot on the target surface, and the coefficients $R_1$ through $R_4$ are the "effective average directional reflectivities." The coefficient $R_1$, for example, is the average reflectivity of the target surface, in the direction of cell 1, over the fractional area of the illuminated spot, $A_1$, that is imaged on cell 1.

Substituting the expressions from (3) and (2) into (1) , the constants, k, and D, cancel giving,

$$E = G\ (A_1R_1-A_2R_2+A_3R_3-A_4R_4)\ /\ (A_1R_1+A_2R_2+A_3R_3+A_4R_4). \qquad (4)$$

As noted above, and indicated in figure 1, when the surface is flat and distortion of the circular spot is neglected,

$$A_1 = A_3, \quad \text{and } A_2 = A_4. \qquad (5)$$

Making these substitutions in (4) yields,

$$E = G\ [A_1(R_1+R_3)-A_2(R_2+R_4)]\ /\ [A_1(R_1+R_3)+A_2(R_2+R_4)]. \qquad (6)$$

This expression shows that the sensor output is independent of the directional reflection coefficients only for the special case where,

$$(R_1 + R_3) = (R_2 + R_4). \qquad (7)$$

Substituting (7) into (6) gives,

$$E = G\ (A_1 - A_2)\ /\ (A_1 + A_2). \qquad (8)$$

This is the ideal sensor output as reported by the Southwest Research Institute, which is implemented in the circuitry of the IR sensor to produce an output.

## 2.2 Theoretical Sensor Outputs

The sensor is calibrated against a reference surface which has uniform reflectance (that is, $R_1=R_2=R_3=R_4$). All target surfaces must satisfy the condition given in equation (7) over the full operating range of the sensor, in order for the sensor output to actually match equation (8) without error.

### 2.2.1 The Effect of Non-Uniform Directional Reflectance.

Displacement of the spot image from its centered position on the photocells is

directly proportional to the displacement of the sensor from its reference height. Thus the area of the spot imaged on each photocell can be calculated as the partial areas of a circle divided into two parts by a cord. The equations required, which were given in the Southwest Research report [1], are shown in Figure 4. The quantity (X) in the figure, defines the cord position relative to a parallel line passing through the center of the circle. Therefore, X, is proportional to the displacement of the sensor from its reference height. With these equations defining the areas $A_1$ through $A_4$, equation (6) was evaluated for several specific reflection coefficient ratios. The arbitrary scaling factor, G, was set equal to one. The results, plotted in figure 4, show that there is a potential for significant errors on the IR sensor output due to nonuniform surface reflectivity.

The curve in Figure 4 passing through the origin is the ideal sensor output obtained when the condition given in equation (7) is satisfied. That is when $(R_1+R_3)=(R_2+R_4)$. Because the illuminated spot is circular, the output is not a perfectly linear function of the spot displacement. Nonetheless, it is reasonably linear, to within about one percent, for values of X/r from -0.5 to +0.5. (A rectangular illuminated spot is shown later to produce a larger usefully linear range.) The three curves in figure 4, representing cases where $(R_1+R_3)$ is not equal to $(R_2+R_4)$, show an offset from the ideal output for a given value of, X/r, and a decrease in the output linearity. Note that nonuniform transmissivity of the protective glass plate in front of the photocells, which can result from an accumulation of dirt, is equivalent to nonuniform directional surface reflectivity, and also causes a change in the sensor calibration indicated by the curves in figure 4.

**2.2.2 The Effect of Transitions of the Surface Reflectivity.** The condition for an ideal sensor output stated in equation (7), deals only with the ratios of the directional reflection coefficients and not with their absolute values. Thus a "dark" surface will produce the same sensor output as a "light" surface, if both exhibit uniform reflectance such that $(R_1+R_3)/(R_2+R_4)=1$. However, during the transition from a light to dark (or dark to light) surface seen by the sensor, as the surface passes under it, this condition is satisfied continuously only when the sensor is at its "zero" reference height, even though each surface in itself exhibits uniform

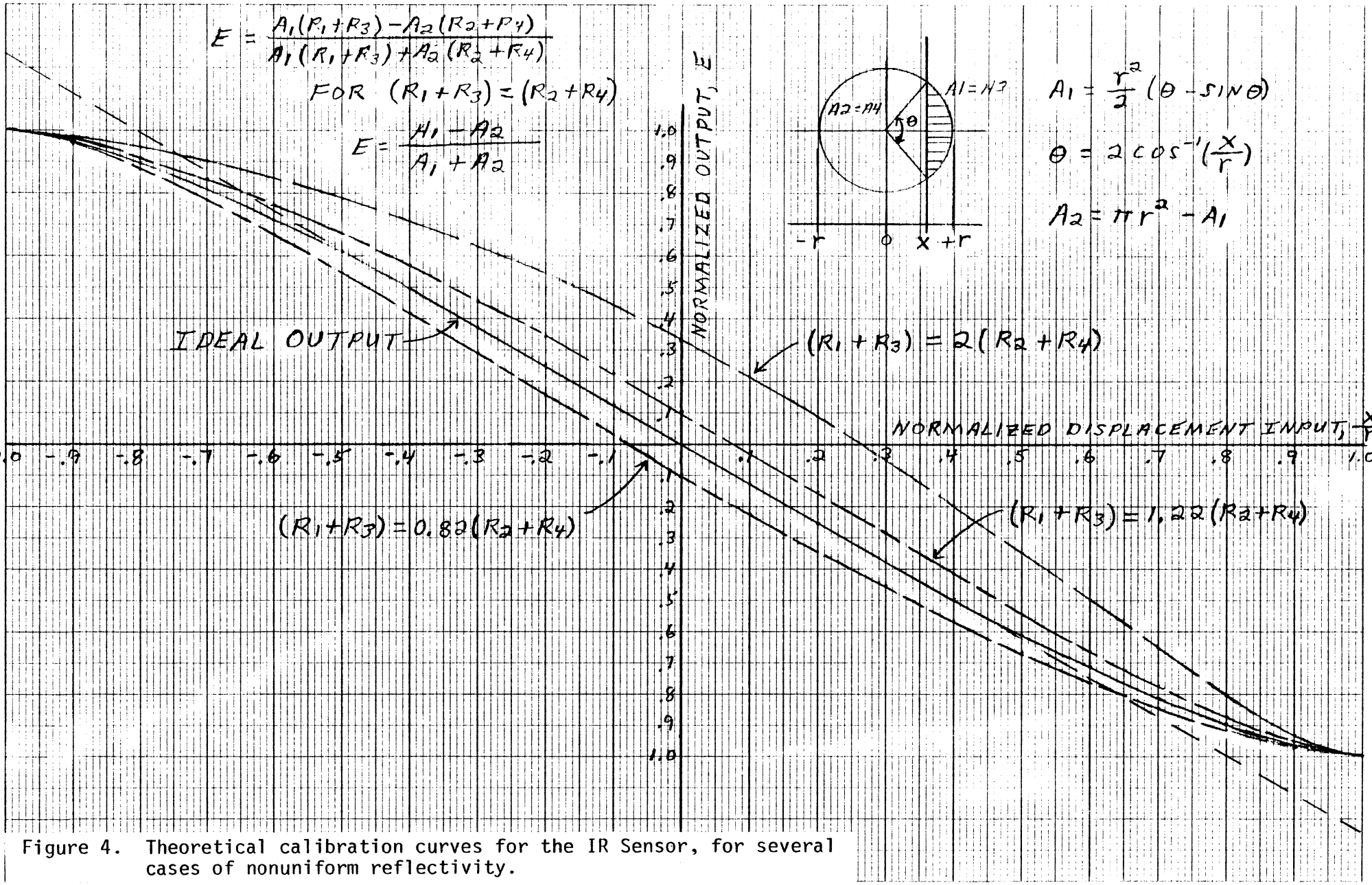


Figure 4. Theoretical calibration curves for the IR Sensor, for several cases of nonuniform reflectivity.

directional reflectance. Because the illuminated surface areas imaged on the photocells ($A_1$ through $A_4$) are not equal when the sensor is displaced from its reference height, the "effective" directional reflectivities do not satisfy the required condition during the transition. This is simply illustrated by the geometric constructions shown in Figure 5, representing a band with uniform reflectivity, $R_N$, moving across the IR spot, replacing a surface with uniform reflectivity, $R_0$.

Figure 5a depicts the sensor at its reference height and Figure 5b depicts the sensor displaced from its reference height. In Figures 5a and 5b the edge of the reflectance change is moving in the direction of the short axis of the IR sensor. From the symmetry in Figure 5a, it is obvious that the average reflectivity of the spot areas imaged on each photocell are the same, although the magnitudes change as the band progresses across the spot. This is shown by the plot of $(R_1+R_3)$ vs $(R_2+R_4)$ at the right side of the Figure, where the slope of the curve is constant and equal to 1. However, in 5b the edge of the band infringes on the areas $A_2$ and $A_4$ before it starts to enter the areas $A_1$ and $A_3$. Thus, the effective directional reflectivities, $R_2$ and $R_4$, change before $R_1$ and $R_3$ start to change and, as shown in the plot at the right, $(R_1+R_3)$ is not equal to $(R_2+R_4)$, except when the edge of the band is at the center of the circle. Because of this inequality, an output error occurs as the band moves across the IR spot. Note that for this particular situation, this error could be eliminated by employing a square or rectangular IR spot shape instead of the circular shape. Even with the sensor displaced from its reference height, the average reflectances would be equal, so that the reflection coefficients would remain equal and no output error would occur.

The result is similar in the case of the band edge moving in the direction of the long axis of the sensor as depicted in Figures 5c and 5d. However, the maximum output error is larger than in the former case, and the error will occur even with square or rectangular IR spot shapes. In both cases the magnitude of the error is proportional to the reflectance ratio, $R_N/R_0$, and to the magnitude of the sensor displacement from its reference height.

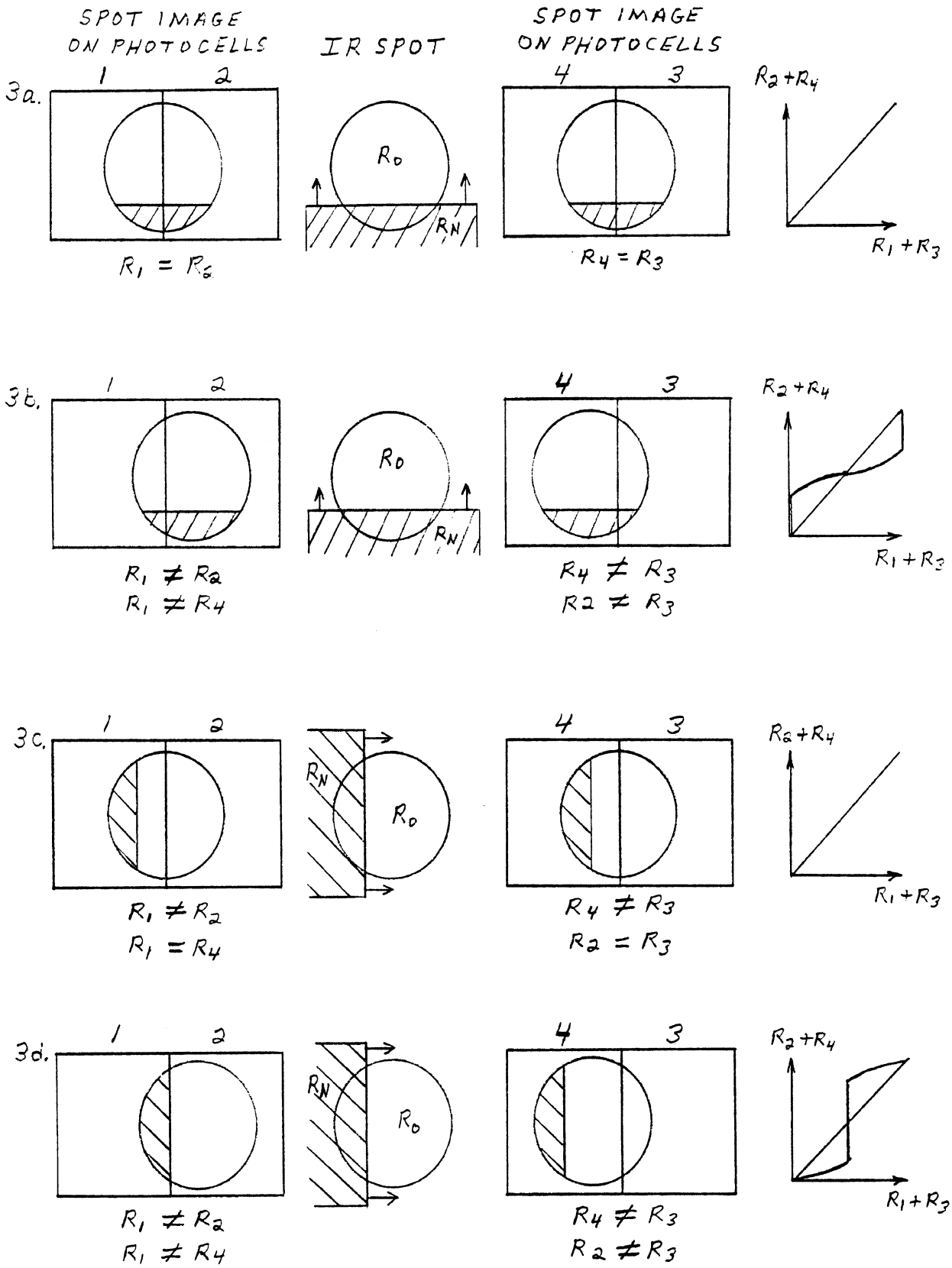


Figure 5. Images seen by the IR Sensor during a step change in surface reflectivity.

2.2.3 **Theoretical Error Magnitudes.** Theoretical IR sensor outputs are shown in Figure 6 for the case of a stripe of width greater than the IR spot diameter, passing completely across the IR spot, and moving in the direction of the long axis of the sensor. That is, in the direction represented in Figures 5c and 5d. The plots show the influence of two parameters; 1) the normalized image spot displacement, X/r, as defined in figure 4; and 2) the ratio, $R_N/R_0$, of the stripe reflectance relative to the background reflectance. Figure 6a displays plots of the sensor output vs the stripe position for a reflection ratio, $R_N/R_0 = 5$, and several values of spot displacement, X/r. The ideal output on these plots for a given value of X/r, is that given by the solid curve in Figure 4. For X/r = +0.5, for example, the ideal output from Figure 4 is -0.6. The maximum error when X/r = +0.5 or -0.5 is almost 50 percent of the ideal output. The error decreases to zero as X/r goes to zero. Figure 6b displays the output plots for X/r = +0.5 and -0.5 with the reflection ratio, $R_N/R_0$, as a parameter. As the reflection ratio decreases the error decreases, and when $R_N/R_0 = 1$, the output is free of errors for all values of X/r. Note that a reflectance change passing under the sensor in the direction of its short axis, but not covering the whole spot as it passes, (for example the band shown in Figure 5d moving at a right angle to the directon indicated by the arrow), will produce an error amplitude, dependent on its position, which can be read from the curves in figure 6. This would occur, for example, when a painted lane delineation stripe encroaches within the illuminated IR spot, as the vehicle-mounted sensor travels down the road. Rather than passing quickly under the spot, the stripe could remain part-in, part-out for some distance, leading to a long wavelength error of significant magnitude.

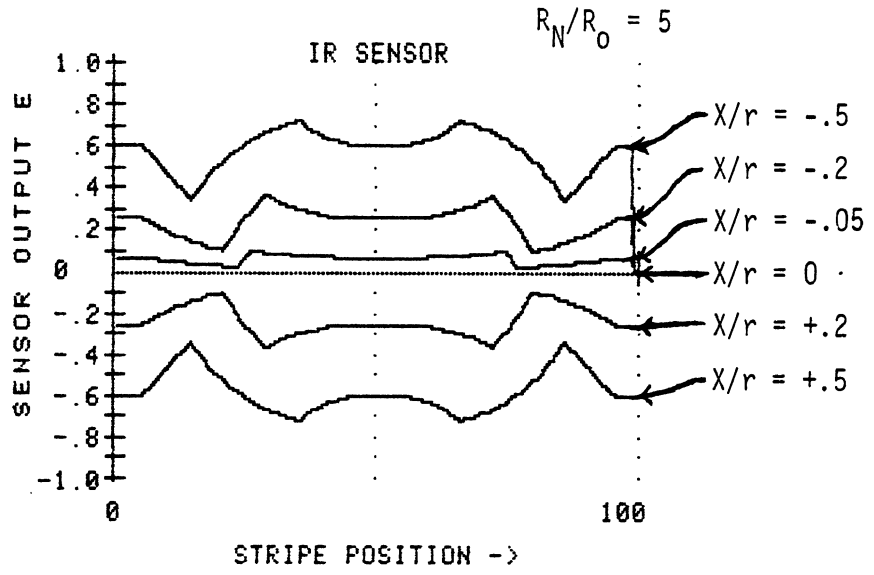


6a. Effect of sensor height

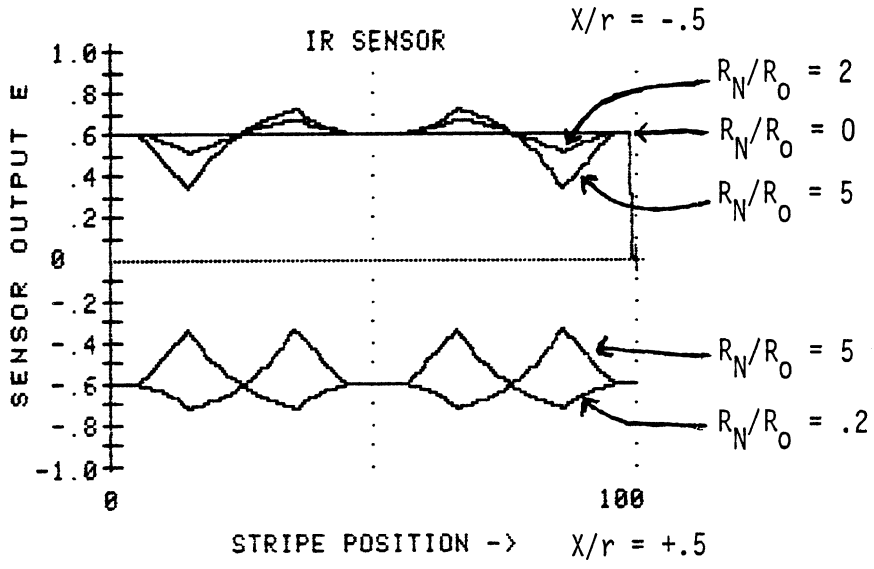


6b. Effect of stripe / background contrast

NOTE: $R_N$ = Reflectivity of stripe  X = Relative Sensor height
$R_o$ = Reflectivity of background  r = Radius of illiuminated circle

Figure 6. Theoretical response of the IR Sensor to a painted stripe, for several combinations of sensor height and stripe/background contrast.

## 3.0 LABORATORY TESTS AND RESULTS

Both quasi-static and dynamic tests of the IR sensor were performed in the laboratory. The dynamic test included surface speeds up to 60 mph. While these test results generally agree with the analysis presented above, they indicate additional errors which are not yet fully explained. After observing these errors, which are described below, the sensor was recalibrated following the procedures given in the Southwest Research Calibration Manual (Appendix A), as detailed in Appendix B. The recalibration generally required only small adjustment changes and produced no significant improvement in the sensor performance.

### 3.1 Quasi-static Tests

Quasi-static tests of the IR Sensor were made with the sensor mounted in the head of a vertical mill, thus permitting accurate vertical displacement of the sensor with its reference (bottom) surface parallel to the target surface laying on the mill bed. Horizontal travel of the test surface was provided by the horizontal displacement of the mill bed.

**3.1.1 Sensor Output vs Displacement.** The output vs displacement curve shown in Figure 7 was made on an X-Y plotter with the displacement signal obtained from a calibrated string pot connected between the head and the table of the mill. The target surface was a white cardboard from a writing tablet. The zero output "reference height" was 13.9 inches. Displacement from this reference height is plotted in Figure 7, where a negative displacement is a decrease in sensor height with a corresponding negative voltage output from the sensor. The output is reasonably linear for displacements from -1.75 inches to +1.5 inches. The curve is seen to be slightly asymmetric. In order to observe the effect of a rectangular illuminated spot on the output linearity, an approximately rectangular spot was obtained by taping a one-half inch wide slit across the IR source output lens, with its long axis centered on the long axis of the sensor. The output curve obtained, shown in Figure 8, has a slightly different gain (slope) and

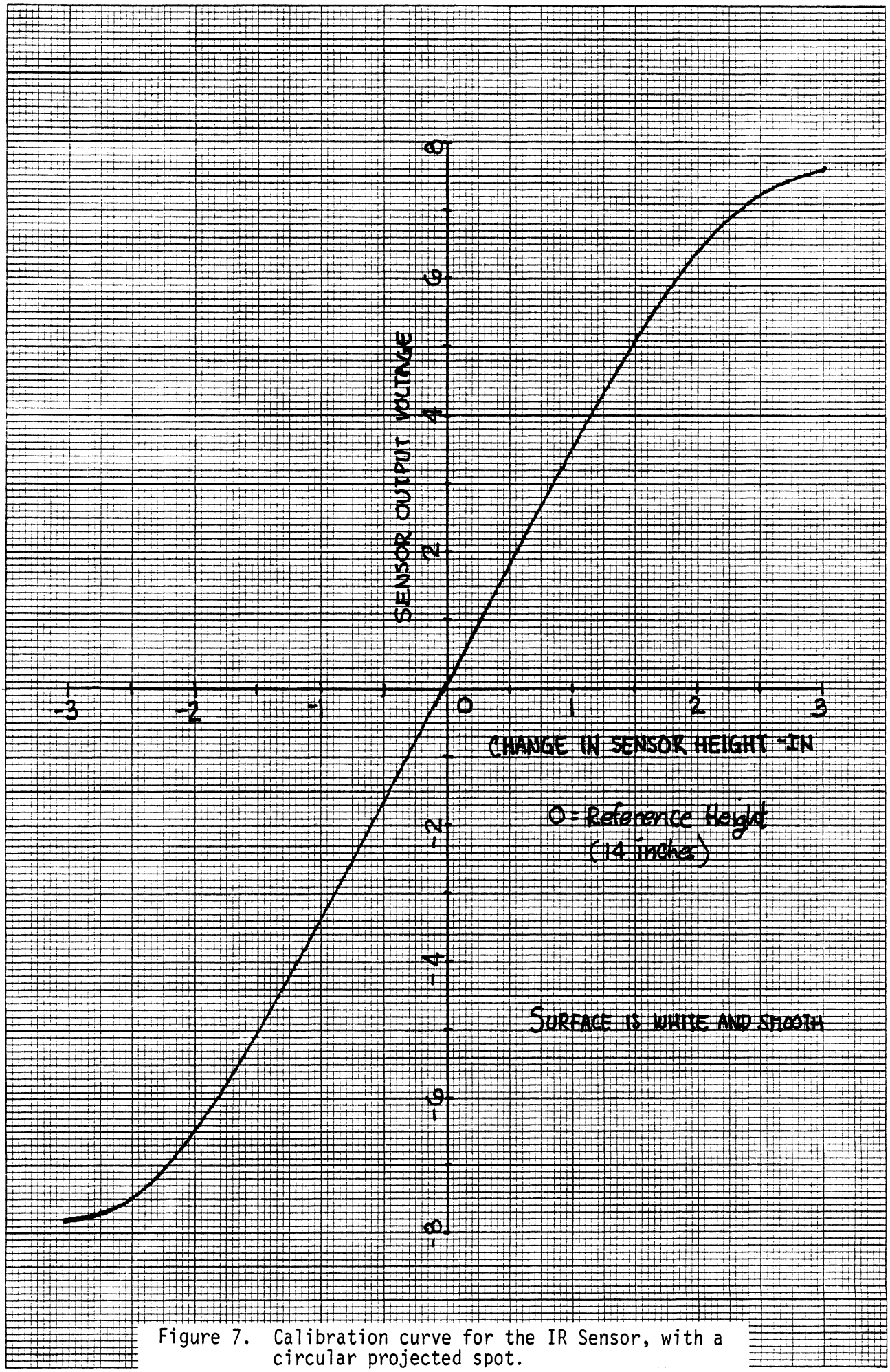


Figure 7. Calibration curve for the IR Sensor, with a circular projected spot.

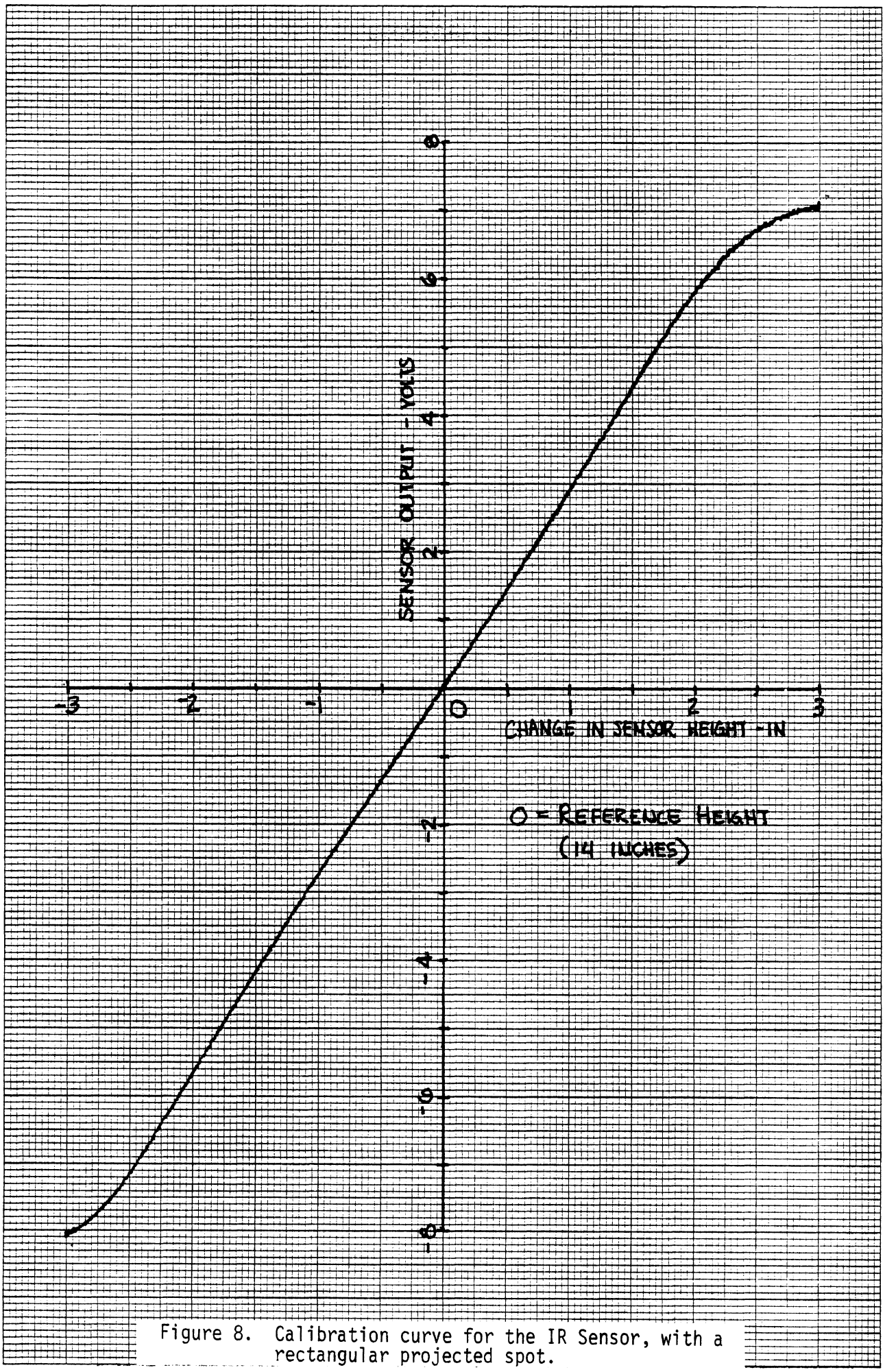


Figure 8. Calibration curve for the IR Sensor, with a rectangular projected spot.

a larger linear range (-2.5 inches to +2.0 inches), than that obtained with the circular spot. The asymmetry observed on both curves (Figures 7 and 8), suggest that the spot image is not perfectly centered on the photocell pairs when the sensor is at the reference or zero-output height. However, other factors, alone or in combination, can also affect the output symmetry:

1. The IR light source is not perfectly collimated. Therefore the spot size changes with height from about 3.2 inches diameter at -2 inches displacement (12 inches height) to 3.6 inches diameter at +2 inches displacement (16 inches height).

2. The four photocells do not have perfectly uniform surface sensitivities. The manufacturer's data sheet specifies a surface uniformity of 2 percent over the photocell surface.

3. The photocell response is not linear. The manufacturer's data sheet specifies the photocell linearity to be ten percent for photocell output current up to 200 microamps.

4. The shape of the spot image on the photocell pairs may be slightly different due to slight geometric asymmetry of the sensor structure.

**3.1.2 Sensor Tilt Sensitivity.** The sensitivity of the sensor output to tilt or rotation of the sensor, around its short axis, was measured with the sensor mounted on the mill. Measurements were made with the sensor mounted at its reference height (14 inches) above a dark-gray target surface. Tilt angles were set by rotation of the calibrated mill head. Since the center of rotation was twenty seven and five eights inches above the target surface, rotation also caused a displacement of the sensor relative to the surface. This displacement was calculated at each measurement angle and subtracted from the sensor output. The sensor output voltage was measured to an accuracy of .01 volt with a digital voltmeter, and converted to inches by the sensor calibration factor (3.5 volts per inch). The tilt-induced error vs tilt angle is tabulated in Table 1, for tilt angles from -10 to +10 degrees. At an angle of 4 degrees the tilt error is only .04 inches. However, as the tilt angle increases above 4 degrees, the tilt error increases rapidly,

TABLE 1

The effect of Sensor Tilt, Combined with Small Displacements From the Reference Height.

| Tilt Angle Deg. | Sensor Output in. | Calculated Height in. | Tilt Error in. |
|---|---|---|---|
| 10 | 0.400 | 0.636 | 0.236 |
| 8 | 0.260 | 0.405 | 0.145 |
| 6 | 0.146 | 0.227 | 0.081 |
| 4 | 0.060 | 0.101 | 0.041 |
| 3 | 0.034 | 0.057 | 0.023 |
| 2 | 0.014 | 0.025 | 0.011 |
| 1 | 0.006 | 0.006 | 0 |
| 0 | 0 | 0 | 0 |
| -1 | 0.006 | 0.006 | 0 |
| -2 | 0.014 | 0.025 | 0.011 |
| -3 | 0.034 | 0.057 | 0.023 |
| -4 | 0.060 | 0.101 | 0.041 |
| -6 | 0.140 | 0.227 | 0.087 |
| -8 | 0.251 | 0.405 | 0.154 |
| -10 | 0.366 | 0.636 | 0.270 |

reaching about .25 inches at plus or minus 10 degrees tilt angle.

Theoretically, the sensor should not be sensitive to tilt around the short axis with the sensor at the reference height. Tilt around the short axis causes different distortions of the spot image shape on one photocell pair compared to that on the other photocell pair. However, at the reference height, the total power on each photocell should not change with tilt angle and the sensor output should not change. When the sensor is displaced from the reference height, however, the change in the shape of the image spots results in a change in the displacement calibration of the sensor. Thus the measured tilt error, shown in table 1, may have resulted from the combined tilt and displacement in the experiment. These measurements must be expanded in order to measure the effect of tilt only, and tilt combined with displacement of the sensor from the reference height.

Theoretically, the sensor is less sensitive to rotation around its long axis, in combination with displacement from the reference height, because the distortion of the spot image shape is the same on both photocell pairs and it is symmetric about a centerline through the spot image parallel to the dividing line between the photocells in each pair. Measurements need to be made to quantify this error and determine the range of tilt and displacement tolerable in a given application of the sensor.

**3.1.3 Sensor color sensitivity.** The sensor response to surface reflectivity, or color changes, was investigated using three control colors: dark-gray; light-gray; and white. An aerosol spray paint was used to obtain a uniformly textured surface. The paints used were:

Dark gray; Krylon No. 1318, All Purpose Gray Primer

Light gray; Dupli-color No. 1699, Gray Primer Sealer

White; Krylon, No. 1502, Flat white

A flat one eighth inch thick aluminum plate was painted dark-gray on both sides. A five inch wide band was painted light gray on one side and white on

the other side. This target surface was then placed on the mill bed under the sensor and moved horizontally under the sensor with the edge of the "color" stripe moving perpendicular to the long axis of the sensor. These are the same conditions assumed for the theoretical plots shown earlier in Figure 6. Figure 9 shows oscillographs of the sensor output as the color stripe passes under the sensor at three different sensor heights. These composite traces were generated on a storage oscilloscope, so that several traces could be compared on one oscillograph. While the vertical sensitivity is the same for each trace in the oscillograph (1.0 volt per division or 0.268 inch per division), the nominal voltage level of each trace relative to the others is not so scaled. The oscilloscope offset control was used to position the traces so they could be easily compared. Obviously, these are not simultaneous time traces, but rather sequential time traces stored for easy comparison. The horizontal time base is 2.0 seconds per division. The mill bed was moved horizontally by hand, thus the surface velocity was not constant, nor was it exactly the same for each trace, and the horizontal scale varies between 4 and 6 inches per division.

In each oscillograph, the center trace is with the sensor at the zero reference height of fourteen inches, the top trace is with the sensor displaced plus one inch from the reference height to a height of fifteen inches, and the bottom trace is with the sensor displaced minus one inch from the reference height to a height of thirteen inches. Figure 9a is with the light-gray stripe and Figure 9b is with the white stripe, both on the dark-gray background. These output curves are seen to be very similar to the theoretical curves in Figure 6. While the IR spot is moving across the color change a transient output is observed similar to the theoretical predictions (Figure 6). For the case of the white stripe on the dark-gray background, a peak to peak output error of about 0.97 inch occurs. With the light-gray stripe the errors are less than with the white stripe as predicted by the analysis. Even larger errors result for displacements greater than the plus and minus one inch illustrated in Figure 9.

These plots were made with the Automatic Gain Control (AGC) circuit in the sensor turned on. When repeated with the AGC turned off, only small changes in the output response were observed.

SCALE: 1V=0.286 in.

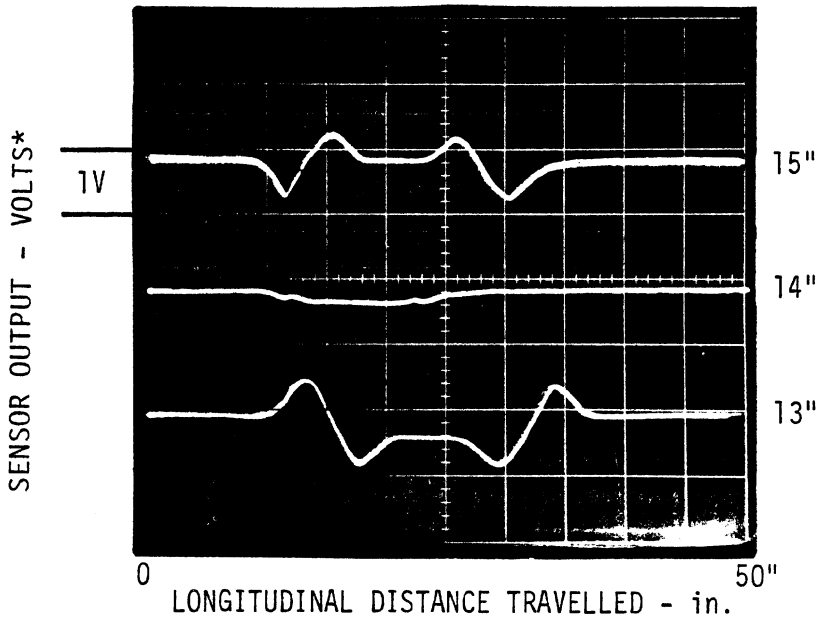


9a. Light-gray stripe on dark-gray background.

---

SCALE: 1V=0.286 in.

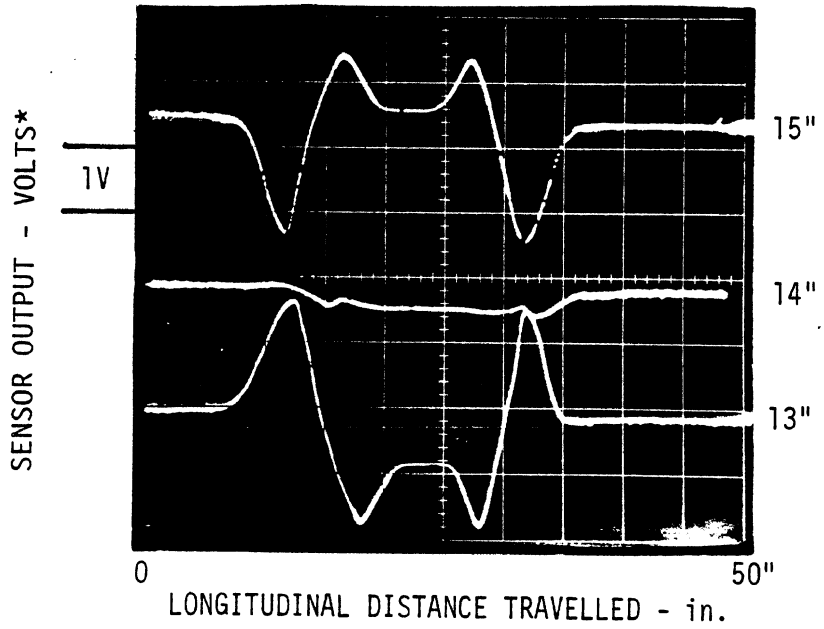


9b. White stripe on dark-gray background.

* NOTE: All plots have been shifted vertically, to allow greater oscilloscope sensitivity. Trace amplitudes are relative not absolute.

Figure 9. Quasi-static response of the IR Sensor to a painted stripe, with the long axis of the sensor oriented in the direction of travel.

While the test results qualitatively corroborate the type of behavior predicted theoretically, there are some additional effects not accounted for by the theory:

1. At the reference height (fourteen inches), where perfect color cancellation should result, there is a residual output of about 0.04 inches for the light-gray stripe and about 0.09 inches for the white stripe.

2. At the center plateau in the waveforms, with the sensor displaced from its reference height, when the IR spot is fully on the stripe the ouput should be the same as when the IR spot is on the dark-gray. Instead, a residual error exists. For example, the residual error is about three small divisions or about 0.17 inch in the bottom trace in Figure 9b.

3. The residual error is not symmetric for positive and negative displacements.

Figure 10 shows oscillographs of the sensor output for the same conditions as in Figure 9a, but with the sensor rotated ninety degrees so that the edge of the white stripe is oriented parallel to the long axis of the sensor, moving in the direction of the short axis of the sensor. This is the condition depicted in Figure 5a and 5b. As predicted in the discussion of Figure 5, the output transient observed, as the stripe moves across the IR spot, is much smaller than it was for the other orientation.

### 3.2 Dynamic tests.

Dynamic tests of the IR sensor were performed with a 67.5 inches diameter drum roller allowing target surface velocities up to 60 mph. The surface input is illustrated in Figure 11. An eight inch square rubber pad, 0.25 inch thick, was glued to the surface of the drum to produce a step input of surface height. The pad and the drum roller surface around the pad were painted dark-gray, making a uniformly reflective surface including the pad. The painted area was 54 inches long in the direction of rotation of the drum roller, and the remainder of the drum was bare steel. The leading edge of the

SCALE: 1V=0.286 in.

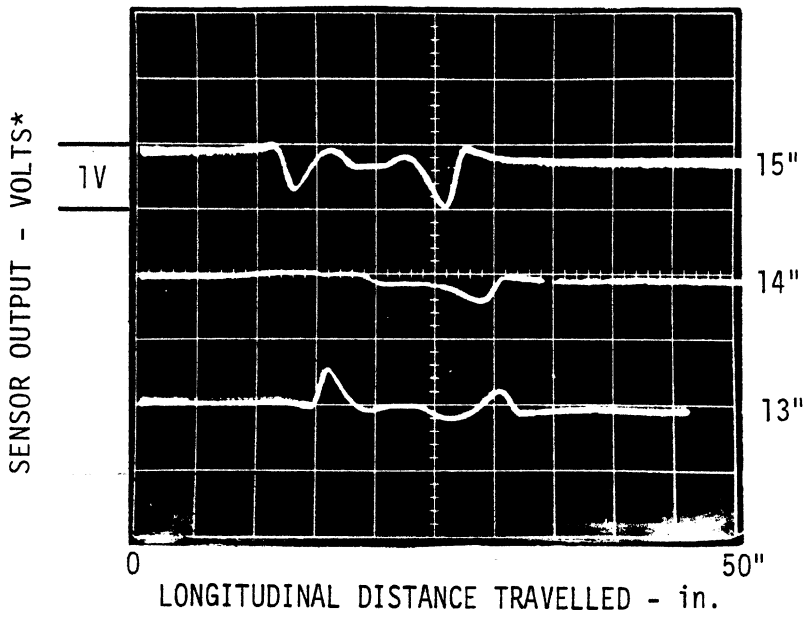


* NOTE: All plots have been shifted vertically, to allow greater oscilloscope sensitivity. Trace amplitudes are relative not absolute.

Figure 10. Quasi-static response of the IR Sensor to a white stripe painted on a dark-gray background, with the short axis of the sensor oriented in the direction of travel.

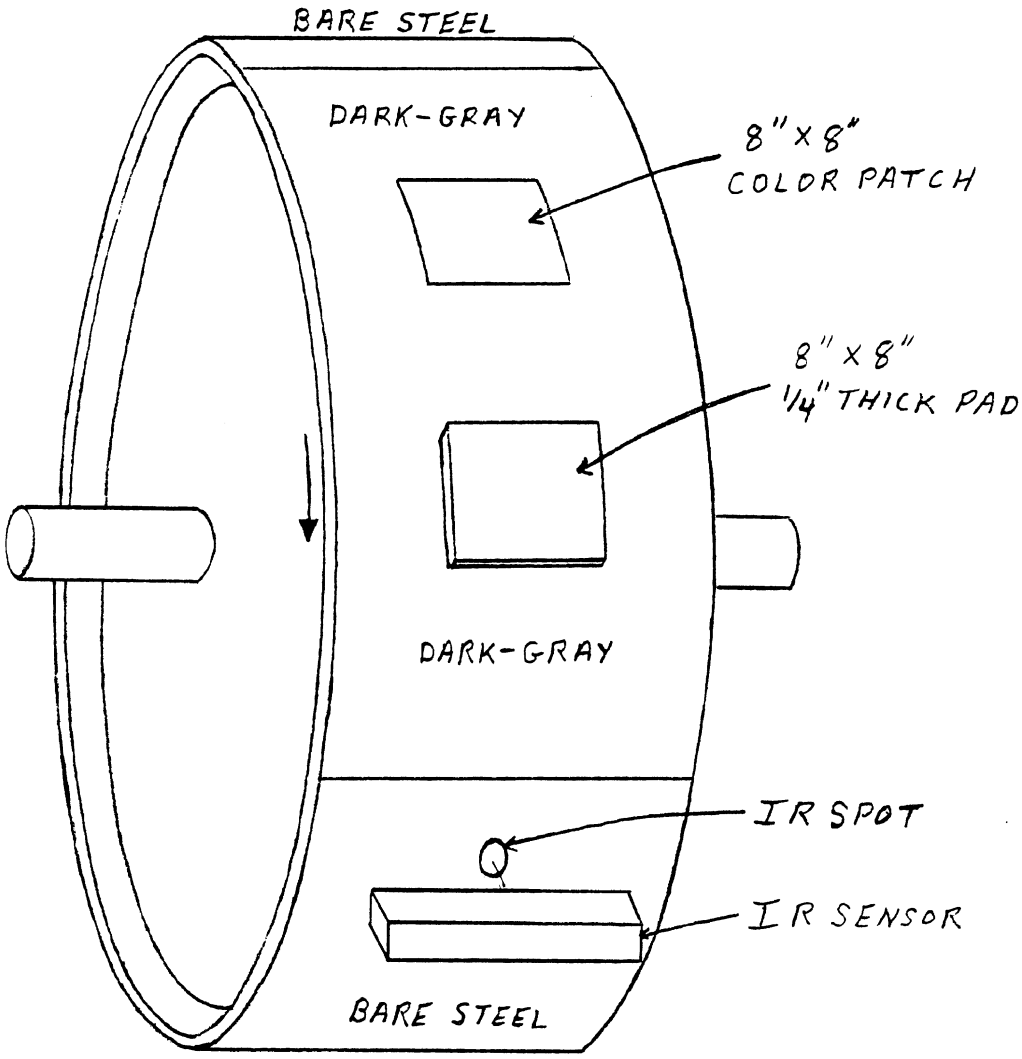


Figure 11. Illustration of the drum roller and test surface used for high speed dynamic testing of the IR Sensor.

rubber pad was about 17 inches from the leading edge of the painted area. A white band, about 3 inches wide, was painted on the drum roller about 18 inches before the edge of the gray painted area in order to obtain a leading pulse on the sensor output for an oscilloscope trigger. The sensor was mounted facing the drum surface, with its long axis parallel to the leading edge of the painted surface, so that the leading edge of the painted surface and of the pad traveled in the direction of the short axis of the sensor. This orientation was chosen to minimize the transient on the sensor output resulting from a color stripe passing the sensor, as demostrated in the analysis and in the quasi-static testing.

3.2.1 **Height Change With No Reflectance or Color Change.** Figure 12 shows oscillographs of the sensor outputs obtained from the uniform dark-gray surface with a 0.25 inch step, for three nominal sensor heights of 13, 14, and 15 inches, and at three surface velocities of 6, 30, and 60 mph. As in figure 9, these are composite storage scope traces. All the traces have the same vertical sensitivity, as is indicated in the Figure, and they are positioned with the oscilloscope offset control to obtain a convenient display. The horizontal time base, for each surface velocity, is selected to obtain the spatial scaling of 0.88 feet (10.56 inches) per division. Starting from the leftside of the oscillographs and following the scope trigger pulse, the inputs to the sensor (see Figure 11) are: the bare steel of the drum; a change in the surface reflectance as the IR spot moves onto the gray painted surface; the gray painted surface; the height change of the rubber pad; again the gray painted surface; and again the bare steel surface. The indicated height change (one volt or 0.286 inch) resulting from the 0.25 inch high rubber pad is fairly accurate at all speeds. Nontheless, the height indicated is slightly smaller at the sensor height of 15 inches than at the sensor height of 14 and 13 inches. (Note that the order of the traces, in terms of the sensor height, is reversed from that in Figures 9 and 10). Although at the higher speeds, the height pulse becomes rounded at its peak, due to the circuit bandwidth, the peak amplitude is the same at 60 mph as at 6 mph.

A false height change of about 0.3 inch is indicated between the bare steel surface and the gray-paint surface. The reflectivity of the bare steel was determined to be only slightly greater than that of the white paint used

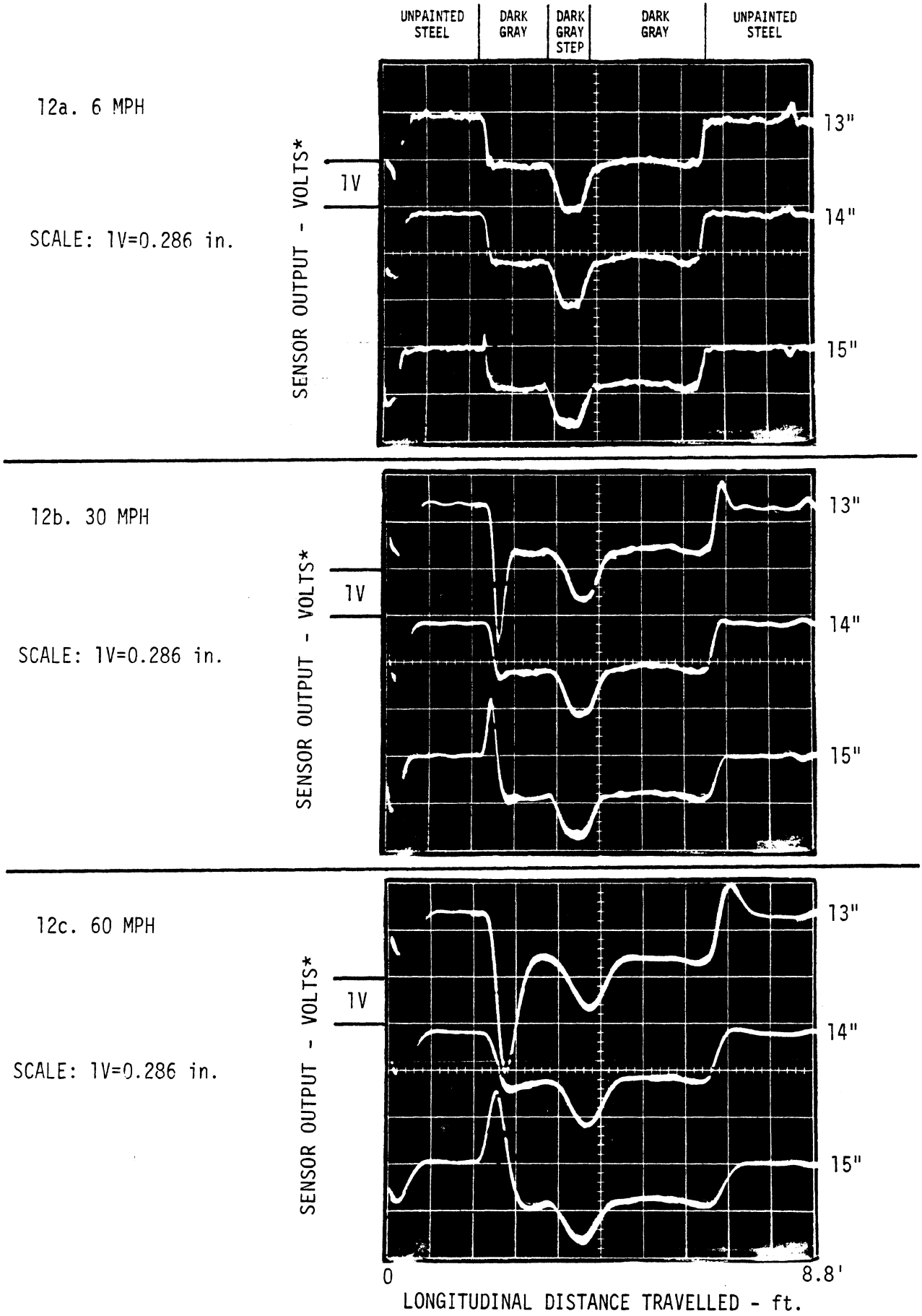


* NOTE: All plots have been shifted vertically, to allow greater oscilloscope sensitivity. Trace amplitudes are relative not absolute.

Figure 12. Dynamic response of the IR Sensor to a raised pad (step change in height).

in the tests for color effects described above, but the color cancellation here is not as effective as with the white paint. We believe this is because of unequal directional reflectivity toward the four photocells, caused by minute grooves in the drum surface left by the machining operation when the drum was made. These grooves are small enough to be completely filled in by the paint and thus do not show through on the painted surfaces. Another significant feature of the oscillographs in Figure 12 is the large signal overshoot at the steel to dark-gray paint transition for 30 and 60 mph surface speeds, when the sensor is displaced from its reference height. The cause of this dynamic response error is not yet understood, but as will be seen below, it can cause significant errors even with moderate surface reflectivity or color changes. Note that the transient error is much smaller at the transition from the dark-gray paint back onto the bare steel.

3.2.2 **Reflectance Change With and Without a Height Change.** The dynamic tests were repeated with a moderate color change added to the drum roller surface. The surface of the eight inch square, 0.25 inch high rubber pad, was painted light-gray and an eight inch square area, about 10 inches past the pad, was also painted light-gray over the dark gray surface (see Figure 11). Oscillographs obtained with this surface are shown in figure 13. Compared with the corresponding oscillographs in Figure 12, at a surface speed of 6 mph, the color change is seen to have caused a perceptible increase in the amplitude of the pad height pulse. Also the light-gray square on the drum surface produces a perceptible but insignificant output. However, at surface speeds of 30 mph and 60 mph, significant signal distortion is apparent, particularly for the sensor height of 13 inches. For the 13 inch height and 60 mph, for example, the light-gray surface area produces a peak-to-peak indicated height change exceeding 0.3 inch, with the indicated height change of the 0.25 inch high pad being 0.48 inch, an error of almost 100 percent.

The same tests were repeated with the light-gray areas of the previous test now painted white. The oscillographs, shown in Figure 14, indicate even greater error. Again the "worst case" occurred with the sensor height of 13 inches, with the white square on the drum surface producing an indicated peak-to-peak height change of more than one inch, and the indicated height of the 0.25 inch high pad also being about one inch. Even at the zero reference height of 14 inches, the errors are about 0.3 inch.

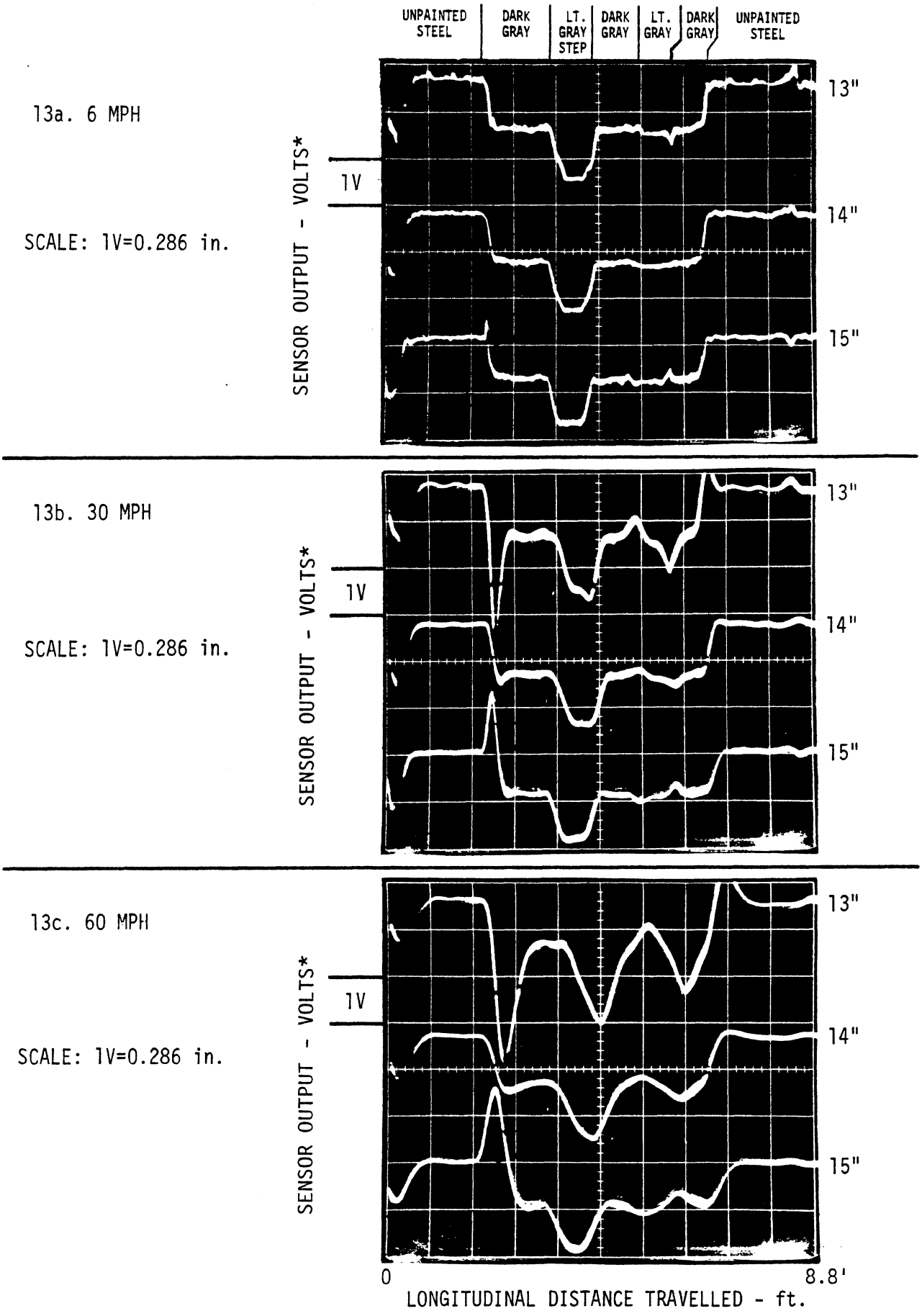


* NOTE: All plots have been shifted vertically, to allow greater oscilloscope sensitivity. Trace amplitudes are relative not absolute.

Figure 13. Dynamic response of the IR Sensor to both height change and moderate color change (dark-gray / light-gray).

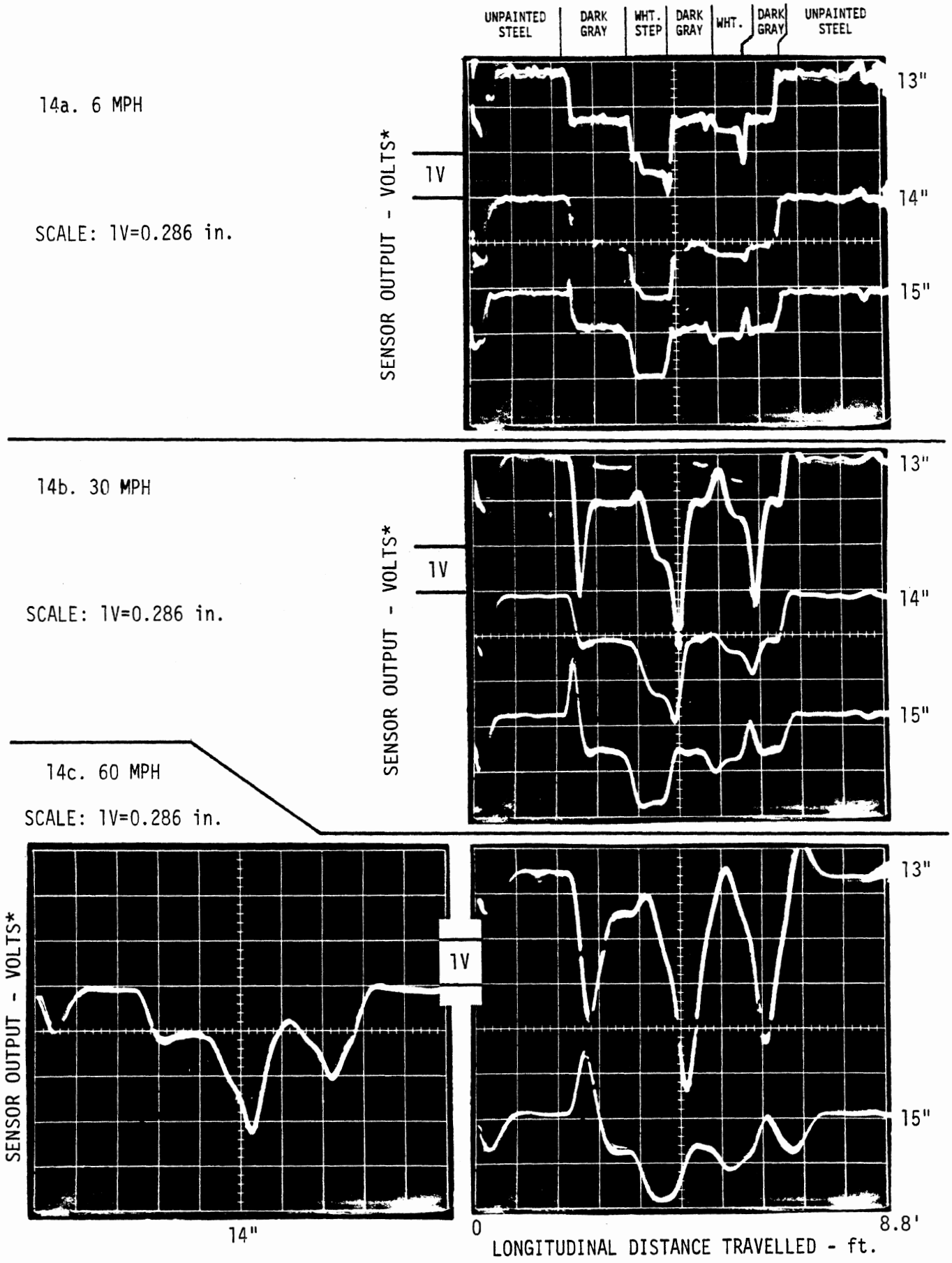


* NOTE: All plots have been shifted vertically, to allow greater oscilloscope sensitivity. Trace amplitudes are relative not absolute.

Figure 14. Dynamic response of the IR Sensor to both height change and major color change (dark-gray / white).

## 4.0 THE IR SENSOR ELECTRONICS

The asymmetry in the sensor outputs in the dynamic tests, for equal plus and minus displacements of the sensor from its reference height, suggest that the sensor is not properly calibrated. Having observed these effects, the sensor was recalibrated following the procedures recomended by the Southwest Research Institute, and the tests were repeated.

### 4.1 Sensor Recalibration

The recalibration did not solve the problems, and in fact, the oscillographs shown in Figures 9 through 14 were made after the recalibration. (The quasi-static output vs displacement curves, in Figures 7 and 8, were made before the recalibration.) Some effort was made to investigate the cause of the observed dynamic behavior before the recalibration was performed, but no specific causes or solutions were found. No significant improvements were realized as a result of the recalibration. Only minor adjustments of the available controls were required to obtain the recommended signal values and waveforms given in the calibration procedure (Appendix A).

Upon completing the calibration an offset of about 0.2 volts remained on the sensor output, where zero output was expected. This residual offset was found to result from unequal gains in the difference amplifier to its four inputs, the gain to photocell inputs 2 and 4 being 3.3 percent greater than the gain to photocell inputs 1 and 3.

An alternate to the piebald disk procedure (see Appendix A), was applied to adjust the sensor for optimum cancellation of surface reflectance changes, while at its reference height. Adjustments of the appropriate controls were made to minimize the tracking error between the D.C. voltages from the photocell channels 1 and 4, and between channels 2 and 3, as a dark-gray to white color transition was moved horizontally under the sensor, in the direction of its long axis. That is, in the direction the sensor is most sensitive to transitions in surface reflectance (See Figure 5). Application

of this procedure allowed the following observations:

1. The sum and difference amplifiers and the analog divider do not contribute to the problem of imperfect cancellation of reflectance changes.

2. The four photocell channels exhibit small differential nonlinearities. Thus perfect tracking between channels 1 and 4, and between channels 2 and 3, necessary for perfect cancellation of reflectance changes at the reference height, cannot be obtained. The photocells are the most likely source of the nonlinearity.

3. Optimum cancellation of reflectance changes, for this particular sensor, is obtained at a reference height of about fourteen and one eight inches, rather than fourteen inches.

Data collected in peformance of the calibration procedures are presented and discussed in detail in Appendix B.

The fact that the dynamic response of the sensor is good when there is no color change involved (see Figure 12), indicates the sum and difference amplifiers and the analog divider do not contribute to or cause the dynamic problem. The signal distortion causing the sensor output signal overshoot is believed to be present on the signals before they are processed by the sum and difference amplifiers. Oscillographs presented below support this theory. If true, the problem is caused either by the photocells or the circuitry between the photocells and the inputs to the sum and difference amplifiers.

## 4.2 The Automatic Gain Control (AGC).

The (AGC) circuit in the IR sensor, controls the voltage applied across the infrared light emitting diode to increase the illumination on surfaces with low reflectivity, and thereby reduce variations of the power level incident on the photocells due to variations of the target surface reflectivity. The gain control signal, or voltage, is derived from the sum signal, that is from the output of the summing amplifier, which also is applied to the denominator input of the divider circuit. Ideally the AGC

controls the light output of the IR diode so that the total power on all four photocells is constant for all surface reflectivities. Then, as the sensor moves up and down from its reference height the photocells see the same range of power levels, regardless of the absolute surface reflectivity. Thus, the photocells are always operating over the optimum linear range of their response curves. It has been proposed, but not confirmed, that the dynamic response problem triggered by surface reflectance changes may be due to differential nonlinearities and/or response times between the four photocells. The imbalanced performance then produces a transient difference between the photocell outputs when a large and rapid change in power level occurs. This theory is supported by the fact that the signal overshoot, occurring at high surface velocities, changes with static sensor height (see Figure 14), which is directly related to the nominal power levels at the photocells.

The reflectance ratio of the white and dark-gray painted surfaces used in our tests is approximately 8:1 as indicated by the ratio of the outputs of each photocell (or the sum signal) when the sensor is viewing one and then the other color while the AGC is turned off. With the AGC turned on, this ratio is reduced to about 1.8:1. Because of this substantial decrease in the effective reflectance ratio with the AGC on, a significant change in the dynamic response of the sensor is expected, if the above theory is true, when the AGC is turned on and off. It will be shown below that such is not the case. However, it is also shown below that the AGC is very slow acting and therefore may not have much effect at the higher surface speeds.

The voltage across the IR diode light source is switched on and off (chopped) at a 5 kilohertz rate. The oscillographs in figure 15 show the voltage on the cathode of the diode relative to the anode (ground). Figure 15a shows the switching waveform, with the AGC off. The diode light source is on when the signal is low or negative, and the light output increases as the voltage increases in the negative direction. The rated turn on and off times of the IR diode are about 15 nanoseconds, much faster than the switching time of the applied waveform. Figure 15b shows the same waveform, but with the AGC on and at a much slower oscilloscope sweep speed such that only the envelope of the waveform is seen. In this case the sensor is viewing the steel surface of the drum roller and the dark-gray/white test surface, as in previous

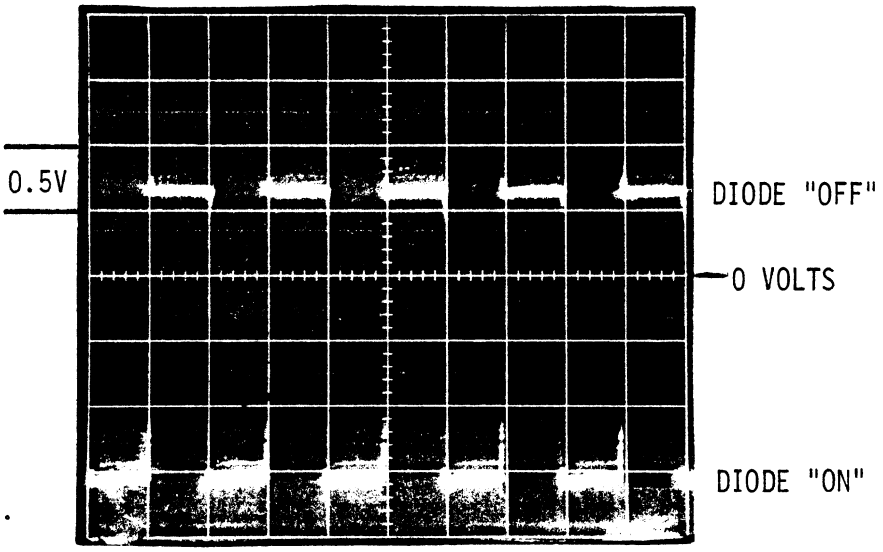


TIME: 0.1 MILLISECOND / DIVISION

15a. 5 KHZ switching voltage with AGC off.

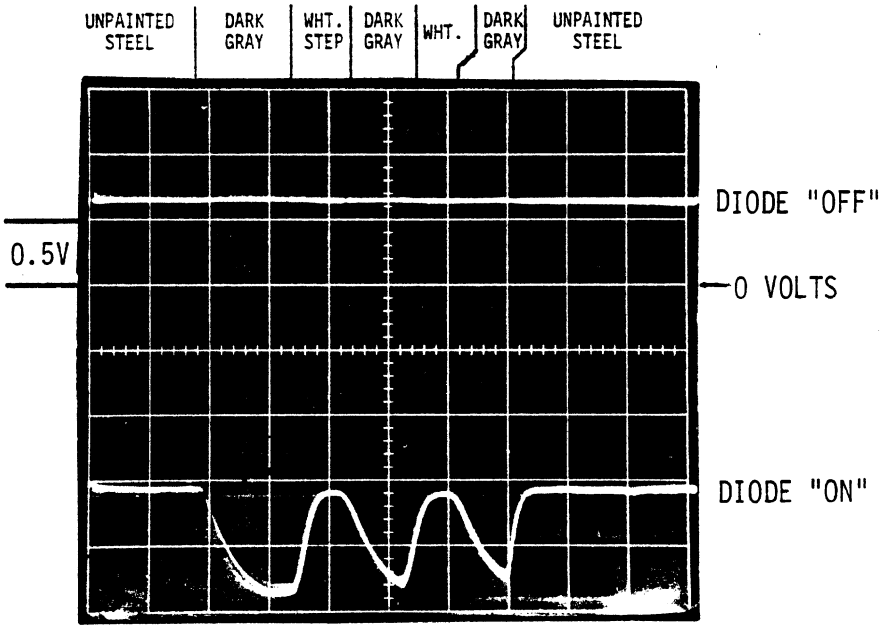


TIME: 0.1 SECOND / DIVISION

15b. Envelope of 5 KHZ switching voltage with AGC on showing AGC response time.

Figure 15. Response of the Automatic Gain Control (AGC) circuit.

oscillographs, with a surface speed of 6 mph. The AGC increases the voltage across the diode, thereby increasing its light output, when the sensor is viewing the dark-gray surface. It then decreases the voltage (and light output) when the steel or white surface is under the sensor. The response time of the AGC circuit is about 0.1 second for increasing the diode voltage and about .05 second for decreasing the diode voltage.

**4.2.1 The Effect of AGC on the Sensor Output.** Oscillographs in Figure 16 allow a comparison of the sensor output in response to the dark-gray/white test pattern on the drum roller, with the AGC on and off, and at surface speeds of 6 and 30 mph. The top trace in these oscillographs is the low level of the IR diode voltage (see figure 15b), and the bottom trace is the sensor output with the sensor at its zero reference height (14 inches). These are the same conditions existing for the center trace in Figure 14a (6 mph) and 14b (30 mph), but in Figure 16 the vertical scale sensitivity is doubled to 0.5 volts (.143 inch) per division, and the signal polarity is inverted in the oscilloscope. Comparing the sensor output traces in Figures 16a and 16b (6 mph), we see that having the AGC on or off results in only a small change in the shape and amplitude of the pulse signals corresponding to the white 0.25 inch high pad and the white 8 inch square surface area. In Figure 16c (30 mph) the waveforms for the AGC on and off are superimposed. Again only a small effect is seen. It will be shown below that the slow acting AGC causes considerable distortion of the individual photocell signals at the higher surface speeds. However, since the sensor output is essentially the same whether the AGC is on or off, it is apparent that the AGC does not directly cause the overshoot on the output signal at the higher speeds.

**4.2.2 The Effect of the AGC on the Photocell Outputs.** The oscillographs in Figure 17 and Figure 18 show the four photocell signals ($E_1$, $E_2$, $E_3$, & $E_4$) as they appear on the test points at the inputs to sum and difference amplifiers (TP9, TP10, TP11, & TP12), with the AGC on and off, and at different surface speeds, while the sensor is viewing the dark-gray/white test surface on the drum roller from the reference height of 14 inches. In Figure 17, the sensor output (top trace) is shown along with only two of the photocell outputs ($E_3$ and $E_4$) in order to help the reader to correlate the changes on the sensor output with the changes on the photocell signals. The

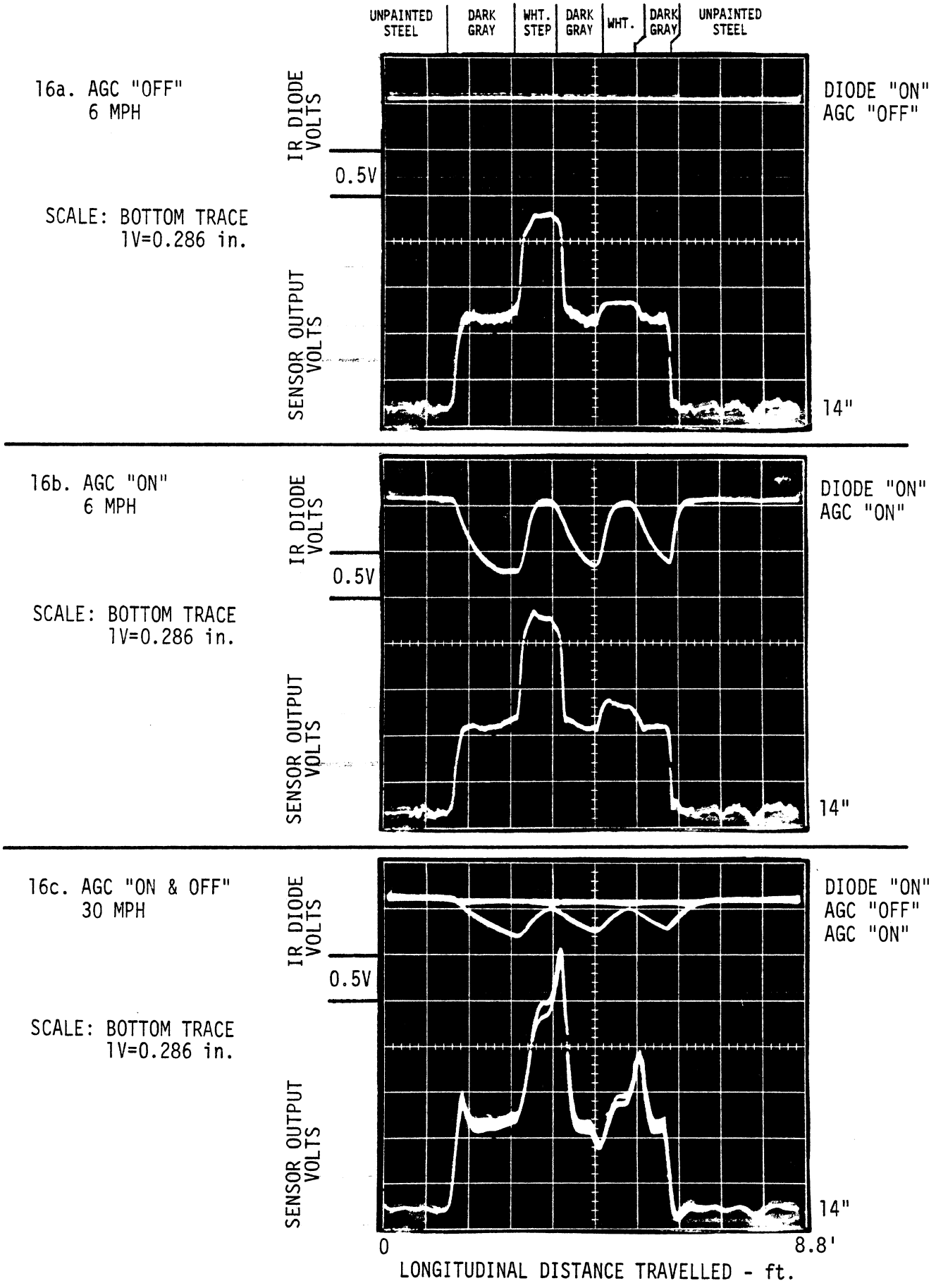


Figure 16. Effect of the Automatic Gain Control (AGC) circuit on the overall sensor response.

17a. AGC "OFF"
30 MPH

SCALE: TOP TRACE
1V=0.286 in.

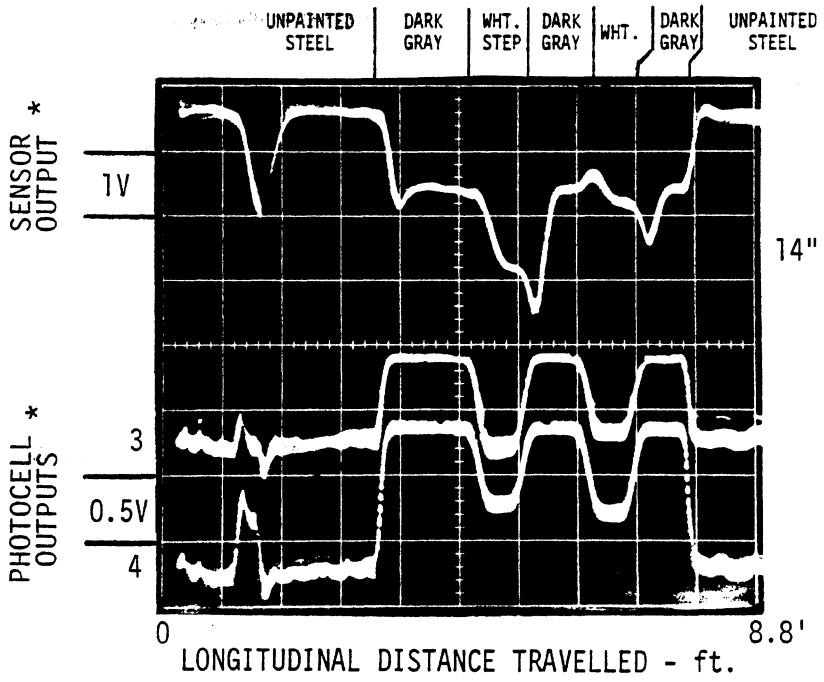


17b. AGC "ON"
30 MPH

SCALE: TOP TRACE
1V=0.286 in.

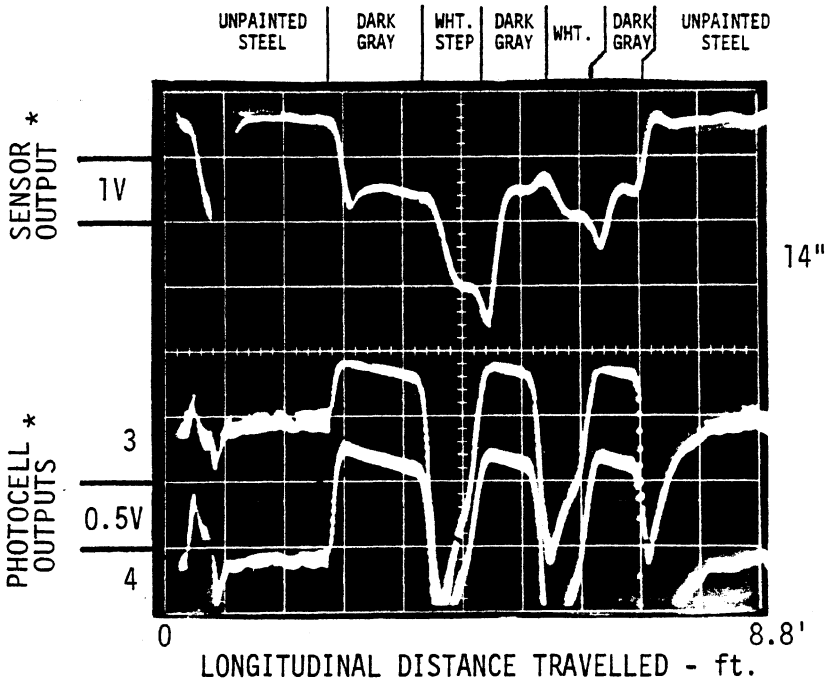


* NOTE: All plots have been shifted vertically, to allow greater oscilloscope sensitivity. Trace amplitudes are relative not absolute.

Figure 17. Effects of the AGC circuit on individual photocell responsesand sensor output.

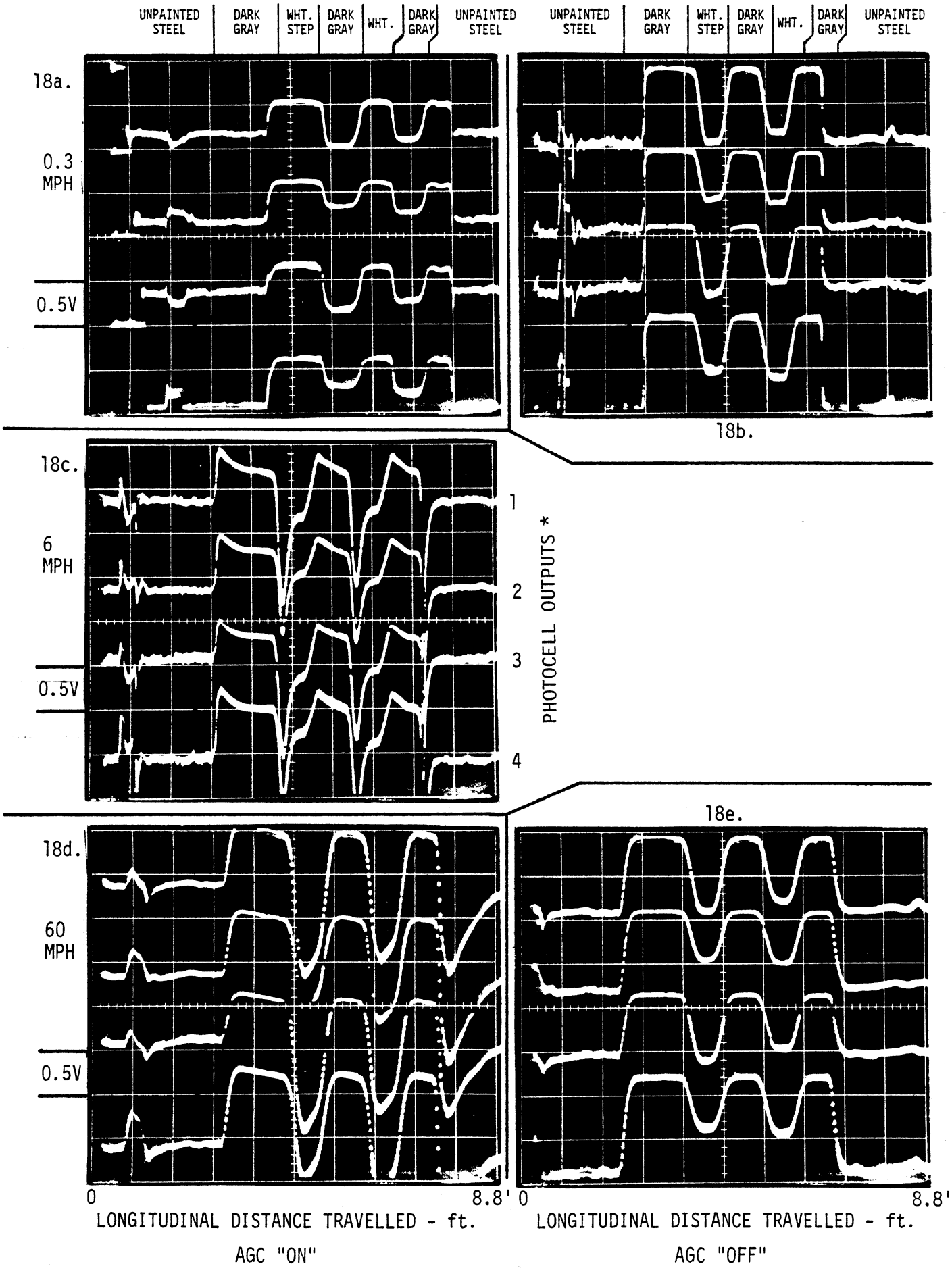


* NOTE: All plots have been shifted vertically, to allow greater oscilloscope sensitivity. Trace amplitudes are relative not absolute.

Figure 18. Dynamic response of the photocells to color and height changes, with AGC on & off.

speed is 30 mph. Figure 17a is with the AGC turned off, and Figure 17b is with the AGC turned on. Note that there is essentially no change in the sensor output waveform when the AGC is switched on and off, while there is a substantial change in the photocell output waveforms. Figure 18 shows that this waveform distortion is a result of the slow acting AGC.

Figure 18 displays all four of the photocell signals for several different speeds. The oscillographs on the left side of the page are with the AGC turned on and those on the right are with the AGC turned off. Comparing the two cases at the very low speed of 0.3 mph, Figures 18a and 18b, the AGC is seen to operate "instantly," reducing the signal level without introducing distortion. However, Figures 18c (6 mph) and 18d (60 mph), show that at the higher surface speeds with the AGC on, the delay in the AGC signal relative to the photocell signals causes considerable distortion of the photocell signals. With the AGC turned off the photocell signals appear to be nearly identical at speeds of 0.3 mph (Figure 18b) to 60 mph (Figure 18e). In Figure 18a, the amplitude of the pulses corresponding to the 0.25 inch height change are larger on the signals E1 and E3 than on the signals E2 and E4, which causes the height pulse output from the sensor seen in the previous oscillographs. On the other hand, the amplitudes of the pulses corresponding to the color change, with no height change, are almost equal and cancel in the difference circuit, thereby producing only the small output change seen in previous oscillographs. Very likely, an Instantaneous Automatic Gain Contol (IAGC) circuit could be incorporated in the sensor (possibly the speed of the present circuit could be sufficiently increased), so that the Automatic Gain Control would not distort the photocell signals at speeds up to 60 mph, just as the present AGC circuit does not distort the signals at very low speeds. Since it was just shown that the distortion of the photocell signals, by the slow action of the AGC, does not significantly influence the dynamic response of the sensor, its incorporation in the sensor is not justified for this reason. However, if the dynamic response problem indeed results from the operation of the photocells over a very large dynamic range, as proposed above, the incorporation of the Instantaneous Automatic Gain Control could yield an improvement in the dynamic performance problem.

## 4.3 The Sum, Difference, and Divider Circuits.

The oscillographs in Figure 19 show the difference amplifier output (top trace), the sum amplifier output (center trace), and the sensor output (bottom trace), with the AGC off, at surface speeds of 6 mph (Figure 19a), 30 mph (Figure 19b), and 60 mph (Figure 19c), and with the sensor at its reference height of 14 inches. Note that the sensor output signal has been inverted in the oscilloscope, consequently its polarity is reversed compared to other oscillographs of the same signal shown previously (Figure 17 for example). As has been shown previously (Figure 14) these oscillographs show an overshoot on the sensor output at the higher speeds, which increases in amplitude with speed. Figures 19b and, particularly Figure 19c, reveal where this overshoot is generated, but not necessarily the cause. In figure 19c a definite time delay can be seen between the sum signal and the difference signal, which results in the overshoot on the output when the signals are divided. However, it is not obvious that the time delay of the difference signal is generated by the difference amplifier. Consider the following:

1. If the time delay is inherent in the difference amplifier we could expect the overshoot on the output to change noticeably because of the signal distortion (change in frequency content) on the input signals when the AGC is turned on. (See Figures 18d and 18e). Such a change is not observed. (See Figure 16c.)

2. The time delay should also occur on the difference signal when there is a height change on the target surface with no color change, and the output should exhibit an overshoot for this condition. It does not. (See Figure 12.)

3. If the difference amplifier is generating the time delay the overshoot should be about the same on the output signals obtained with plus and minus displacements of the sensor from its reference height. This is not the case. (See Figure 14.)

Investigation into the cause of the poor dynamic performance of the IR sensor will be continued only if a decision is made to attempt to apply the

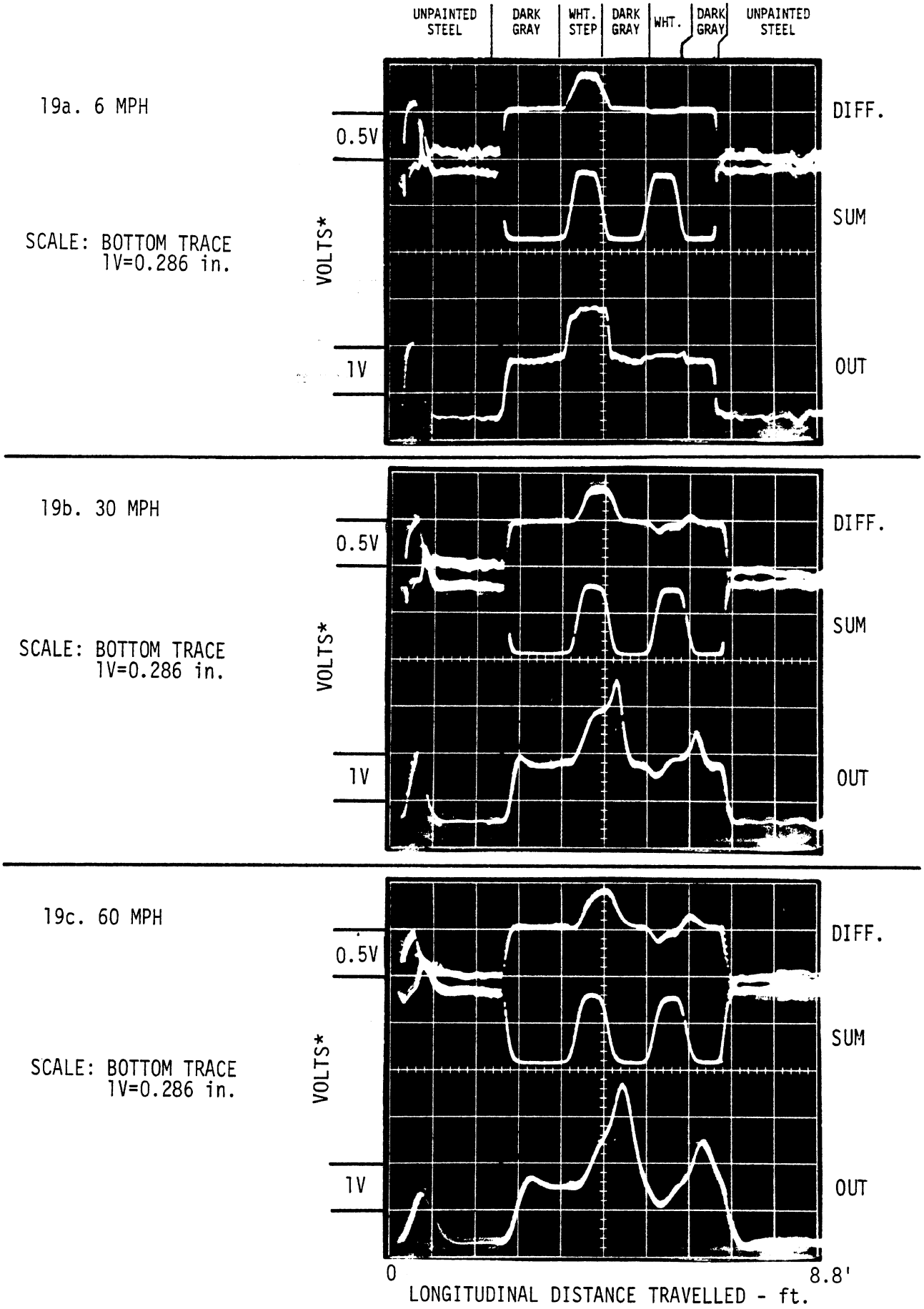


* NOTE: All plots have been shifted vertically, to allow greater oscilloscope sensitivity. Trace amplitudes are relative not absolute.

Figure 19. Sum and difference amplifier outputs and sensor output at three surface speeds.

sensor in the profilometer/rut-depth measurement system, despite its other deficiencies. This decision will be based primarily on the results of quasi-static tests performed on actual road surfaces, which are reported below.

## 5.0 QUASI-STATIC ROAD TEST AND RESULTS

Quasi-static tests of the IR Sensor were performed on a variety of real road surfaces, representative of road surfaces over which the device should operate. In this section, the test procedures and equipment used are described, the road surfaces used in the tests are illustrated, and the data plots obtained are presented. A quick check on the sensor's temperature sensitivity and tilt sensitivity was made, and also is described here.

### 5.1 Instrumentation and Methodology

A test fixture, shown in Figure 20, was designed and fabricated for this purpose. The test fixture consists of an aluminum angle frame with rails, on which a carrier rolls above the pavement. The IR sensor sits on the carrier, oriented either parallel or perpendicular to the direction of travel. Precision spacers permit quick adjustment of the sensor height above the road. A string pot transduces the horizontal motion of the carrier, so that a plot of the indicated road surface height variations, from the IR Sensor, vs horizontal position can be made on an X-Y plotter. The recording equipment, located in the rear of the van used for the road test, can be seen in Figure 20. In order to obtain a plot of the "true road input," the IR Sensor is replaced by a surface follower device, transduced by a string pot. This device is shown in Figure 21. A three inch diameter wheel rests on and follows the surface as the carrier is slowly rolled along the rails.

The results of tests of the IR sensor obtained with this device (that is the X-Y recorder plots), on a variety of road surfaces, are shown in the Figures that follow. A photograph of each test surface is also shown. The plots appearing on the X-Y recorder chart obtained for each road surface are organized as follows (see Figure 23 for an example):

- The uppermost plot is the "true road surface input" as transduced by the road surface follower wheel. The vertical scale is 0.025 inch per small chart division.

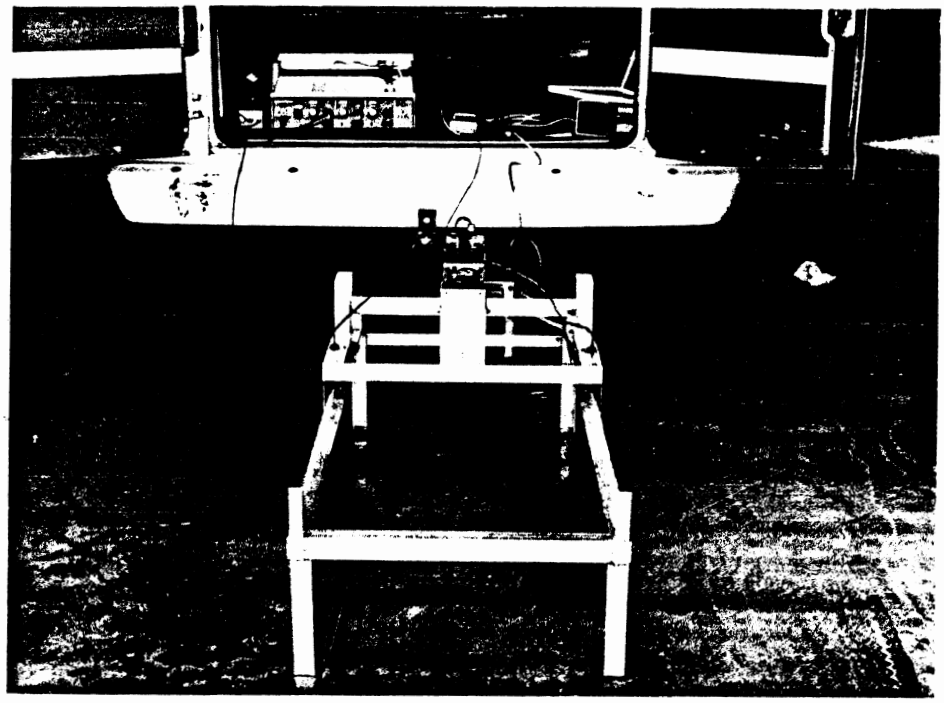

Figure 20. The test fixture used for road tests of the IR Sensor, and the data recording instrumentation.

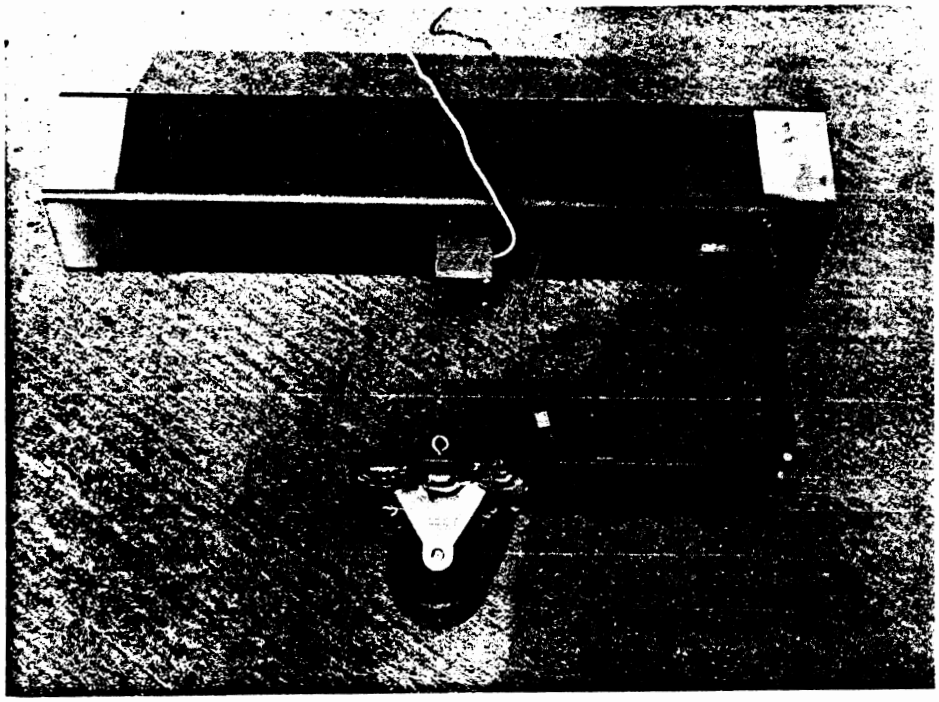

Figure 21. The road follower device used to measure the true road profile.

- The three central plots are the IR sensor output at three heights. The middle sensor-ouput-plot is with the sensor nominally located at its zero output reference height. The other two sensor-output-plots are with the sensor displaced precisely plus one inch (up) and minus one inch (down) from this height. Height changes were made by placing precision spacers between the sensor and the carrier on which it rested. The vertical scale is 0.025 inch per small chart division.

- The two plots at the bottom of the charts are the sensor SUM amplifier output voltage, one with the AGC turned on, and the other with the AGC turned off. These plots show the relative reflectivities of the various test surfaces.

- The horizontal scale of all the plots is 4 inches per major chart division.

## 5.2 Road Test Data.

The road tests agreed with the laboratory test in that: 1) on smooth surfaces with uniform reflectance, the sensor is accurate and linear, within about 0.02 inch, with displacements of the sensor from the reference height up to plus and minus one inch; and 2) surface reflectance variations, due to roughness and/or changes in the overall surface reflectivity, produce significant errors at the sensor output when the sensor is displaced from the reference height. In the worst case measured, a transition from PCC to new asphalt produced a peak error of about 0.5 inches with the sensor displaced either plus or minus one inch from its reference height. Similarly, an oil spot produced an error of 0.23 inch; cracked asphalt, an error of 0.2 inch; a yellow marker stripe, an error of 0.35 inch; a tar joint in PCC, an error of 0.45 inch; and an old surface treated, but smooth surface, produced an error of 0.13 inch. The wavelength of these errors is typically two to eight inches. Because of the amplitude and asymmetry of the error waveform it may be impossible to filter the signal so as to achieve accurate profile measurements for wavelengths shorter than one and possibly two feet.

Unless noted otherwise, all of the sensor output plots were made with the sensor moving in the direction of its long axis, and with the AGC turned on. The SUM amplifier output plot, with the AGC turned off, was made to show the relative magnitudes of surface reflectivities.

**Painted Concrete.** A smooth painted concrete test surface (laboratory floor), is pictured in Figure 22. The data plots for this surface are shown in Figure 23. Color variations in the surface account for the slight ripple on the sensor output plots for plus and minus one inch displacement. Over this range, the sensor is in agreement with the surface follower within about 0.025 inches. Because the SUM amplifier ouput is the sum of the outputs of all four photocells, it does not show the same ripple frequency that appears on the sensor output.

**Color Test Pattern.** Figure 24 shows a smooth dark-gray, light-gray, white test pattern, which was painted with the same colors used in the laboratory test described previously. Plots obtained with this test surface are shown in Figure 25 and Figure 26. Figure 25 is with the sensor moving in the direction of its long axis, and Figure 26 is with the sensor moving in the direction of its short axis, that is, the orientation shown in Figure 24. These tests were made for comparison with the previous laboratory test, and the results are seen to be essentially the same as in those tests (see figures 9 and 10).

**Oil Spot on PCC.** A "natural" oil spot on a PCC surface is shown in Figure 27. Figure 28 shows the sensor outputs for this surface condition. At the reference height the sensor ouput agrees with the surface follower measurement within 0.025 inch, but with the sensor displaced from this height by plus or minus one inch, the sensor ouput has a peak error of 0.23 inch

**Old Cracked Asphalt.** Figure 29 shows an old and cracked asphalt road surface with moisture in the cracks. The sensor output, shown in Figure 30, has a maximum error of about 0.2 inch. The surface "texture" shown by the IR sensor at the reference height is different from that shown by the surface follower because the sensor tends to average over the illuminated area. The chalk marks seen on the surface were made after obtaining the sensor output

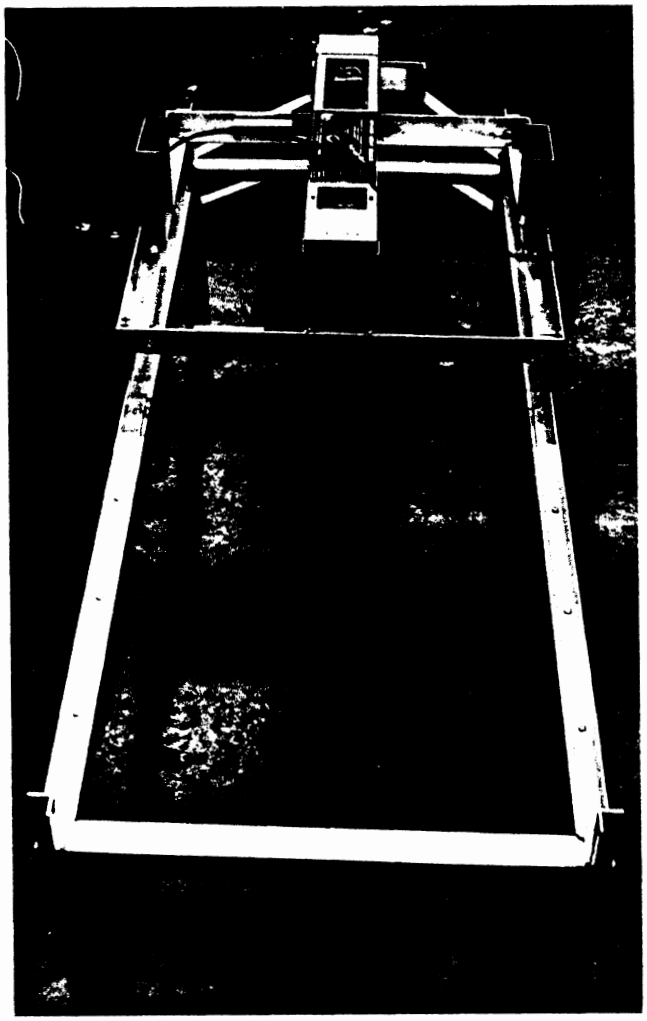

Figure 22. The concrete (laboratory floor) test surface for the plots appearing in Figure 23.

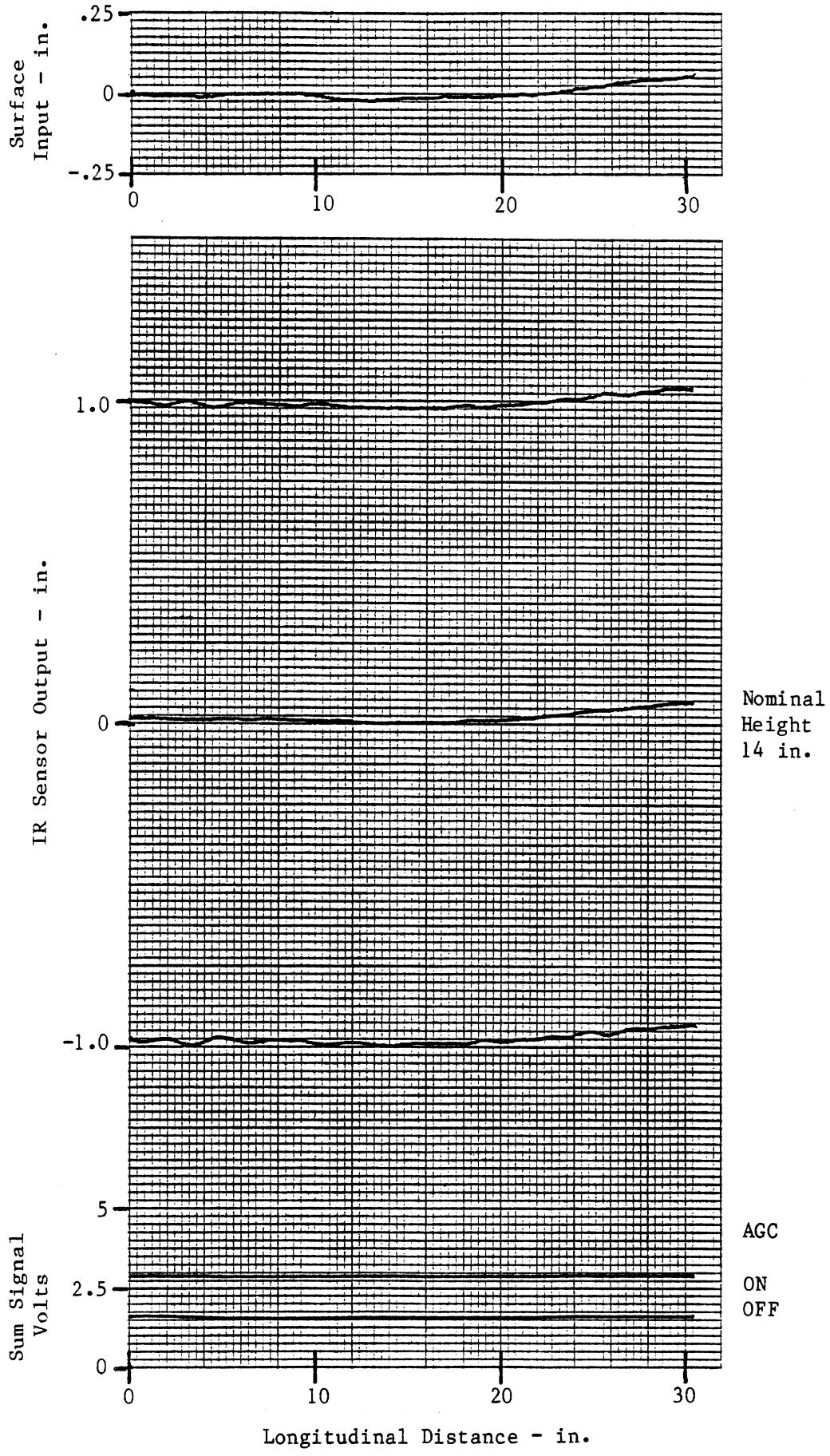


Figure 23. The IR Sensor response on the smooth concrete surface shown in Figure 22.

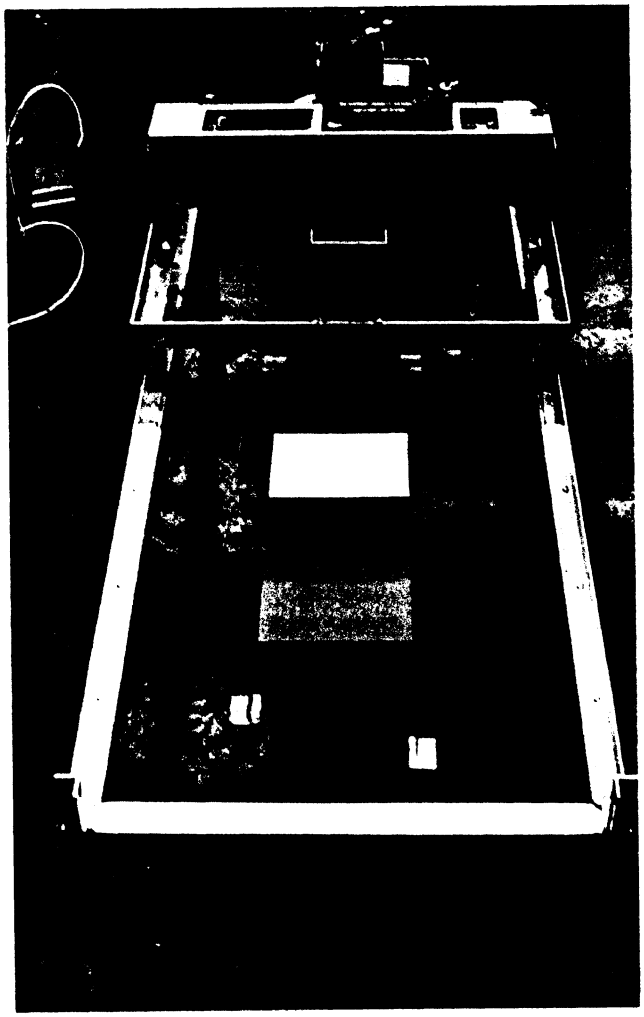

Figure 24. A dark-gray, light-gray, and white test surface for the plots appearing in Figures 25 and 26.

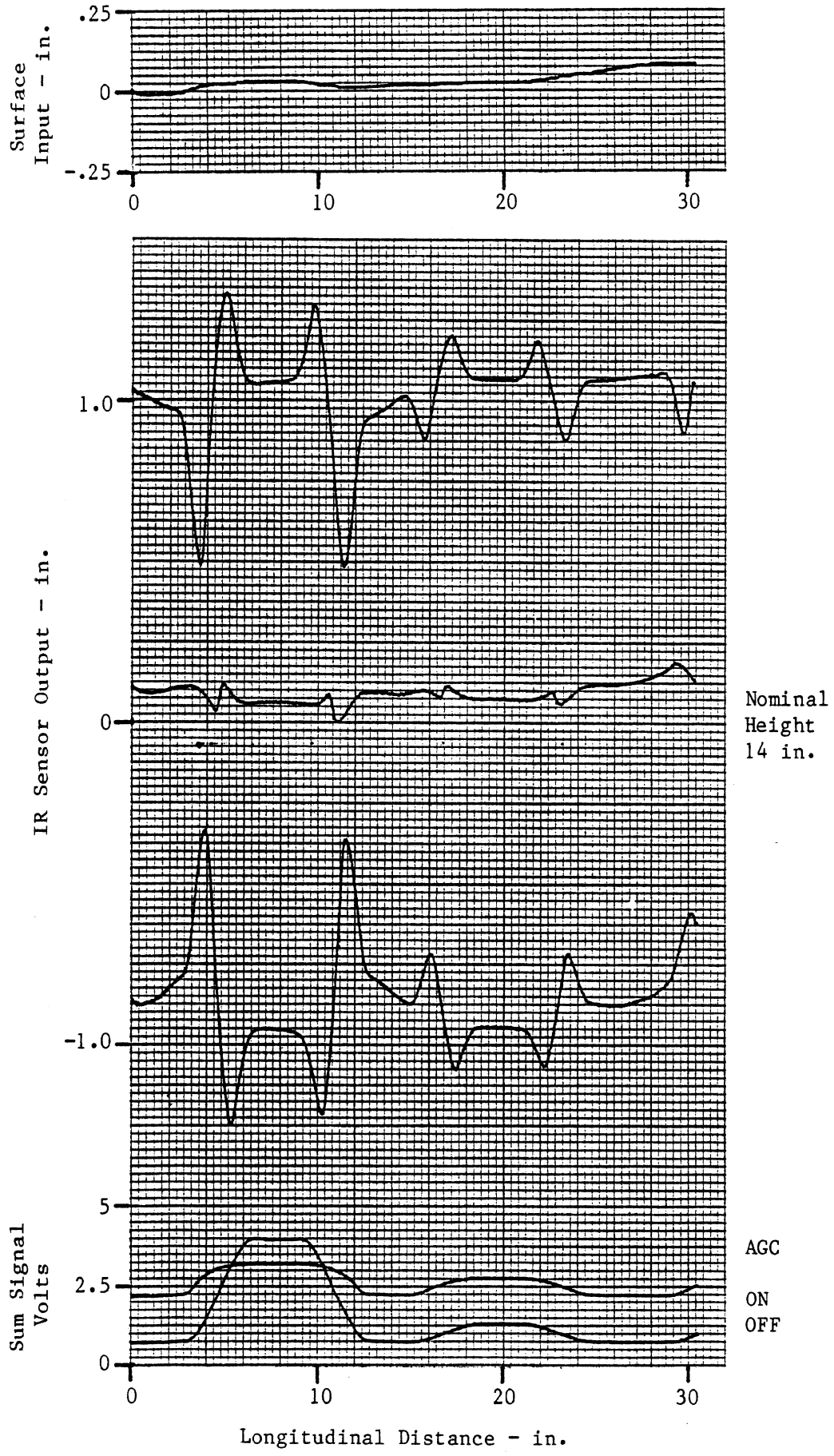


Figure 25. The IR Sensor response on the dark-gray, light-gray, and white test surface shown in Figure 24. The Sensor was moved in the direction of its long axis.

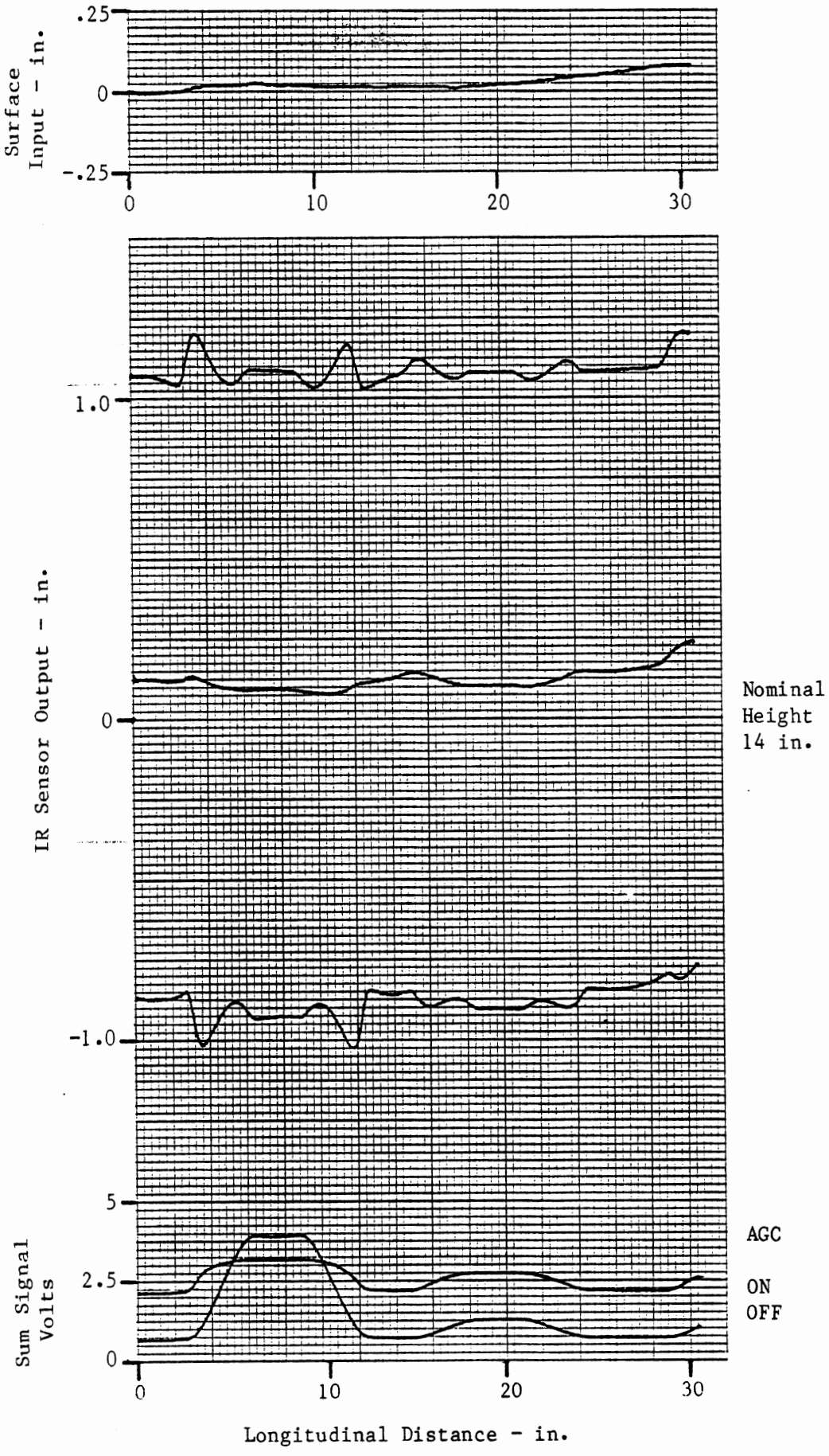


Figure 26. The IR Sensor response to the dark-gray, light-gray, and white test surface shown in Figure 24. The Sensor was moved in the direction of its short axis.

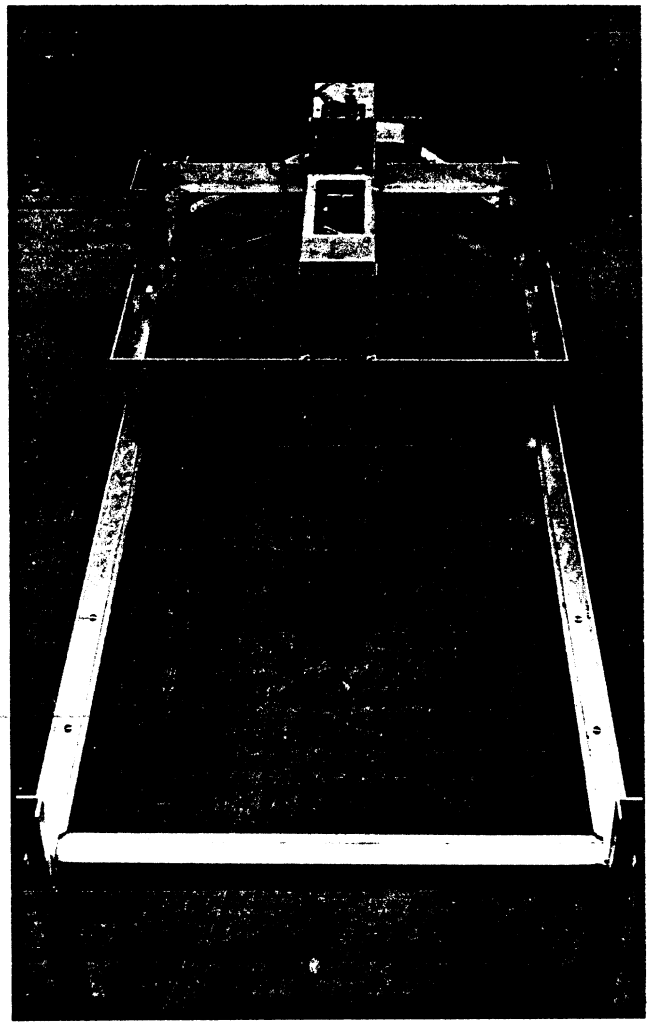

Figure 27. PCC with an oil spot, the test surface used for the plots appearing in Figure 28.

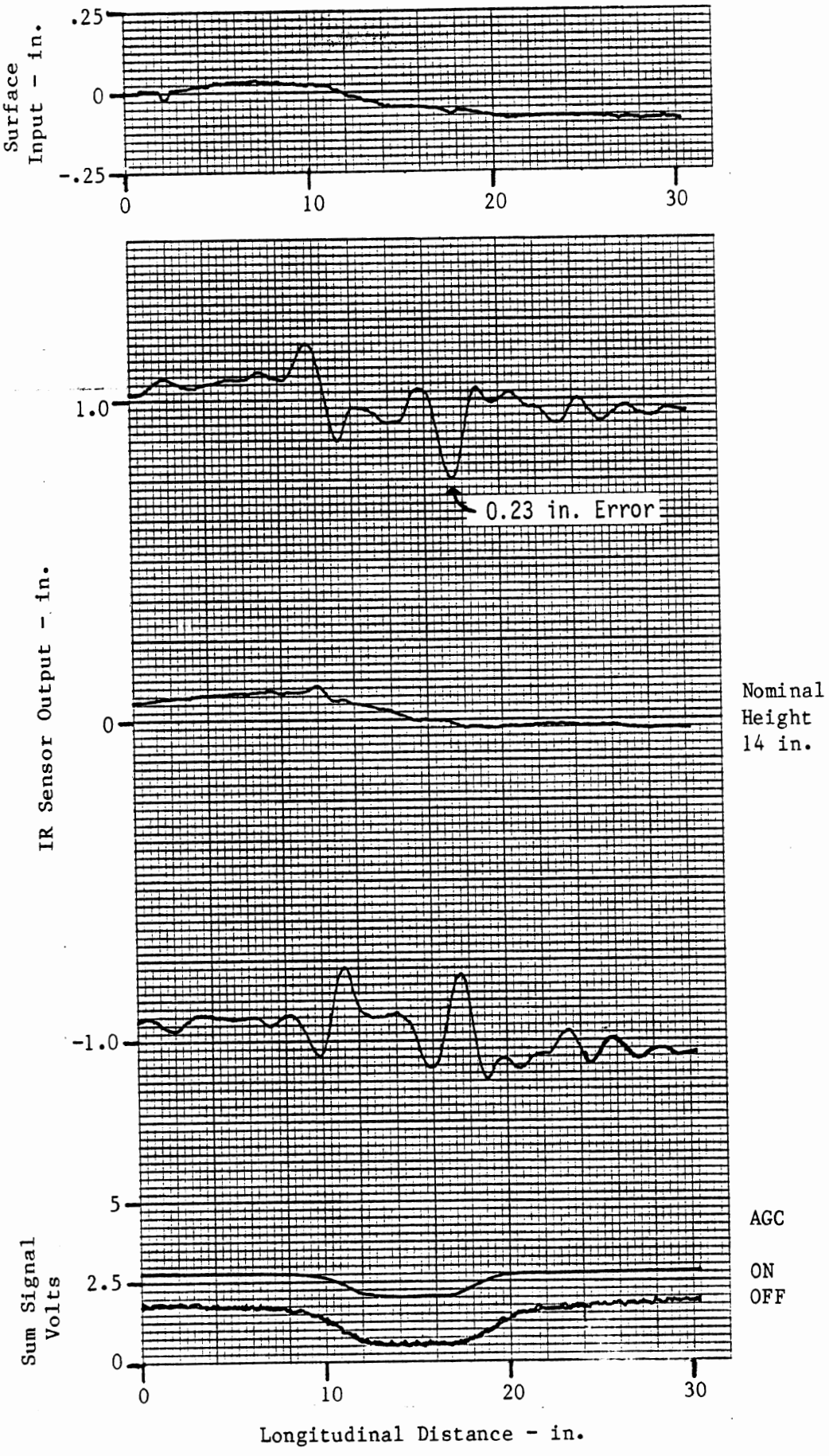


Figure 28. The IR Sensor response to an oil spot on PCC. The surface is shown in Figure 27.

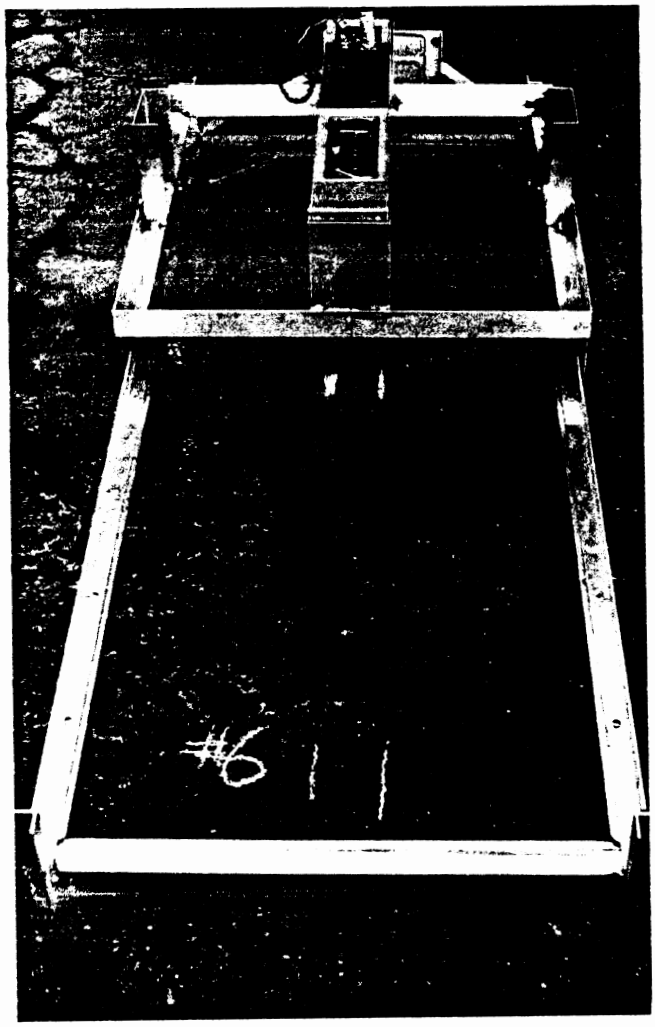


Figure 29. Old and cracked asphalt, the test surface for the plots appearing in Figure 30.

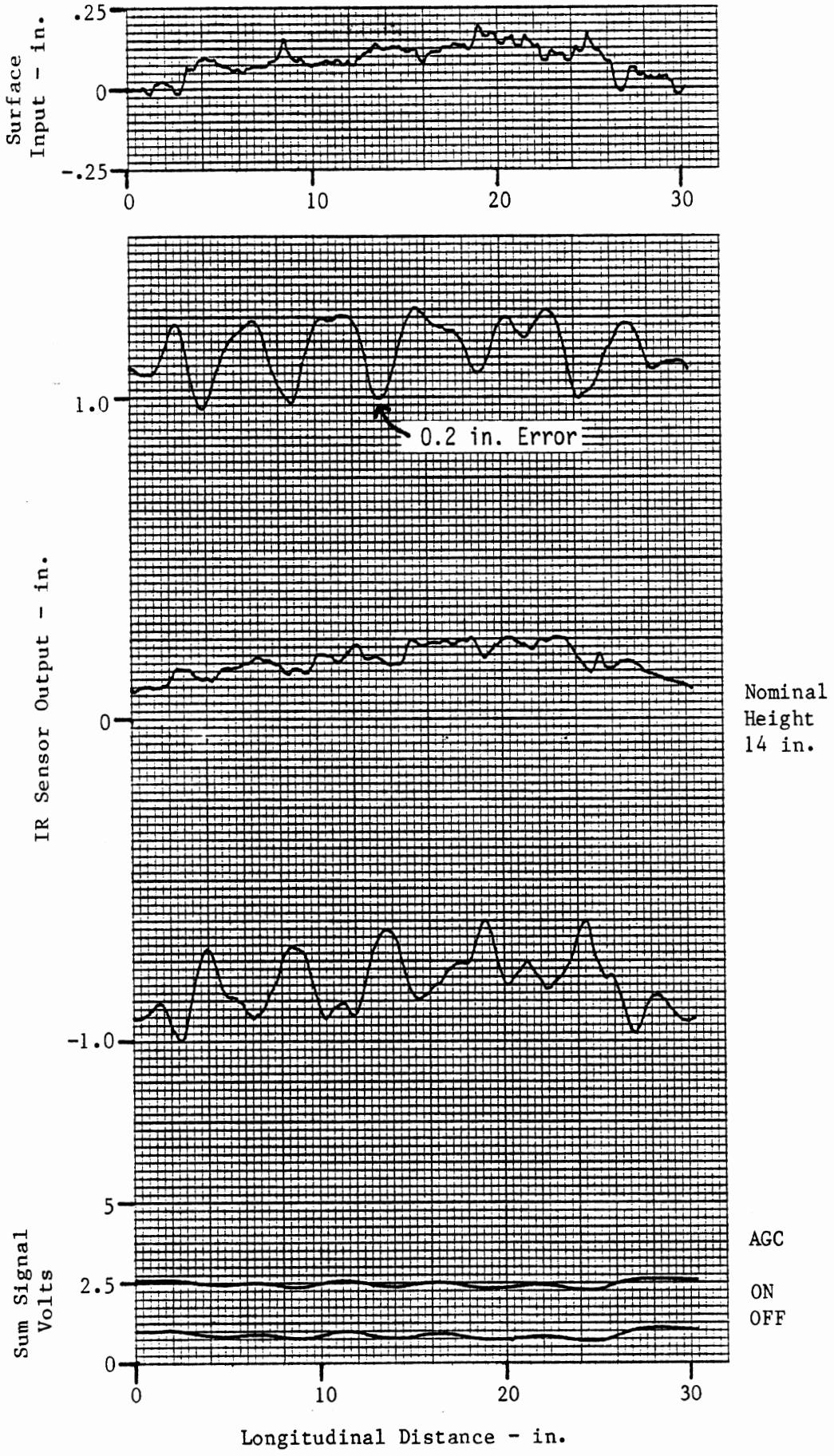


Figure 30. The IR Sensor response to the old, cracked asphalt surface in Figure 29.

plots. These marks indicate the area scanned by the sensor.

**A Yellow Marker Stripe on Old Asphalt.** A test surface of old, but fairly smooth, asphalt with a yellow painted marker stripe is shown in Figure 31. This surface produces a maximum sensor error of about 0.35 inch, as seen in Figure 32. At the reference height the error is about .025 inch.

**Dry PCC and Wet PCC.** Figure 33 shows a fairly smooth PCC surface with a very thin film of water on one half of the test section. The data plots are shown in Figure 34. On the dry PCC the sensor output agrees with the surface follower measurement within about 0.025 inch, however on the wet PCC all three sensor output plots have a slight bias of about .025 inch in the positive direction compared with the surface follower. The SUM amplifier output, with the AGC turned off, shows only a very small change in the overall reflectivity between the dry and wet surface, indicating the shift on the sensor output may be due to a change in the directional reflectivity of the surface when wet compared to dry. During the transition from the dry to wet surface a peak error of about 0.08 inch occurs.

**Surface Treatment.** The surface shown in Figure 35 is characteristic of an asphalt surface with surface treatment. As shown by the surface follower output in Figure 36, the surface is quite smooth, however it exhibits significant variations in reflectivity, which can be seen in the photograph, and which is in evident on the SUM amplifier output. This reflectivity variation results in a maximum error of about 0.13 inch.

**A Pebbled Surface.** The photograph in Figure 37 shows a stone/asphaltic surface where the binder is eroded leaving a pebbled surface. The roughness of this surface is shown by the surface follower plot in Figure 38. At the reference height the IR sensor indicates a smoother than actual surface, and when displaced plus or minus one inch, the sensor output indicates only a slightly rougher texture than does the surface follower.

**Grooved PCC.** This surface, which is pictured in Figure 39, is PCC with small grooves running perpendicular to the direction of the sensor travel. As seen from the plots in Figure 40, the IR sensor output is in

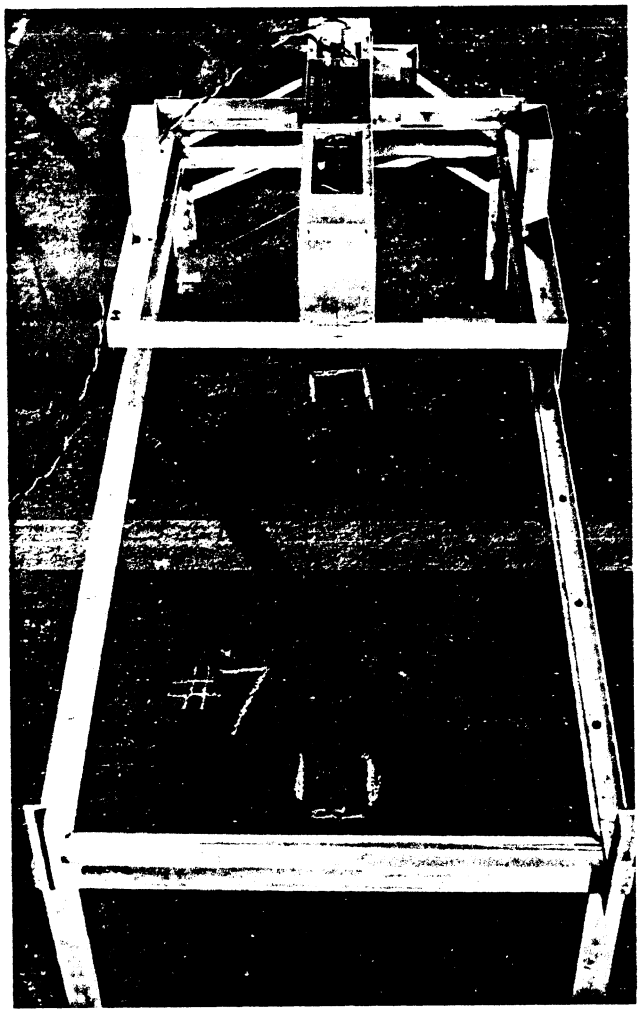


Figure 31. Old asphalt with a yellow stripe, the test surface for the plots appearing in Figure 32.

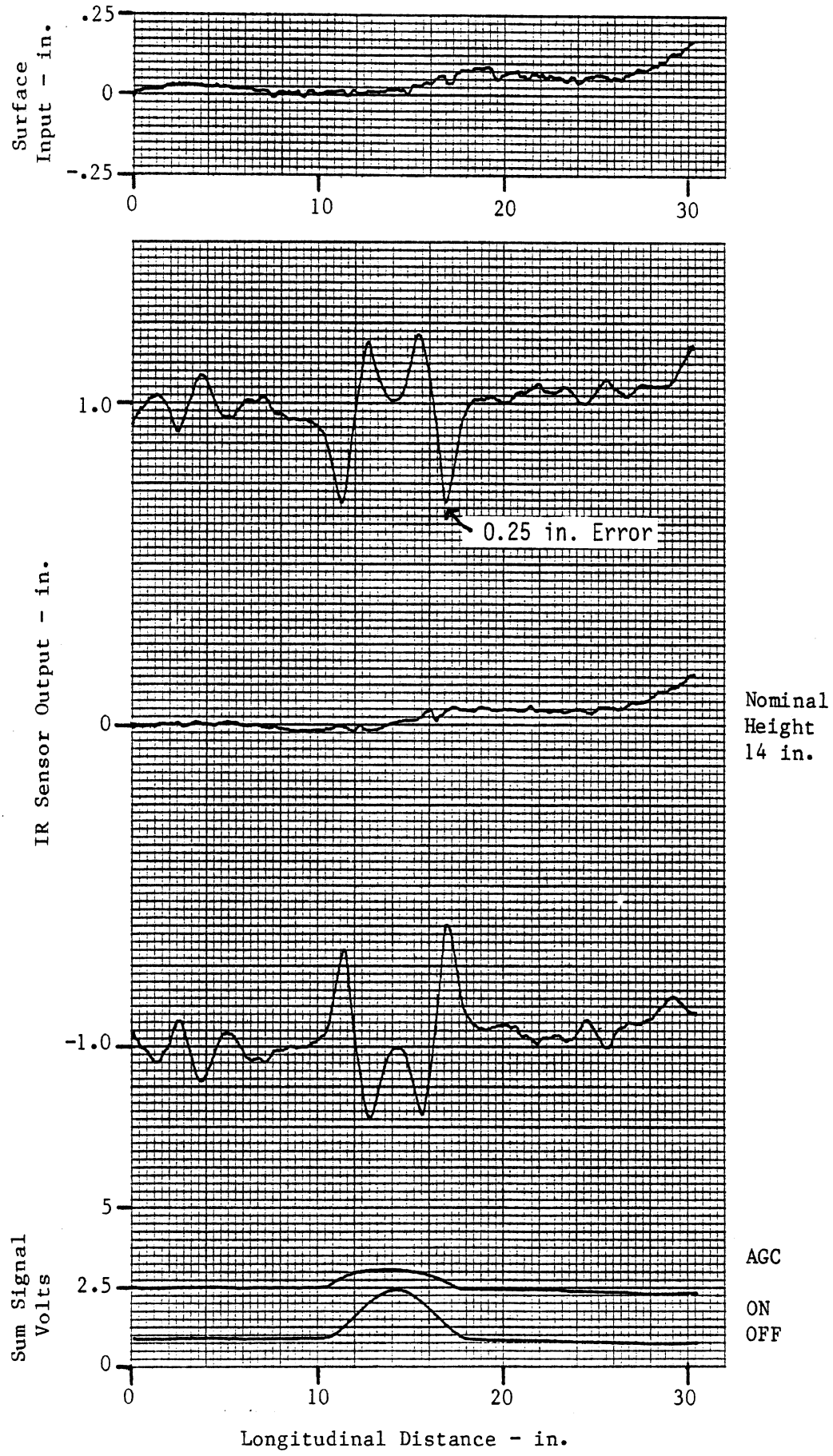


Figure 32. The IR Sensor response to a yellow marker stripe on old asphalt. The surface is shown in Figure 31.

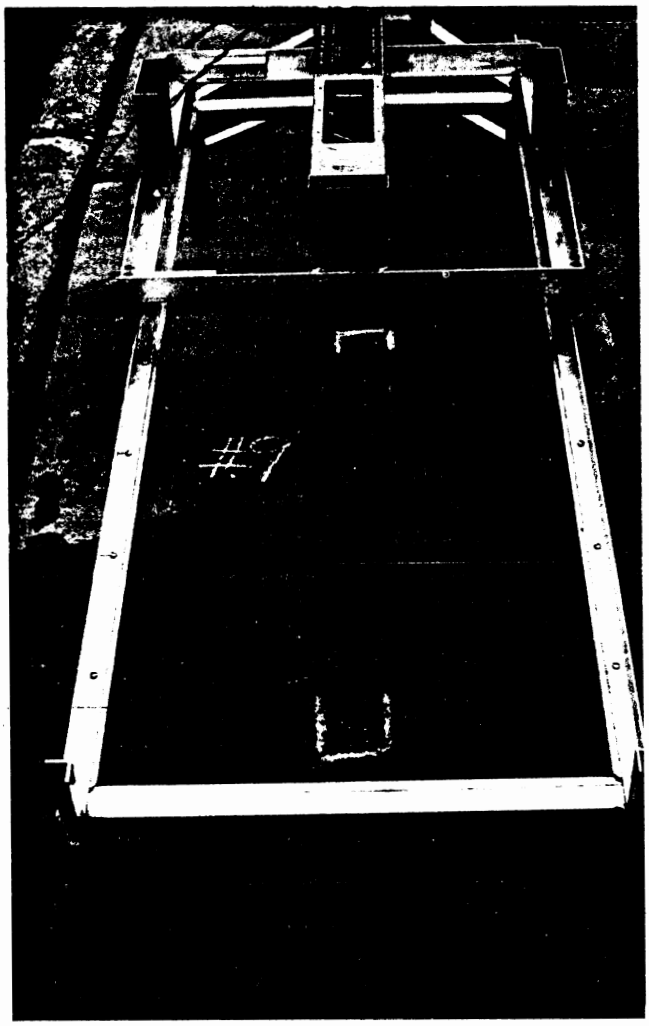


Figure 33. Dry and wet PCC, the test surface for the plots appearing in Figure 34.

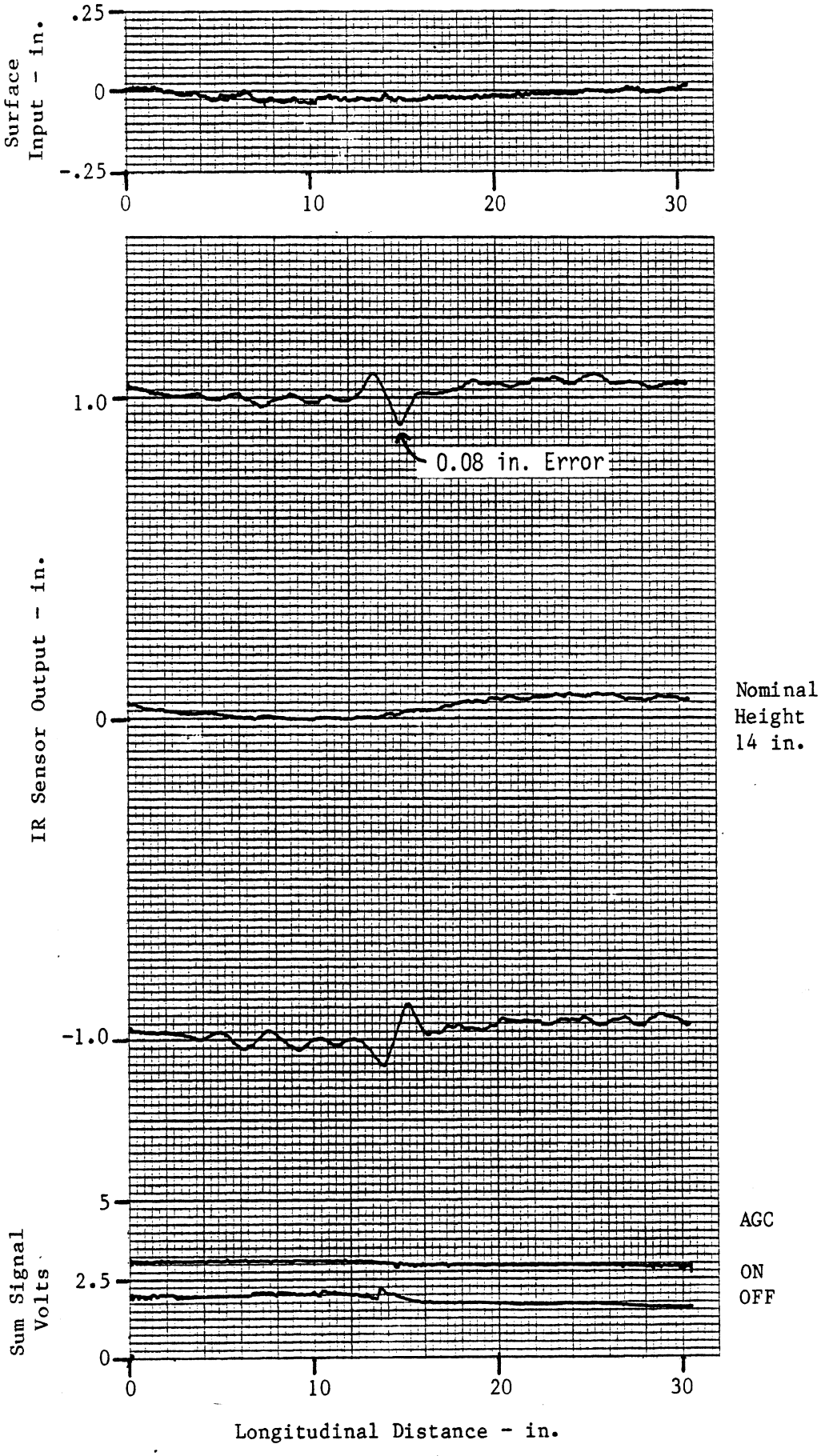


Figure 34. The IR Sensor response to dry and wet PCC. The surface is shown in Figure 33.

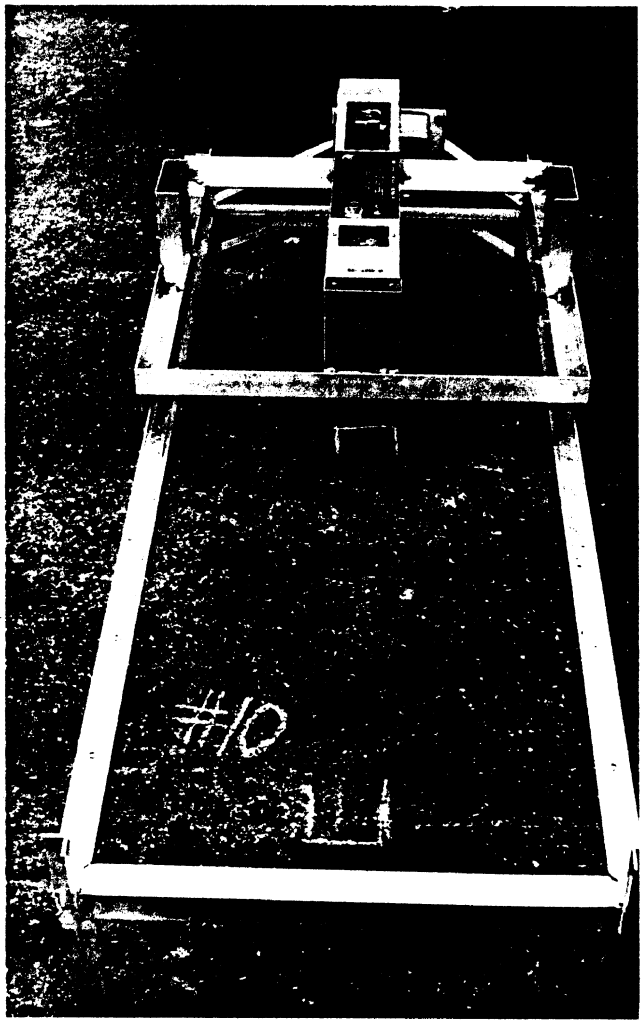


Figure 35. Surface treated asphalt, the test surface for the plots appearing in Figure 36.

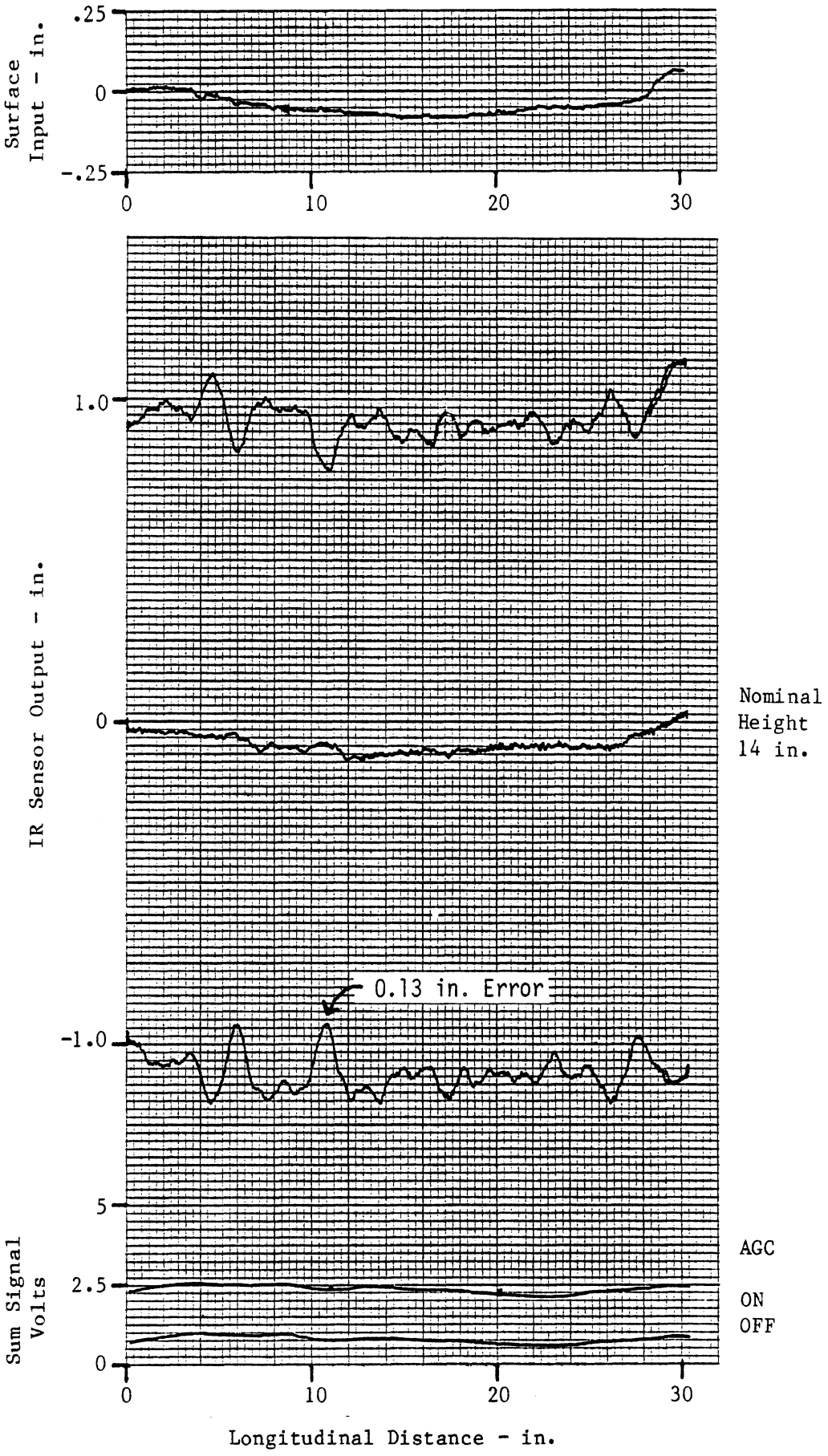


Figure 36. The IR Sensor response to surface treated asphalt. The surface is shown in Figure 35.

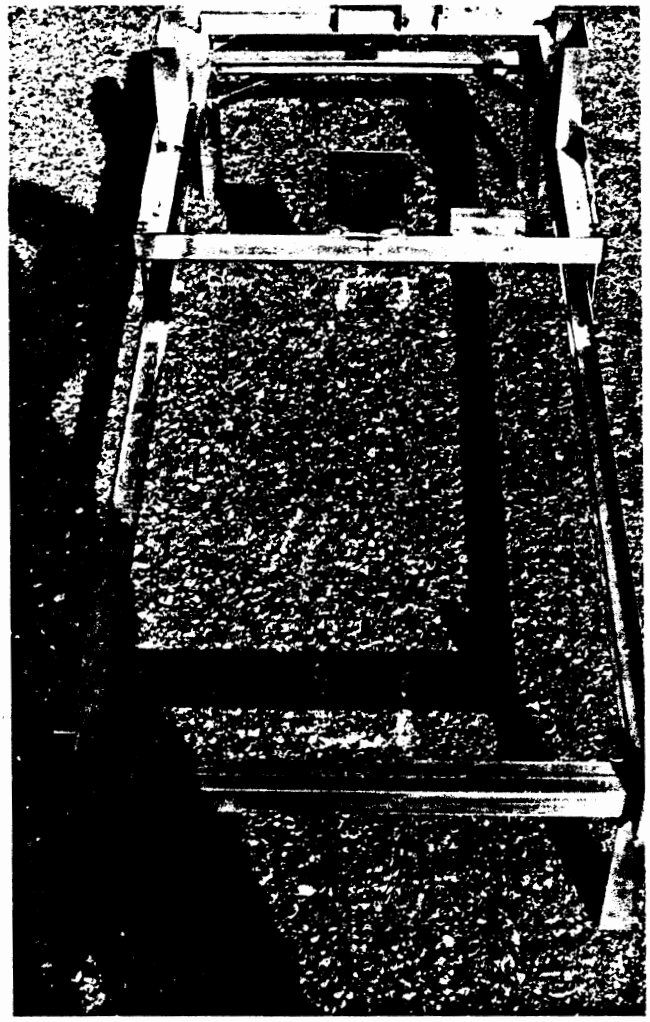

Figure 37. Pebbled test surface for the plots appearing in Figure 38.

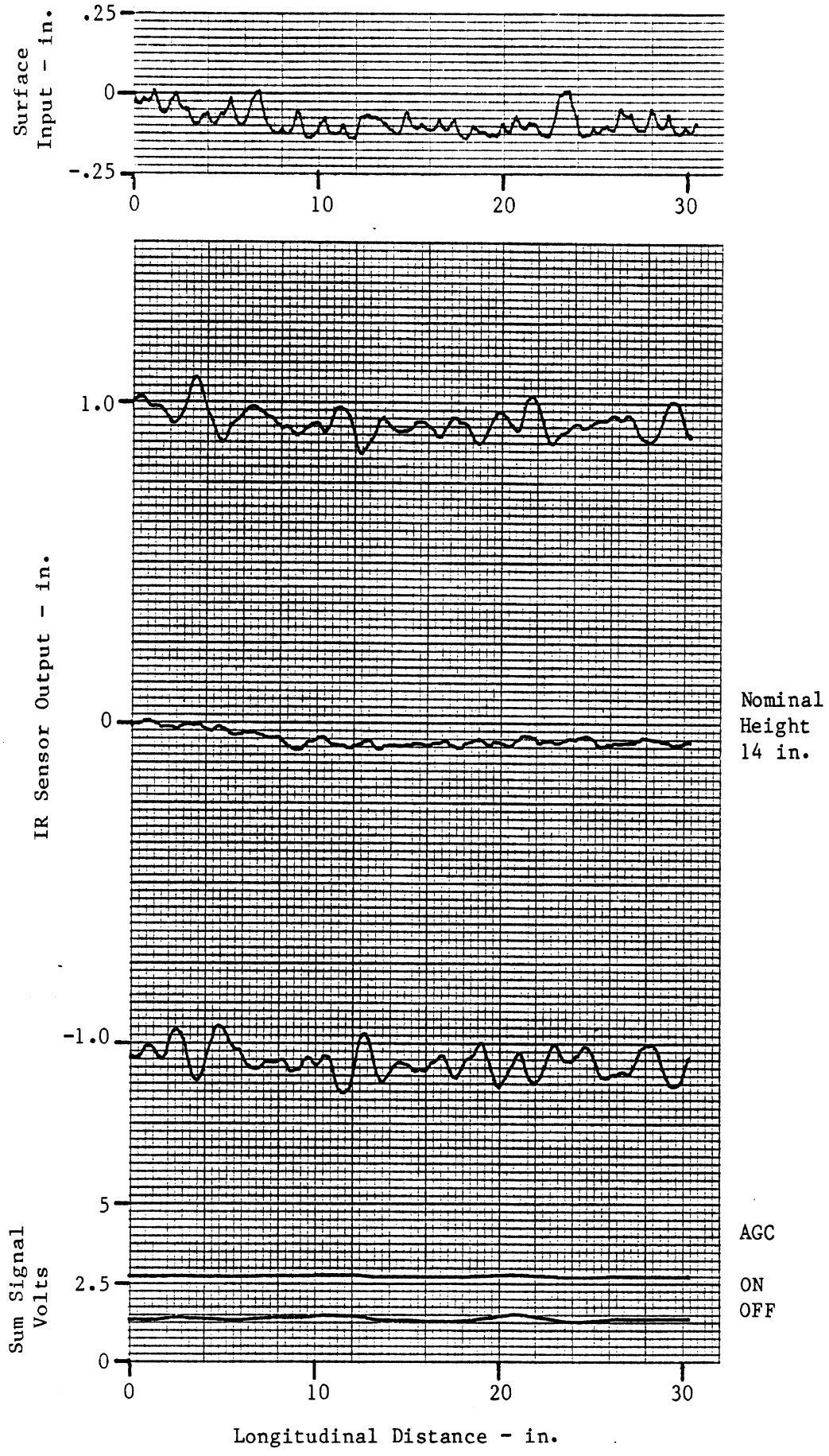


Figure 38. The IR Sensor response to a pebbled surface. The surface is shown in Figure 37.

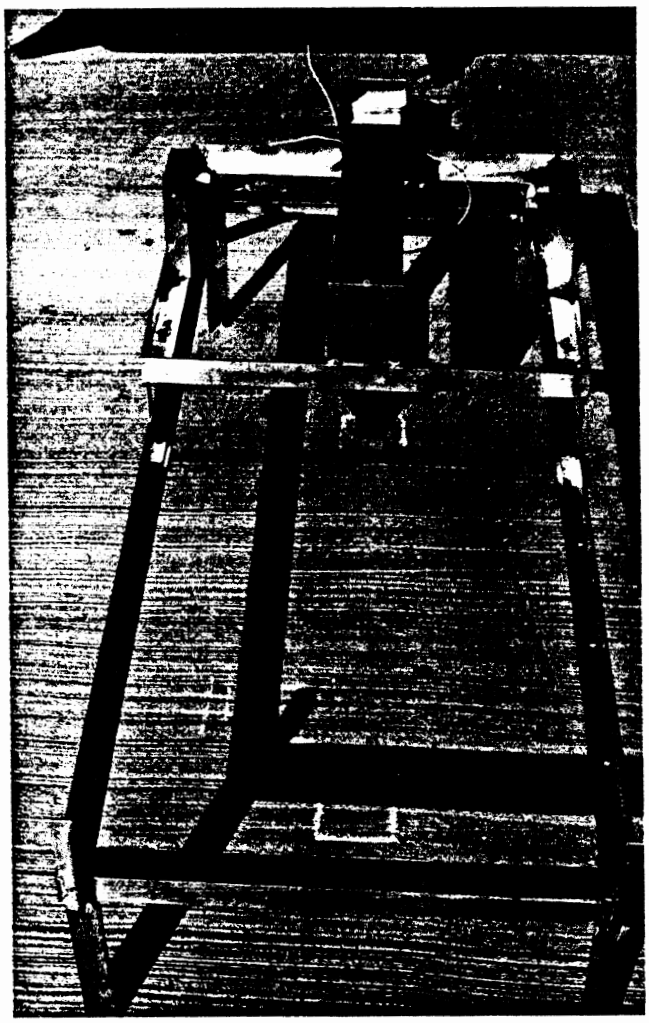

Figure 39. Grooved PCC, the test surface for the plots appearing in Figure 40.

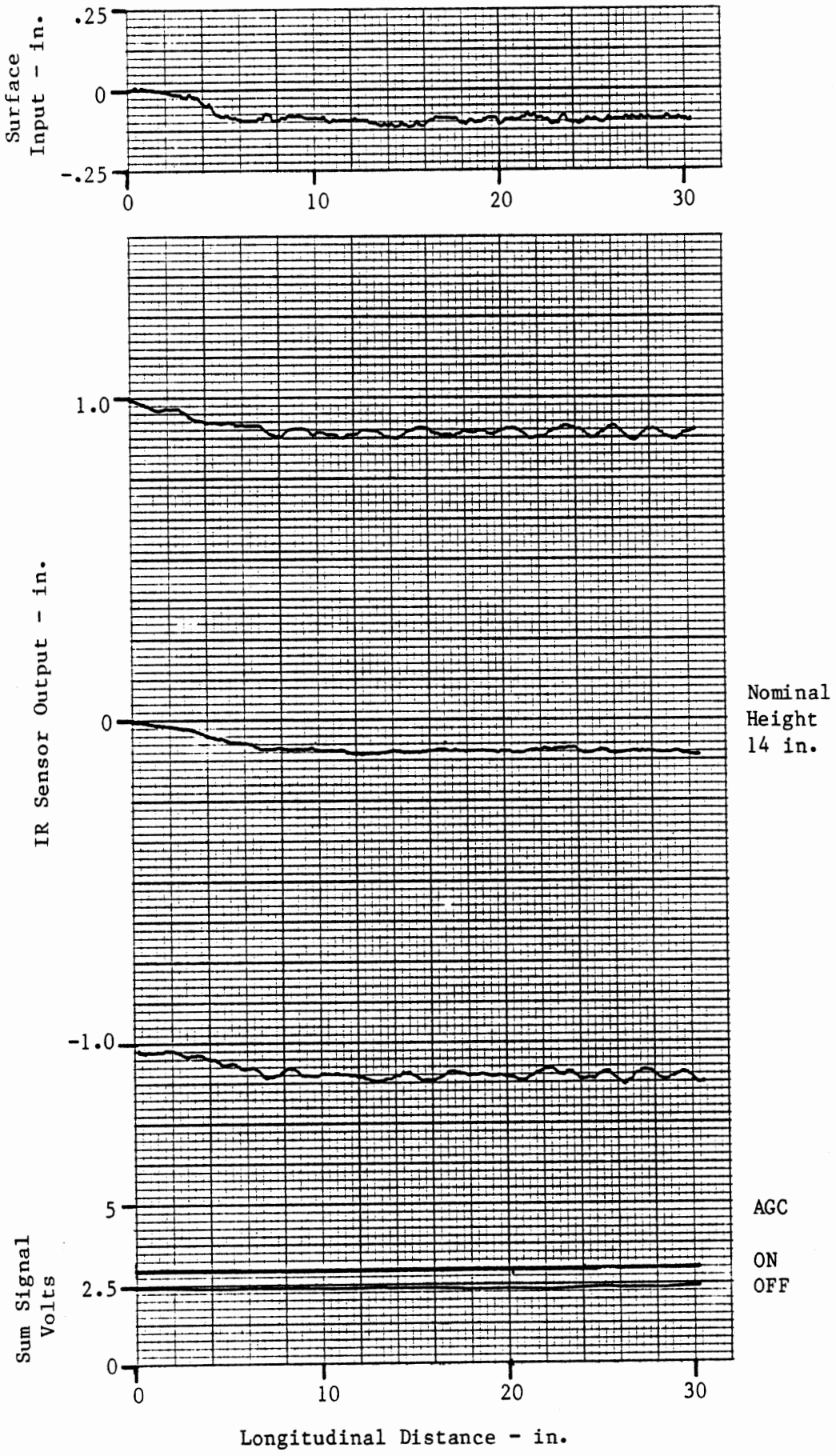


Figure 40. The IR Sensor response to grooved PCC. The surface is shown in Figure 39.

agreement with the surface follower measurement within about 0.025 inch at all three sensor heights.

**PCC With a Tar Joint.** A tar joint, two to three inches wide, between two slabs of PCC is shown in Figure 41. The plots shown in Figure 42 reveal a maximum error on the sensor output, as the sensor passes over the tar joint, of 0.45 inch. While the surface has an overall height variation of about .23 inch, on each side of the tar strip, the sensor output agrees with the surface follower height indication within 0.025 inch at all three sensor heights.

**PCC to Asphalt Transition.** Figure 43 shows a junction between a slab of PCC and an asphaltic surface layed over PCC. The data from this surface is plotted in Figure 44. Except at the junction of the two surfaces and with the sensor displaced from the reference height, the sensor output and the surface follower indication match within about 0.025 inch. The maximum error during the transition is about 0.25 inch. The SUM amplifier output shows that the difference in reflectivity between the PCC and the asphalt is very small in this case.

**A Manhole Cover.** The response of the sensor while passing over the manhole cover shown in Figure 45 was surprisingly good. As seen in Figure 46, when the the short wavelength ripple on the curves is smoothed, the sensor output is in agreement with the surface follower output within about 0.05 inch.

**A Worst Case Reflectance Change.** In order to simulate an extreme reflectance change, representing a junction between new PCC and new asphalt (a live example could not be found in the area), a section of light colored PCC was coated with a black asphalt surface coating. This test patch is shown in Figure 47. Comparing the SUM amplifier output for this surface, shown in Figure 48, with the SUM amplifier output for the dark-gray/ white test patches, shown in Figure 25, (with the AGC off) the reflectance of the asphalted area is seen to be less than that of the dark-gray test surface used in the laboratory tests, and the reflectance of the light PCC surface also is less than the reflectance of the white test surface. Since it seems only

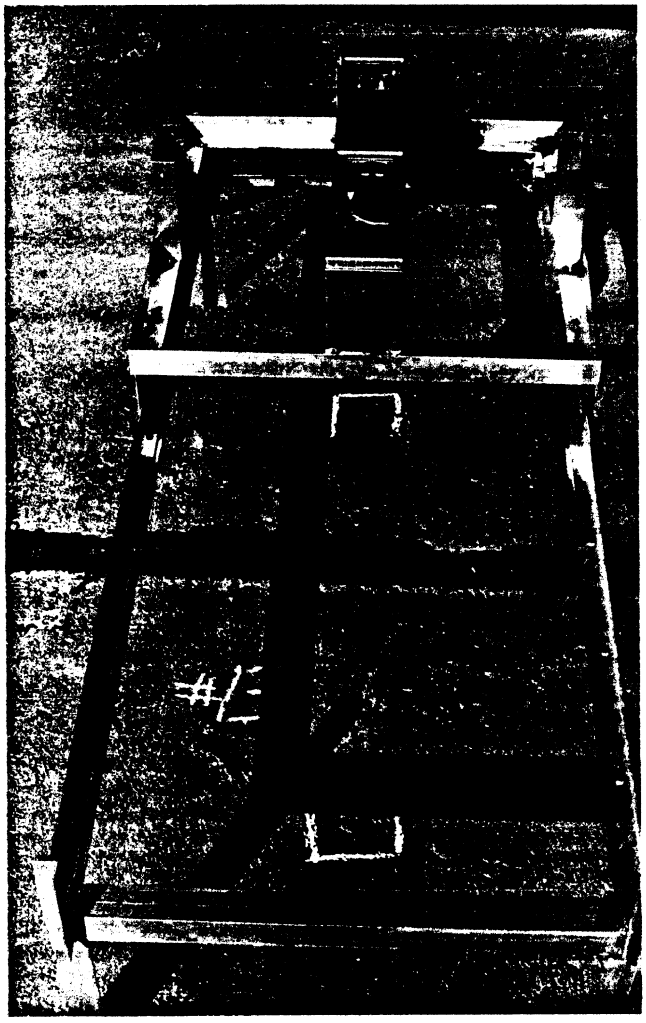

Figure 41. PCC with a tar joint, the test surface for the plots appearing in Figure 42.

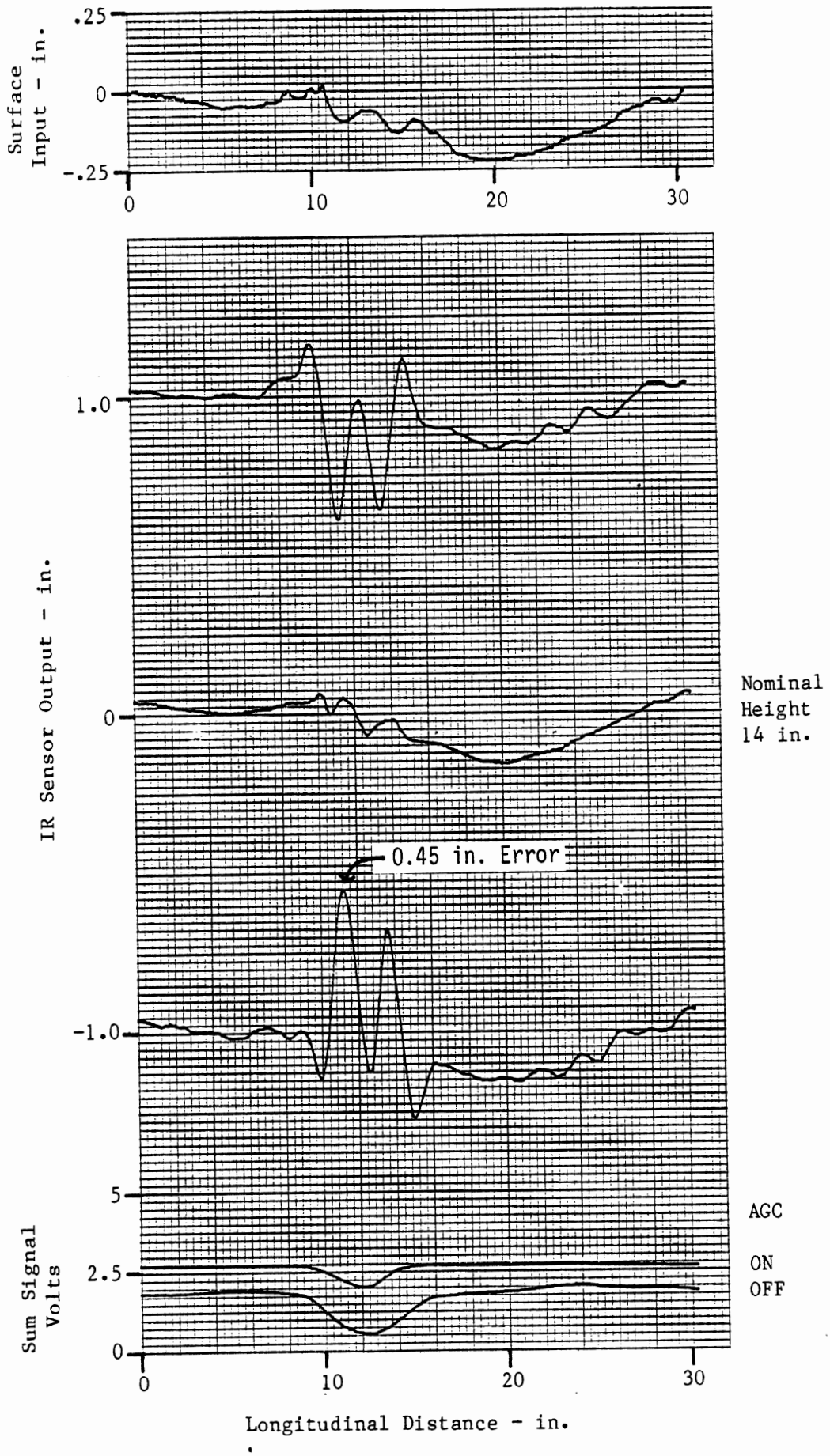


Figure 42. The IR Sensor response to a tar joint in PCC. The surface is shown in Figure 41.

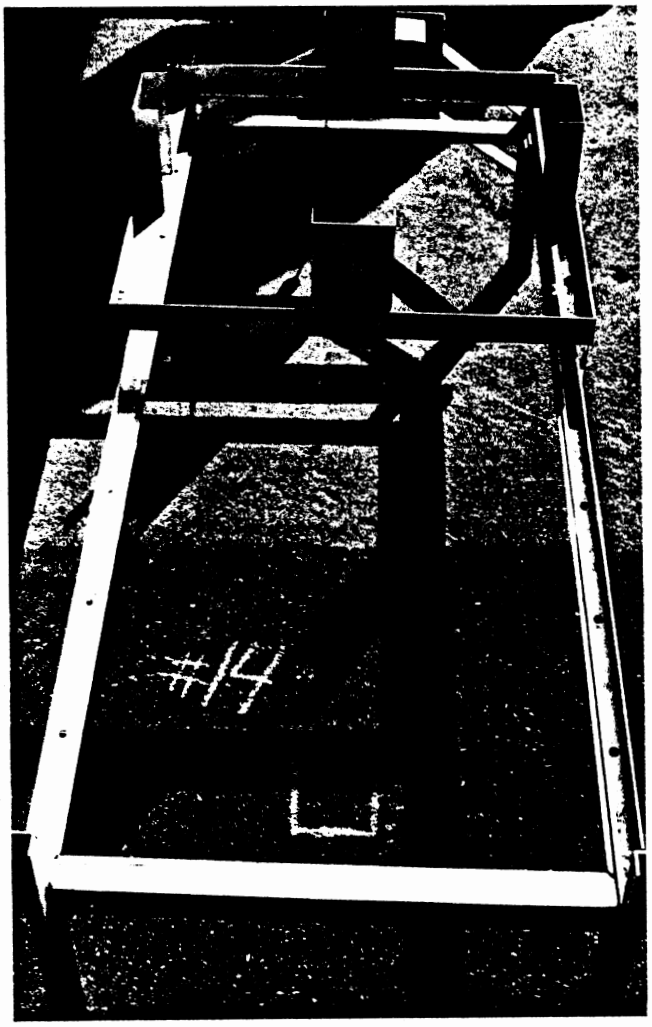


Figure 43. Junction between PCC and old asphalt, the test surface for the plots appearing in Figure 44.

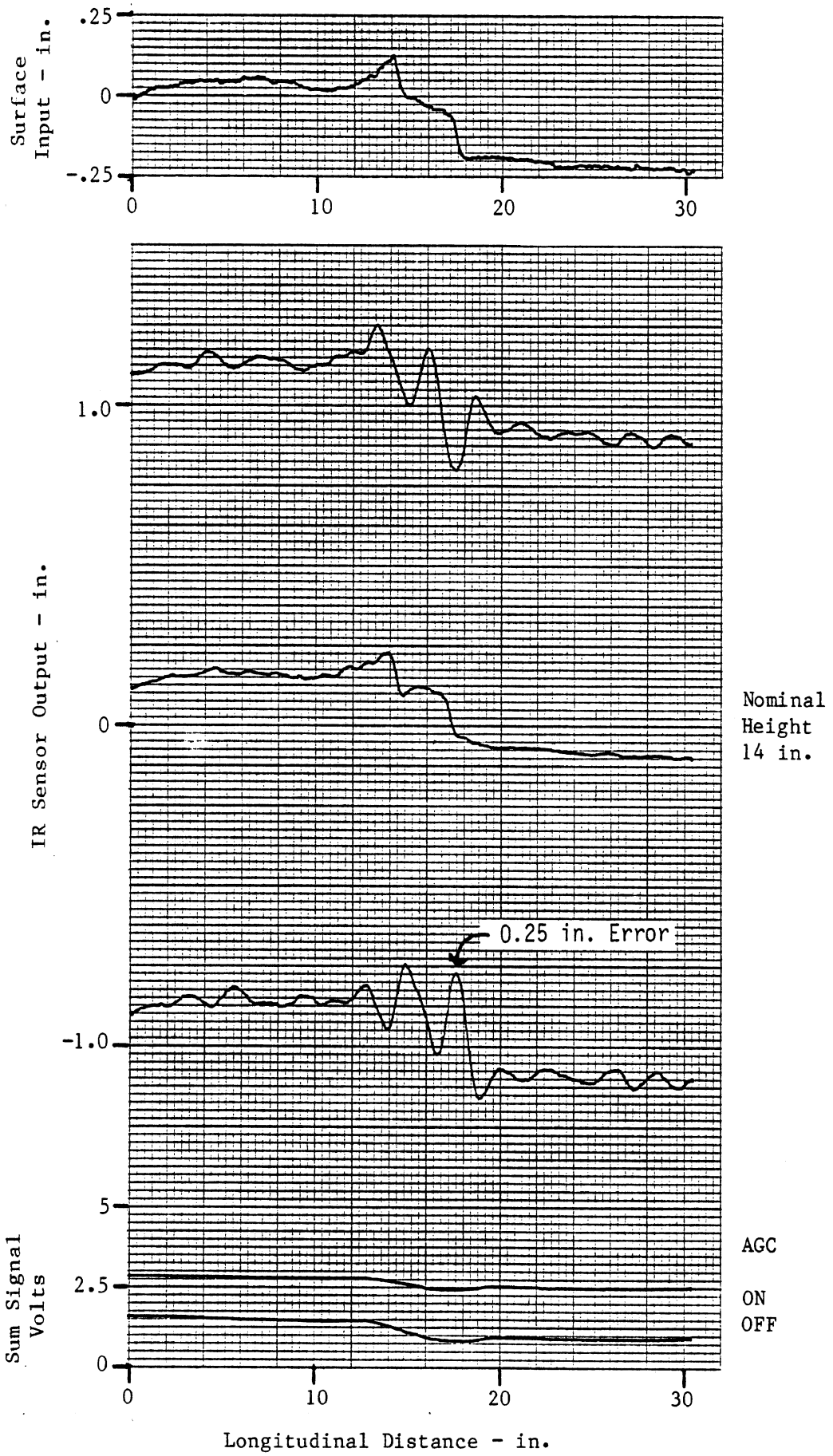


Figure 44. The IR Sensor response to a junction between PCC and asphalt. The surface is shown in Figure 43.

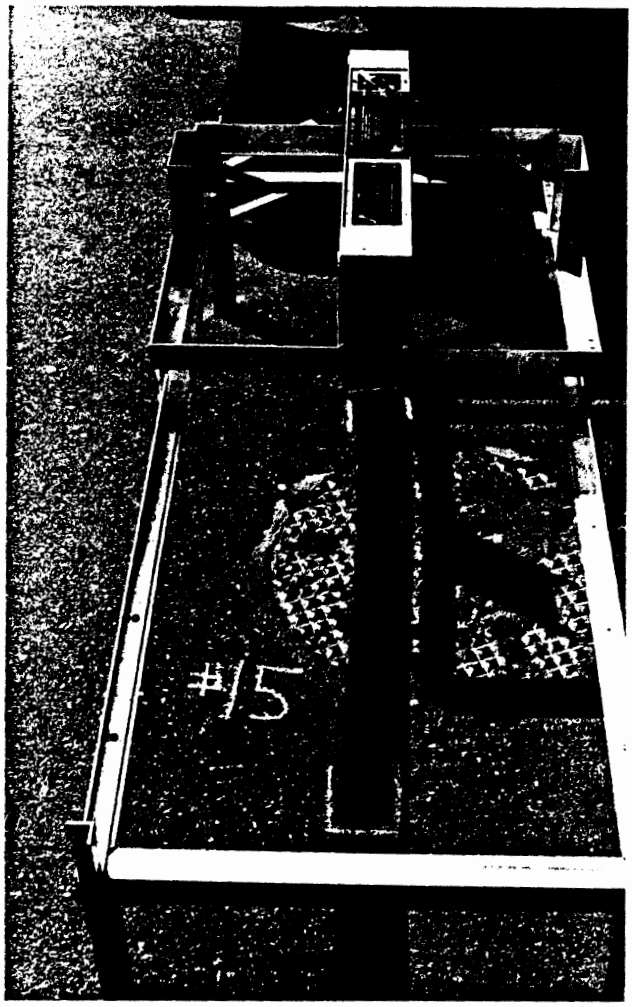


Figure 45. Asphalt around a manhole cover, the test surface for the plots appearing in Figure 46.

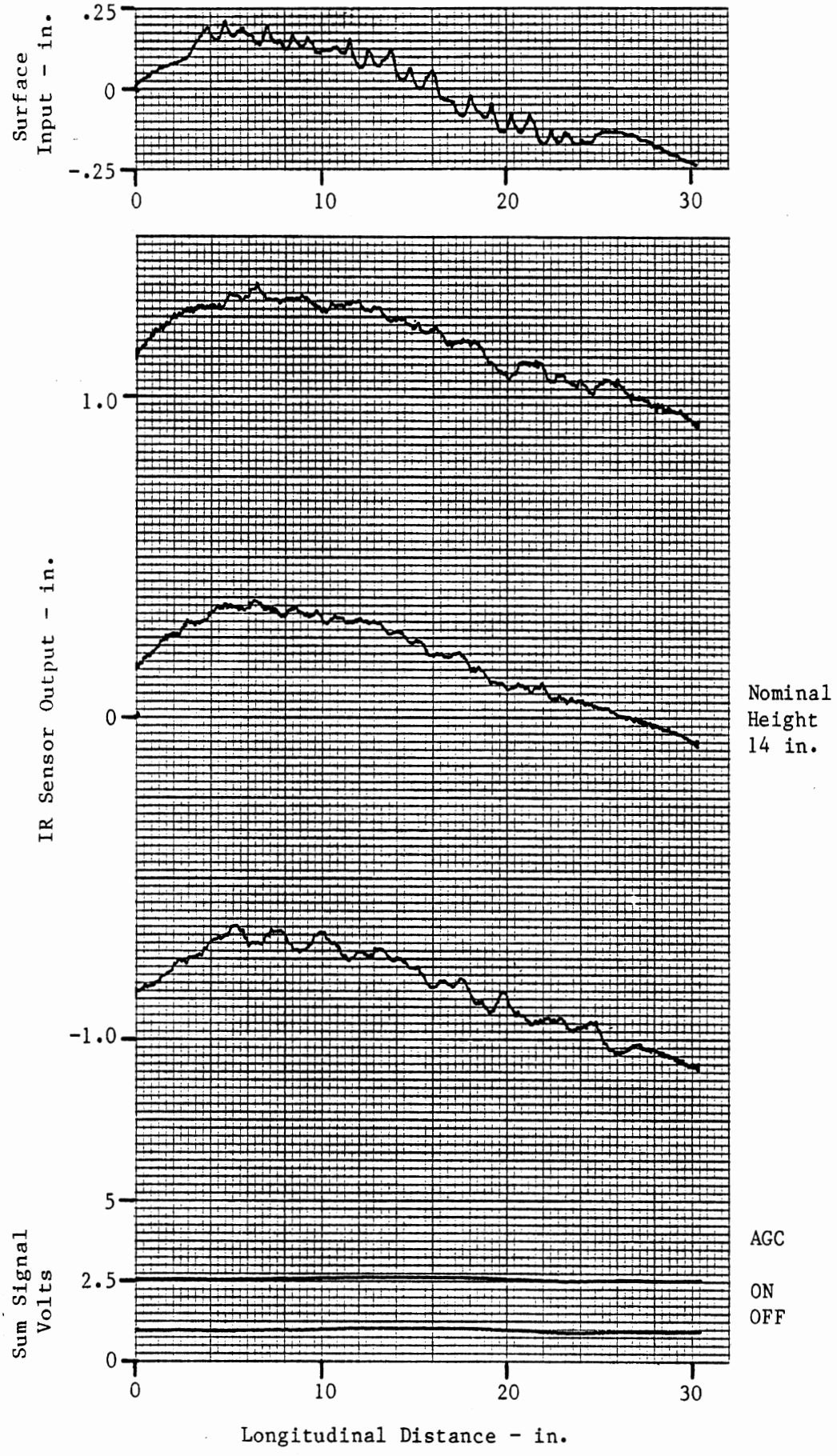


Figure 46. The IR Sensor response to a manhole cover in asphalt. The surface is shown in Figure 45.

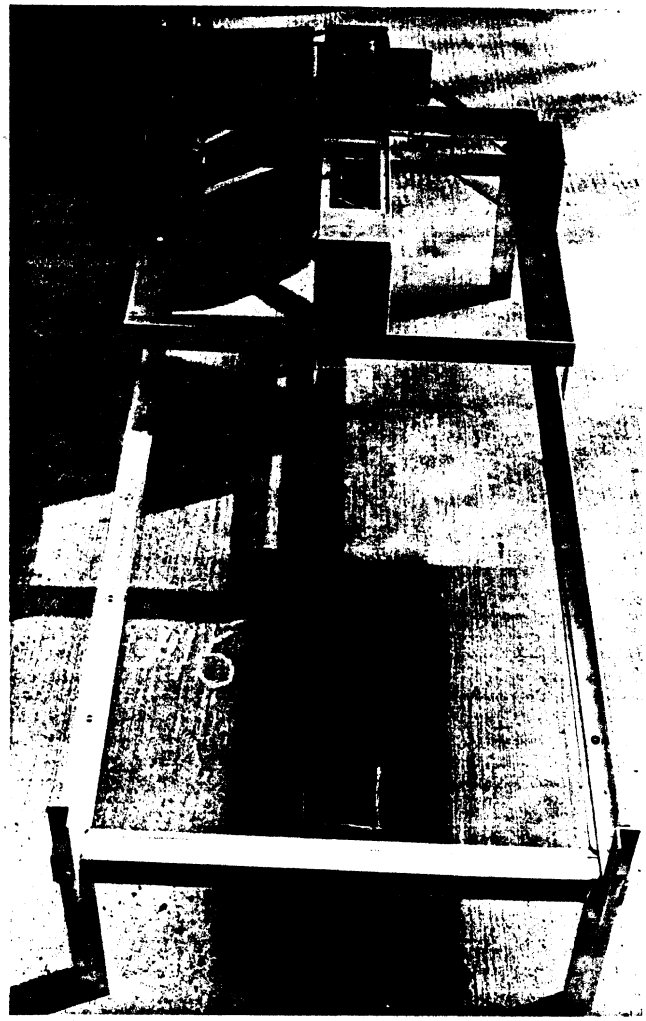

Figure 47. PCC coated with asphalt surface sealer, the test surface for the plots appearing in Figures 48 and 49.

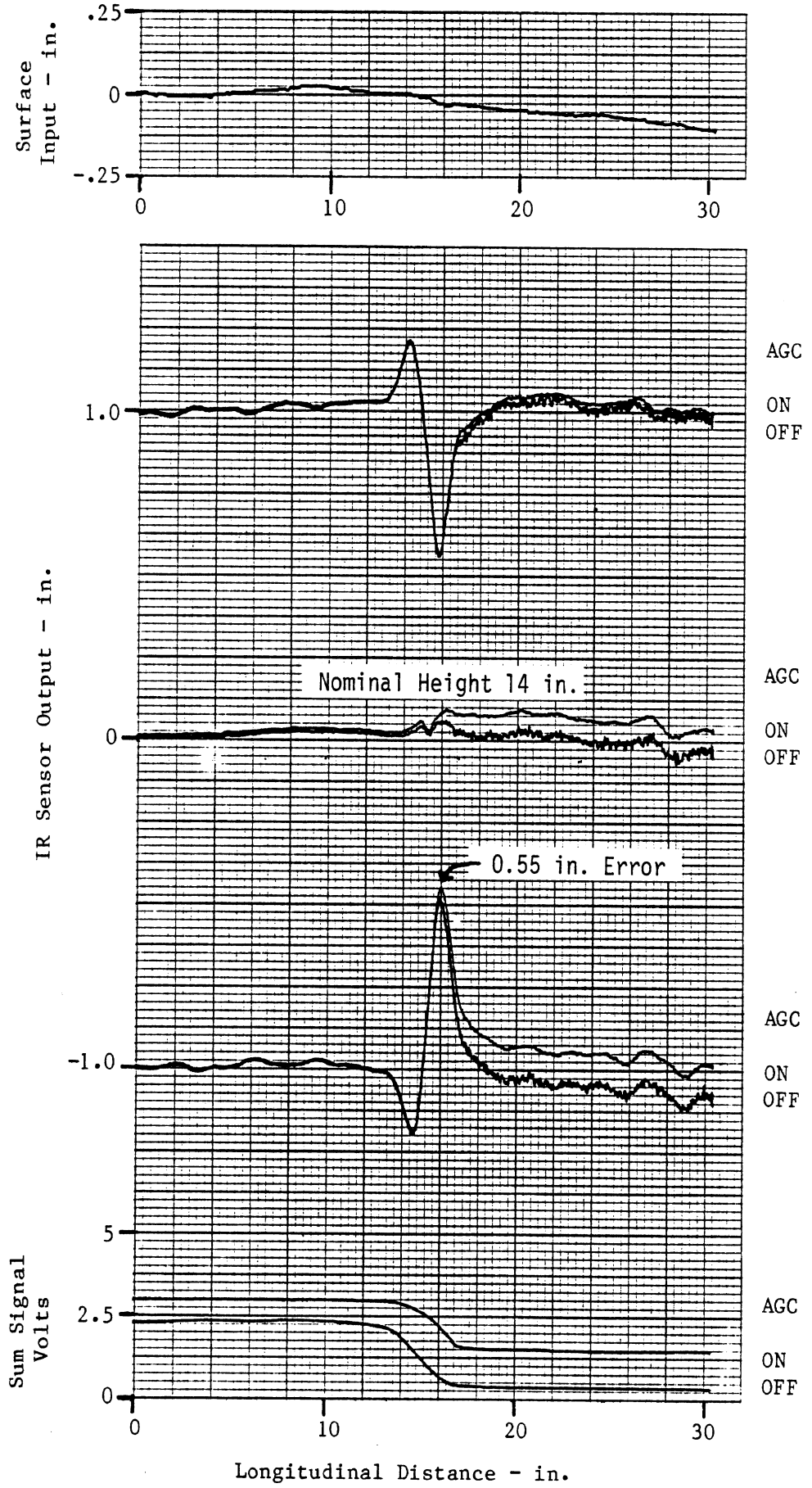


Figure 48. The IR Sensor response to PCC and new asphalt surface sealer. The surface is shown in Figure 47. The direction of motion is along the long axis of the sensor.

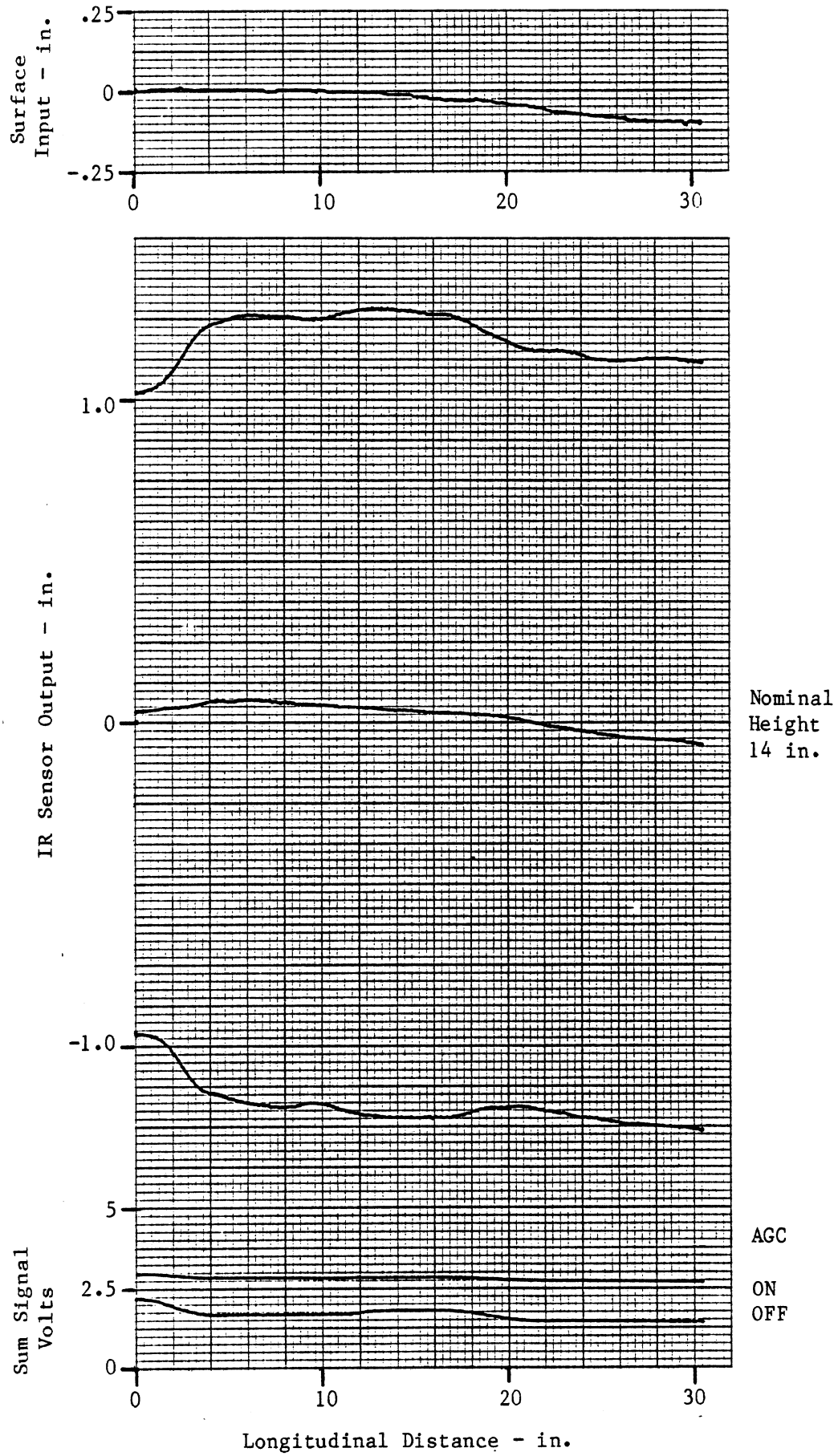


Figure 49. The IR Sensor response to PCC and new asphalt surface sealer. The surface is shown in Figure 47. The direction of motion is along the short axis of the sensor.

reasonable to calibrate the sensor on a surface with a reflectivity falling within the range of surface reflectivities to be encounted in the field, the light-gray test surface would be a more reasonable choice than a piece of white bond paper or the white painted surface. (White bond paper is recommended for a calibration surface in the calibration procedure, Appendix A.) The reflectivity of the light-gray surface is seen (see Figures 25 and 48) to fall approximately midway between the light PCC and the dark asphalt surfaces.

In Figure 48, the sensor outputs with the AGC turned off are superimposed on those with the AGC turned on (the normal case). The AGC makes no difference on the sensor output for the light colored PCC surface, but it makes a significant difference for the dark surface, particularly with the sensor at the nominal heights of 14 inches (reference height) and 13 inches. On the light PCC surface the IR sensor and the surface follower outputs agree to within 0.025 inch. However, on the dark surface, with the AGC turned on, the sensor output has a static error of 0.1 to 0.12 inch at the three sensor heights, and with the AGC turned off the error is less, being a minimum when the sensor is at a height of 13 inches. Differential nonlinearities between the four photocells is the most likely cause of these errors. During the transition from the light PCC to the dark asphaltic surface a peak error of 0.55 inches occurred.

Figure 49 shows additional plots on the surface shown in Figure 47, but with the sensor turned with its short axis in the direction of travel. In this example the edge of the dark strip is only partially in the spot illuminated by the sensor. These plots illustrate the long wavelength errors that occur when the sensor is oriented with its short axis in the direction of travel and it is tracking reflectivity variations which are parallel with its track.

## 5.3 Temperature Sensitivity

A quick check of the IR sensor's temperature sensitivity was made before conducting the road surface tests. The outside temperature ranged from about 35 degrees F. to 50 degrees F. during the road tests. The temperature

sensitivity check was made by moving the sensor from the 70 degrees F. laboratory temperature into the 35 degrees F. outside temperature. With the sensor sitting on the test frame at the reference height, its output was monitored for a period of one half hour. The indicated height output from the sensor changed by only 0.01 inch during the first 15 minutes, and by only 0.002 inch during the second 15 minutes. This result indicates that temperature sensitivity of the sensor is not a significant problem.

## 5.4 Tilt Sensitivity

Using the road test fixture and appropriate shims, the sensitivity of the sensor to tilt was measured, for tilt in both the lateral and longitudinal directions. The height variation at the center of the sensor was held to less than 0.02 inch during the tilt tests. The tests were performed over the surface shown in Figure 22. Figure 50 shows the results of the longitudinal tilt tests, that is for rotation of the sensor about its short axis. The measurement was made for tilt angles of plus and minus 5 degrees only, at sensor displacements of zero and plus and minus one inch from the reference height. The plots show an error of 0.1 inch for plus and minus 5 degrees tilt at all three heights. However, the center of the sensor was about 0.02 inches higher when the sensor was tilted than when it was level. Thus the actual tilt error is 0.08 inch, which is in good agreement with the value of about 0.07 inch, interpolated from the tilt measurement data that was given in Table 1.

Errors resulting from tilt around the long axis of the sensor are shown in Figure 51. This data is for two values of tilt angle (4 degrees and 8 degrees), at three sensor heights (zero and plus and minus one inch displacement from the reference height), and for tilt in one direction only. With the sensor at the reference height and at the reference height plus one inch, the tilt errors are 0.04 inch and 0.075 inch, at tilt angles of 4 degrees and 8 degrees respectively. The corresponding errors are slightly smaller, 0.025 inch and 0.05 inch with the sensor at the reference height minus one inch. The reason for this difference has not been determined.

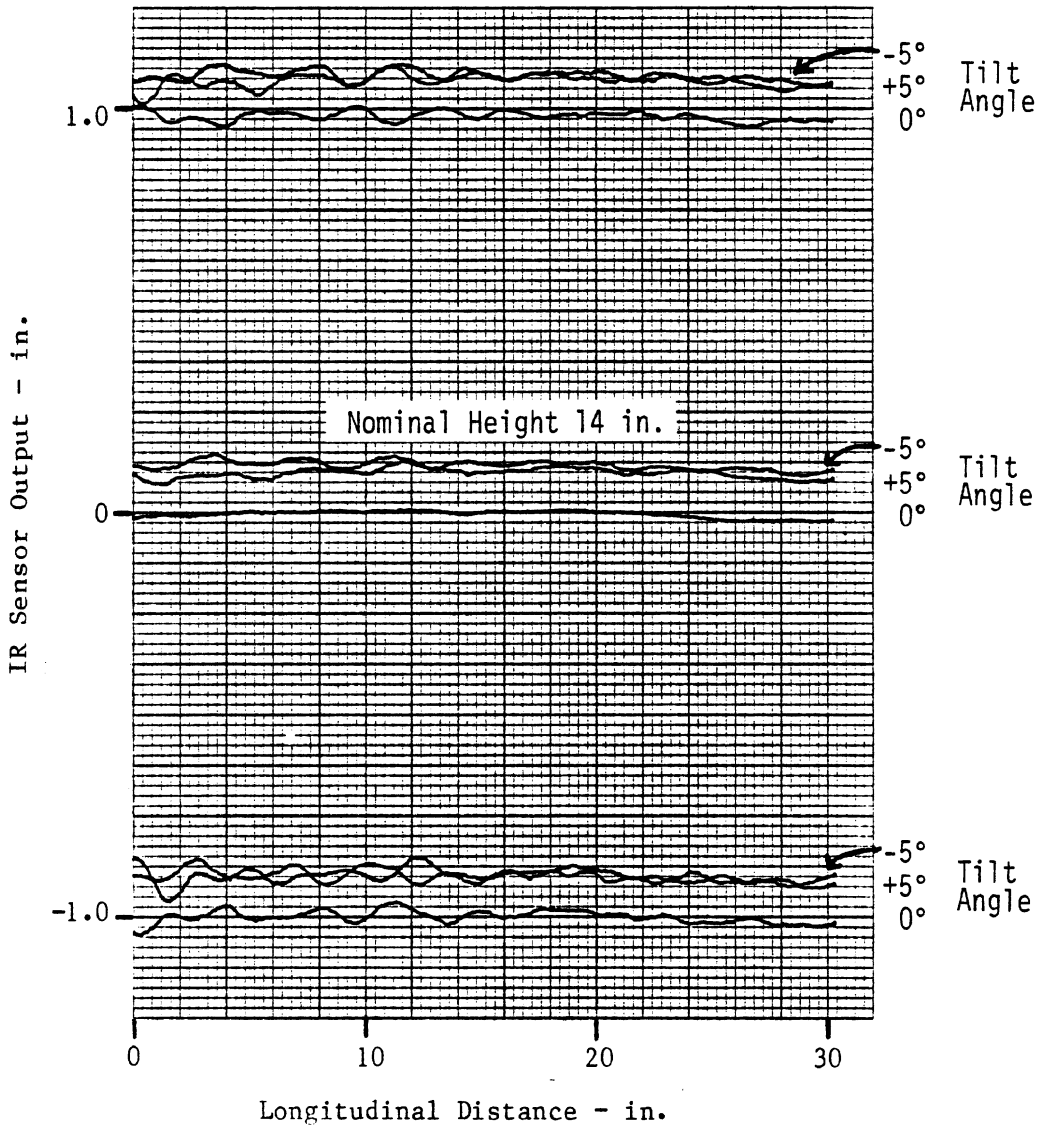


Figure 50. The IR Sensor's sensitivity to tilt around its short axis for ±5 degrees tilt.

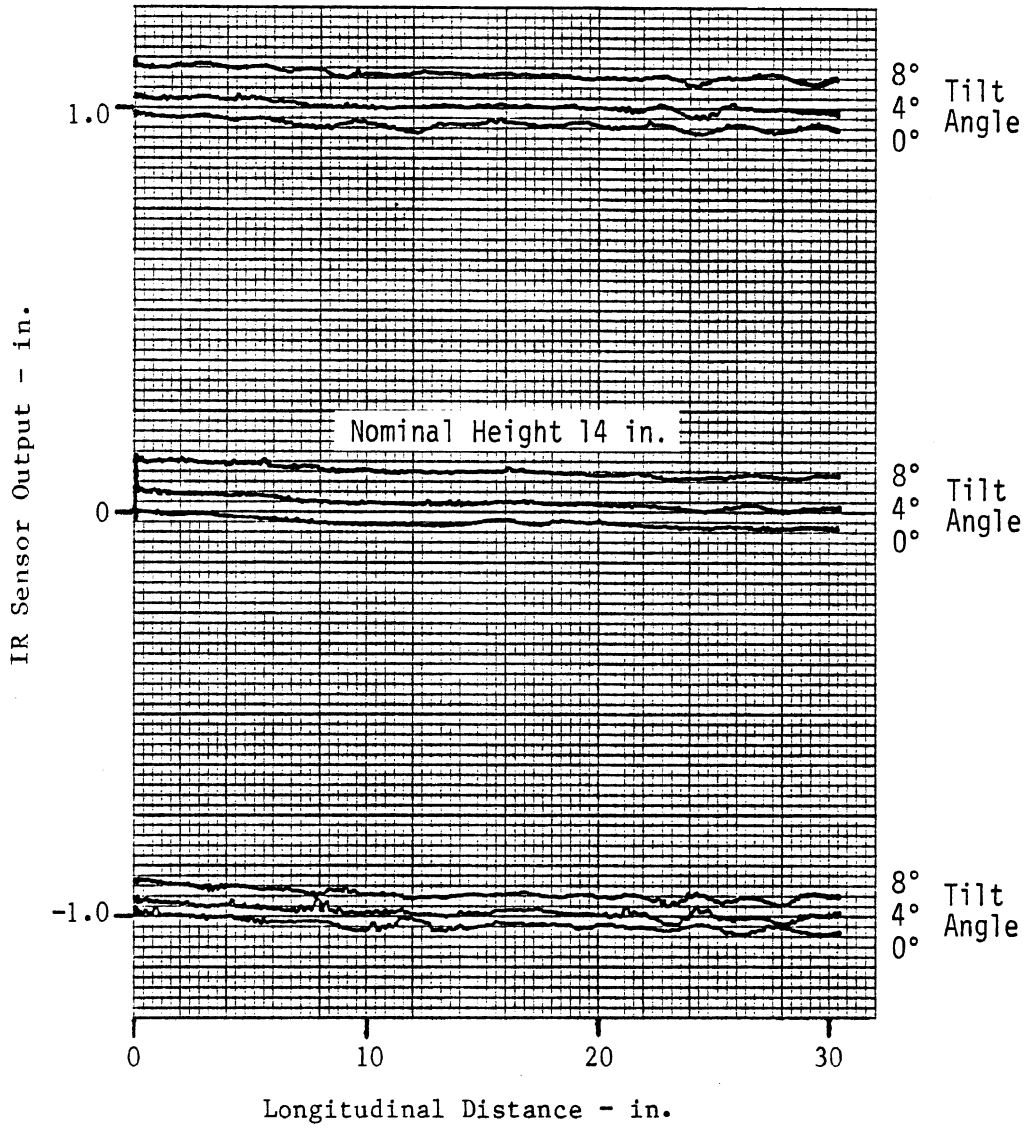


Figure 51. The IR Sensor's sensitivity to tilt around its long axis for 4 degrees and 8 degrees tilt.

# 6.0 CONCLUSIONS AND RECOMMENDATIONS

Analysis and laboratory tests of the FHWA IR Height Sensor have shown that the design concept is technically correct only under certain limiting conditions. When the part of the road surface illuminated by the spot of IR light is flat and has a reflectivity that is homogeonous and uniform in direction, the concept appears sound. Changes in reflectivity are cancelled, as they are intended to be, when the height of the sensor is invariant **and** happens to correspond to the reference height, nominally 14 inches. When these conditions are not satisfied, the theoretical sensor output is confounded by the reflectivity properties of the road surface which produce significant errors. Laboratory tests support the theoretical expectations, and indicate additional errors that are not explained by the simple theory. These are: 1) a large dynamic error that occurs when surface reflectivity changes pass under the sensor at high speeds; 2) a small static offset resulting from changes in the average surface reflectivity; and 3) a small static offset related to the sensor tilt angle. The sum and difference amplifiers and the analog divider circuits do not compromise the performance of the sensor. The sensor's temperature sensitivity does not appear to be a problem. Wavelengths of the dynamic errors and of the errors predicted by theory are typically in the range of 2 inches to 12 inches. However, in certain circumstances, longer error wavelengths can occur.

**Dynamic Performance**

When a surface reflectance change passes under the sensor, a transient overshoot appears on the sensor output. The error amplitude may be as large as one inch, depending on the magnitude (ratio) of the reflectivity change, the sensor height, and the surface velocity relative to the sensor. Unlike the errors predicted by theory, resulting from surface reflectance changes when the sensor is displaced from its reference height (which also appear at high surface velocities, of course), this dynamic error appears even when the sensor is at the reference height. The longest wavelength of this dynamic error is about one foot. Thus, in order to apply the IR sensor to high-speed

profilometer measurements, including wavelengths in the range of about two feet or less, this dynamic problem will need to be solved. Tests to date have not revealed the source of the dynamic error beyond establishing that it is not caused by the sum-difference-divider circuit. Indications are that it is caused by differential photocell responses and/or by the bandpass filter/demodulator circuits. Hence we think the dynamic problem is solvable.

Quasi-Static Performance

The dynamic problem mentioned above is currently not the most critical, because there is the more fundamental issue of whether the sensor is usable even in a quasi-static mode for profile measurement. When measuring height relative to a flat and uniformly reflective surface, the IR sensor exhibits a linearity of about 2 percent over a displacement range of $\pm$1.5 inches, with an accuracy of about 2 percent on surfaces with reflectivities not too different from that of the surface on which it is calibrated. Based on earlier studies at UMTRI, this accuracy appears sufficient for evaluating roughness on all but the smoothest roads. However, it has been shown theoretically and experimentally that the sensor will produce significant measurement errors when the reflectivity of the surface is not uniform and the sensor is displaced from its reference height.

With the sensor displaced only one inch from its zero output reference height, tests on actual road surfaces showed the following peak error magnitudes:

- a transition from PCC to new asphalt, 0.5 inch;
- an oil spot on PCC, 0.23 inch;
- old and cracked asphalt, 0.2 inch;
- a yellow marker stripe on asphalt, 0.35 inch;
- a tar joint in PCC, 0.45 inch;
- surface treated asphalt, 0.13 inch.

The wavelength of these transient errors varied from about 2 inches up to about 10 inches when the direction of travel was in the direction of the long axis of the sensor. Longer wavelengths result when the direction of travel is

in the direction of the short axis of the sensor, and the sensor is tracking along a reflectance transition with its edge lying in the direction of travel. A lane delineation marker is an extreme example. Other less extreme cases are often seen even in the wheel track on road surfaces. Examples are skid marks and natural coloration changes due to surface aging and contamination.

A small static error occurs when the sensor is viewing a surface with reflectivity greatly different from the reflectivity of the surface on which it had been calibrated. For example, a change from PCC to a dark blacktop caused a change on the sensor output of 0.1 inch due only to the reflectivity change. The sensor had been calibrated against a white painted surface with reflectivity slightly greater than the PCC.

A small output error occurs when the sensor is tilted about either its long axis or its short axis. For tilt around the long axis and with no height change, the measured error was 0.04 inch for 4 degrees of tilt, and 0.075 inch for 8 degrees of tilt. When the sensor was rotated around its short axis the measured error was 0.04 inch for 4 degrees tilt and 0.145 inch for 8 degrees tilt. Tilt errors are believed to be caused primarily by distortion of the spot image on the surface of the photocells.

**Temperature Sensitivity**

The manufacturer's data sheet on the divider module (Analog Devices model 436), specifies a worst case output temperature drift of only 2 millivolts per degree C. (1.1 millivolts per degree F). This translates to 0.00027 inch per degree F. at the sensor output. A rough measure of the temperature drift of the overall sensor was made by monitoring the sensor output after moving it from a 70 degrees F. environment into a 35 degrees F. environment. A drift of 0.01 inch was observed during the first 15 minutes, and only 0.002 inch drift occurred during the second 15 minutes. While some additional drift may have occurred with a longer soak period at the 35 degree temperature, this result, together with the the divider drift specificaton, indicates temperature drift is not a major concern.

**Use of the Sensor to Measure Longitudinal Profile.**

The transient response of the IR sensor precludes its use for measuring road roughness for wavelengths in the range of about 2 feet or less. Special filtering techniques would be required to remove noise, in this wavelength range, from the measurement. For the longer wavelength measurements, the overall sensor accuracy, at best, would be about 5 percent of its $\pm$1.5 inch "linear" range. The sensor linearity is about 2 percent over this range. The range of surface reflectivities that are encountered on the road can result in offset and gain changes of several percent, although this could be improved some by an improved calibration procedure. Angular motions of the sensor lead to errors of about 4 percent at 4 degrees of pitch or roll. Larger roll angles during steady cornering would cause larger errors. A larger displacement range is desirable, so that the system can operate at normal speeds on rougher roads.

**Use of the Sensor to Measure Rut Depth**

Since rut depth measures are basically simple static measures, which can be summarized over lengths 10 ft or longer, the short-wavelength performance of the sensor is not as critical as when measuring longitudinal profile for roughness evaluation. Problems with dynamic overshoot and incorrect transient responses to reflectivity changes should have little effect on the very long wavelengths of interest. Thus, the problem can perhaps be "solved" for the application of rut depth measurement simply by filtering the signals sufficiently to remove all medium and short wavelength content.

Although the short wavelength response of the sensor is not critical for rut depth measurement, the absolute static measurement must be accurate. Nonlinearities in the calibration curve of the sensor can of course be compensated by computer, yet any offsets, drift, or change in gain due to reflectivity will change the apparent rut depth. The accuracy estimates stated above, of course, also apply here.

The computation of rut depth from the signals of three height sensors (see Figure 1) effectively cancels any vehicle bouncing motions, if the three

sensors are matched in their response characteristic (amplitude and phase). Rolling and pitch motions are also cancelled if all three of the sensors respond identically to the angular deviations from true vertical. As shown in Figure 1, the outermost sensors must be aimed differently from the others (which are aimed straight down), in order to measure the height of a track outboard of the vehicle. Because the sensor has been shown to behave differently when aimed at different angles, due (we think) to a distortion of the image of the spot seen by the photocells, the outboard sensor may respond differently than the other two when the vehicle rolls even a small amount.

**Recommendations.**

The IR sensor has been shown to have a number of design and performance problems which would compromise the performance of either a longitudinal road profilometer or a rut depth measurement system employing the sensor, restrictions on the profilometer being the greater. Because these limitations would complicate the design and operation of the final system, we recommend that an effort be made to find a sensor with significantly better performance than the IR sensor, before proceeding with the effort required to optimize the IR sensor for this application. Of course any "better" sensor should be thoroughly tested to assure that it does not have unexpected limitations, before expending the considerable effort required to build it into an operating system.

If a decision is made to use the IR sensor for development of the profilometer/rut depth measurement system, then the following issues must be addressed and problems solved.

1. The cause of the large dynamic errors that occur at higher speeds must be identified and eliminated.

2. Tilt angle errors must be quantified more completely, and if needed, means for correction devised.

3. Temperature sensitivity of the sensor should be quantified more carefully.

4. A better calibration method must be devised, with an eye towards computer-controlled methods that can be employed to reduce the technical demands on the user, and which will provide the optimum sensor accuracy obtainable for a selected range of road surface conditions.

5. The shortest wavelength to be included in the measurements must be selected, consistent with data reduction methods, which will permit suitable accuracy for longer wavelengths by rejecting noise at the shorter wavelengths

6. Guidelines must be prepared to permit users of the IR sensor to exclude measurements over surface features which have been determined to cause errors which can not be handled by the data reduction procedures.

## 7.0 REFERENCE

1. King, J.D. and Cerwin, S.A. System for Inventorying Road Surface Topography. Final Report, Contract No. DOT-FH-11-8494, Report No. FHWA/RD-82/062, August 1982.

# 8.0 APPENDIX

## Instructions for Adjustment and Calibration

## of

## Modified Infrared Height Sensors

Developed under:

Contract No. DTFH6-81-C-00046
SwRI Project No. 15-6527

For: U. S. Department of Transportation
Federal Highway Administration
Washington, D.C. 20590

Prepared by: Steve A. Cerwin

## ADJUSTMENT AND CALIBRATION

### A. EQUIPMENT

1. Height Sensor
2. Bench and Test Target (white poster board or white bond paper).
3. Single Axis Linear Translation Stage (4-inch or more travel, .005 inch resolution)
4. Two-Channel Oscilloscope, 5 mHz or greater bandwidth
5. Digital Volt Meter
6. 12v, 5 amp power source
7. 0-10 volt, 10 ma adjustable voltage source
8. An Infrared Viewer is very helpful in positioning the test targets but is essential only for the optional fine tuning procedure in Section D.

### B. SET-UP

1. A sketch of a typical test set-up is given in Figure 1. References to test points and potentiometer adjustments may be located on electrical schematics shown in drawing numbers 15-6527-001 and 15-6527-002 and on the parts location photograph given in Figure 2.
2. Position the target surface at the reference distance of 14.00" from the bottom surface of the height sensor (surface containing plastic windows). The target surface must be parallel to the height sensor and should be of a uniform light color and texture. A section of flat, stiff poster board is suggested. It should be noted that the amplitudes of many of the signals within the height sensor are dependent upon the reflectivity of the target surface. The target surface must be either a piece of white poster board or white bond paper for the gain adjustment, and once the alignment procedure is started the target surface must not be moved relative to the height sensor until the procedure is completed.
3. Remove the covers from both access ports on the top of the height sensor.
4. Connect the height sensor to a nominal 12 volt D.C. power source capable of supplying currents up to 5.0 amperes.

   CAUTION: OBSERVE POLARITY. REVERSING POWER SUPPLY POLARITY TO THE HEIGHT SENSOR WILL BLOW FUSE F-1. In addition to the inline 3 amp fuse there is a 5 amp fuse located on PCB6 within the height sensor.

b. Connect oscilloscope channel 1 to TP1 and channel 2 to TP5.

c. Adjust Center frequency of the 5 kHz band-pass filter using potentiometer P1 such that there is zero phase shift between the sine wave displayed on channel 2 and the square wave displayed on channel 1. It may be useful to superimpose the two wave forms using the centering controls on the oscilloscope for this adjustment. Typical wave forms are shown in Figure 3b.

d. Repeat the adjustment for the second band-pass filter using TP6 and pot P2.

e. Repeat the adjustment for the third band-pass filter using TP7 and pot P3.

f. Repeat the adjustment for the fourth band-pass filter using TP8 and pot P4.

3. Gain Adjustment

a. The automatic brightness control circuitry must be disabled before the gain control potentiometers P5, P6, P7 and P8 can be adjusted.

b. The automatic brightness control loop is broken and the circuitry disabled by interrupting the SUM line which runs from PCB 5 to PCB 6 by setting switch S1 (located between PCB6 and PCB7) from the normal (N) position to the test (T) position.

c. Measure the sum voltage at TP14 with a digital voltmeter (DC) and with switch S1 in the Test (T) position. With a piece of white bond paper or white posterboard as the test target, the voltage at TP14 should be approximately +5 VDC. Also, if the target surface is positioned at the reference height, the DC voltages at TP9, TP10, TP11, and TP12 should be equal and nominally -1.25 VDC each.

d. If required, adjust the gain of channel 1 using potentiometer P5 to set the voltage at TP9 to -1.25 VDC.

e. Repeat the adjustment for channel 2 using potentiometer P6 and TP10.

5. The nominal 4-in. diameter circular spot of infrared light projected downward through the center window of the height sensor onto the target surface should be observed with an infrared viewer. Reposition the target or sensor if necessary to cause the area of the target surface illuminated by the spot to be uniform and free from any markings or smudges.

C. ALIGNMENT PROCEDURE

1. Detector Aiming Alignment

a. Adjust the oscilloscope controls as follows:

(1) Select "Alternate" mode for vertical, 2-channel display.

(2) Set vertical sensitivity to 200 millivolts per division, AC coupled.

(3) Set horizontal sweep to 50 microseconds per division.

(4) Trigger on either channel 1 or channel 2.

(5) Insure that all variable oscilloscope controls are in calibrate position.

b. Connect one channel of a dual trace oscilloscope to test point TP1 and the other channel to test point TP2. Typical waveforms should be as shown in Figure 3a.

c. Adjust detector 1 alignment screw until the AC peak to peak voltages at TP1 and TP2 are equal. Lock the alignment screw with the shaft lock provided after making the adjustment.

d. Connect oscilloscope to TP3 and TP4 and repeat for detector 2 using the detector 2 alignment screw.

2. Adjustment of Band-pass Amplifier Center Frequency

a. Adjust oscilloscope settings as follows:

(1) Select "Chop" mode of vertical display.

(2) Set vertical sensitivity to 200 mV per division, DC coupled, for both channels

(3) Set horizontal sweep to 50 microseconds per division.

(4) Trigger on channel 1.

(5) Insure all variable oscilloscope controls are in calibrate position.

f. Repeat the adjustment for channel 3 using potentiometer P7 and TP 11.

g. Repeat the adjustment for channel 4 using potentiometer P8 and TP12.

h. Recheck the voltages on TP9 through TP12 to insure that each voltage is -1.25 VDC. The voltage at TP14 should be the sum of the voltages on TP9 through TP12 (with a sign inversion) and should be +5 VDC when the voltages on TP9 through TP12 are each -1.25 VDC.

i. Return toggle switch S1 to the Normal (N) position.

4. Sum and Difference Offset Adjustments

a. Using a piece of heavy cardboard and masking tape block the center window of the height sensor to prevent any infrared light from reaching the target surface. The infrared viewer may be used to check for this condition.

b. Connect one channel of the dual channel oscilloscope to TP13. Turn up the sensitivity of the oscilloscope until the electronic noise on TP13 is evident on the trace. This will typically occur at a sensitivity of 50 mV per division. The oscilloscope should be DC coupled for this operation. Alternately block each of the two detecter windows (near each end of the bottom surface of the height sensor) with an opaque object while observing the signal at TP13. There should be no change when either window is blocked. If there is a change, then some IR light is reaching the target. Repeat step a.

c. Adjust the Difference null potentiometer P12 for 0.00 volts output at TP13.

d. Connect the oscilloscope to TP14 and adjust the SUM null potentiometer P13 for 0.00 volts output at TP14.

5. Analog Divider Trimming Procedure

The performance of the electro-optical height sensor is critically dependent upon proper operation of the analog divider circuit. The analog divider typically can be trimmed to an accuracy of better than 0.1 percent of full scale for a denominator signal in the range of 10 mV to 10 V (60 DB). To achieve this level of performance, the following alignment procedure should be followed.

b. Alignment of the analog divider requires independent access to Z (or numerator) input and the X (or denominator) input. A minature toggle switch, S2, has been provided on PCB 5 for this purpose. The switch is placed in the "N" (or normal) position for normal height sensor operation and in the "T" (or test) position for the alignment procedure. In the test position, the Z (or numerator) input is connected to TP-16 and the X (or denominator) input is connected to TP-15.

c. Apply power to the height sensor and allow a five minute (minimum) warm up period. Place toggle switch S2 on PCB 5 to the "T" (test) position.

d. Set the external variable voltage (test) power supply to +10.00 V, and connect the positive output line to the denominator input, TP-15, and the negative to TP-18 (ground). Connect the numerator input TP-16 to TP-18 (ground). Note: For purposes of the analog divider alignment procedure, all ground returns for the test points and external power supply should be connected to the ground terminal TP-18 provided on PCB 5.

e. Adjust output offset potentiometer P11 for 0 mv output at TP-17.

f. Connect the variable power supply voltage through a 1000:1 resistive voltage divider (100k to 100 ohm) to provide an input of +10 mV to TP-15 and leave the numerator input connected to ground. Adjust the numerator (Z) offset potentiometer P10 for 0 mV output at TP17.

g. Disconnect TP 16 from ground and connect both TP 15 and TP 16 to the variable power supply. Set the test power supply output to +10.00 volts and set the scale adjust potentiometer P14 for +10.00 V output at TP-17.

h. Connect both TP15 and TP16 to the +10 mV obtained through the divider described in f. Adjust the denominator (x) offset potentiometer P9 for +10.00 V output at TP17.

i. Remove the connections to TP-15 and TP-16 and return toggle switch S2 on PCB 5 to the "N" position.

## D. FINE TUNING OF NOISE CANCELLATION CIRCUITRY (optional)

NOTE: Read all of the alignment instructions before beginning the procedure. In addition to the equipment requirements listed in Section A, a special rotating target fixture and a four or more channel strip chart recorder will be required to perform this procedure.

1. The height sensor is designed to cancel height measurement error caused by nonuniform reflectance distributions in the target spot area. This is accomplished geometrically by orienting the incident, or transmitted light path perpendicular to the target surface and using two position sensor pickups at complementary angles on either

side. Thus positive or negative height displacements produce in-phase electrical responses from the two pickups, but because of the complementary symmetry the error components caused by nonuniform reflectance produce out-of-phase responses which cancel when the two sensor responses are combined in the difference and sum amplifiers. The effects of this type of error are particularly noticeable under transient reflectance conditions, such as those encountered when running over painted stripes. Rejection of these errors may be fine-tuned by the optional procedure outlined in this section.

2. A rotating test surface with a known reflectance variance is used for this procedure. A piebald surface with one half dark and one half light is easiest to generate. A piece of flat poster board or cardboard of the type found on tablet backs is suggested. Mask one half of the target and paint the other half a moderately dark grey. Extreme differences in reflectances (such as black/white) should be avoided. Light grey/dark grey combinations will produce best results. The finished texture of the test surface should be flatly reflective, as glossy surfaces will produce erroneous results. Unpainted sandpaper should be avoided because the shiny and lens-like sand crystals on many sandpapers have a preferred orientation and will also cause erroneous results. The finished test surface should be bonded to a rotatable disk 5 to 6 inches in diameter. The following criteria should be observed:

   a. The finished surface must be flat (to at least $\pm$ .010 in.)

   b. The rotatable disk must rotate the target surface in-plane and without runout.

   c. The center of rotation must pass through the dividing line between the light and dark areas of the target surface.

   d. Disk rotational speed must be compatible with either stripchart or oscillographic display. Two to ten revolutions per second is recommended for stripchart recording.

3. Perform the static alignment procedure outlined in section C using a uniform target surface (white or grey poster board). Substitute the rotatable piebald target surface for the uniform target. The rotatable target must be placed at exactly the same height distance as the uniform target, and the dividing line between the two piebald halves must be positioned in the center of the infrared spot in both x and y directions. An infrared viewer and scale may be used to center the target. Centering the target in both x and y directions is facilitated by manually orienting the dividing line either parallel or perpendicular to the height sensor chassis while using the infrared viewer and scale.

4. Five electronic signals are monitored for the procedure: the four DC output signals corresponding to the responses of the two detector halves of both detectors and the height output signal. The DC outputs of detector 1, -E1 and -E2, are available at TP9 and TP10; the DC outputs of detector 2, -E3 and -E4, are available at TP11 and TP12. The height output signal is available at the output BNC connector.

5. Connect TP-9, TP-10, TP11, and TP12 respectively to ch1, ch2, ch3, and ch4 of a four or more channel stripchart recorder. Set the scale factors of the stripchart recorder to -2VFS, or as required after beginning the procedure. The output signal may be displayed on an additional channel if available, or on an external oscilloscope.

6. Apply power and start rotation of the piebald target. Triangular shaped signals should appear on the four channels of the strip chart recorder, caused by the alternating light and dark areas of the piebald target passing over the respective detector halves. Typical signals are shown in Figure 4. Note that both of the detector 1 outputs (ch1 and ch2) and the detector 2 outputs (ch3 and ch4) each have large and small AC components, ch1 and ch4 are in phase, ch2 and ch3 are in phase, and ch1 and ch4 are 180° out of phase with ch2 and ch3. If the 180° phase relationship is not present, recheck the target centering in step 3 and make sure the rotating target is at the same height distance as the static target was for the static alignment procedure.

7. The relative phase and amplitudes of the four signals are responsible for the error cancellation: the AC components (amplitude and phase) on ch1 and ch3 should be equal and opposite; and the AC components on ch2 and ch4 should also be equal and opposite (thus, their effects will cancel in the summation circuitry). Fine tuning of the cancellation is made by making minor adjustments to the phase and amplitude levels of these signals. The degree of cancellation obtained is reflected in the magnitude of the AC component present on the output signal (BNC output connector), and all adjustments are made to minimize this signal.

8. Observation of the signals on the strip chart recorder will tell which parameter to adjust first. If it is not obvious from the traces which parameter needs adjustment, then minor adjustments should be made to each control input while noting the effect on the output signal. Best results will be obtained by optimizing the cancellation through small adjustments of all control inputs, as opposed to gross adjustment of any one input. Control inputs are as follows:

```
Amplitude (gain) of ch1 (TP9)      : P5
Amplitude (gain) of ch2 (TP10)     : P6
Amplitude (gain) of ch3 (TP11)     : P7
Amplitude (gain) of ch4 (TP12)     : P8
Phase relationship of ch1 and ch2 : detector 1 aligment screw
Phase relationship of ch3 and ch4 : detector 2 aligment screw
```

9. Reductions in the height measurement error caused by nonuniform reflectance of 60 to 70:1 should be achievable. If one of the two detectors is blocked by placing an opaque card over the lens window, then the height sensor output will show the error with no cancellation. Figure 5 shows typical height sensor output with the rotating piebald disk as a target surface under conditions of 1) detector 1 blocked, 2) detector 2 blocked, and 3) both detectors operating. With either detector blocked, a 14 vp-p error signal is

present on the output (note the 180° phase difference between the error signals of Figure 5a and Figure 5b). When both detectors are allowed to operate, the error signal is reduced to 0.2 vp-p, shown on the right hand portion of Figures 5A and 5B, and on an expanded scale in Figure 5c. Thus the measurement error is reduced by 70 times, or 37dB.

E. RESPONSE CURVE AND SCALE FACTOR ADJUSTMENT

This completes the height sensor alignment procedure. Before replacing the cover plates, be sure that both S1 and S2 have been returned to the Normal (N) position. A calibration curve should be taken at a range of $\pm$ 2 inches about the reference height. Height increments of not greater than 0.2 inches are recommended. A typical response curve is given in Figure 6. Scale factor of the response curve may be set with potentiometer P15. The scale factor should be set to 3.5 v/inch, set by displacing the target surface + 1 inch from the reference height (0.00 volts) and setting the output voltage to +3.5 v with P15.

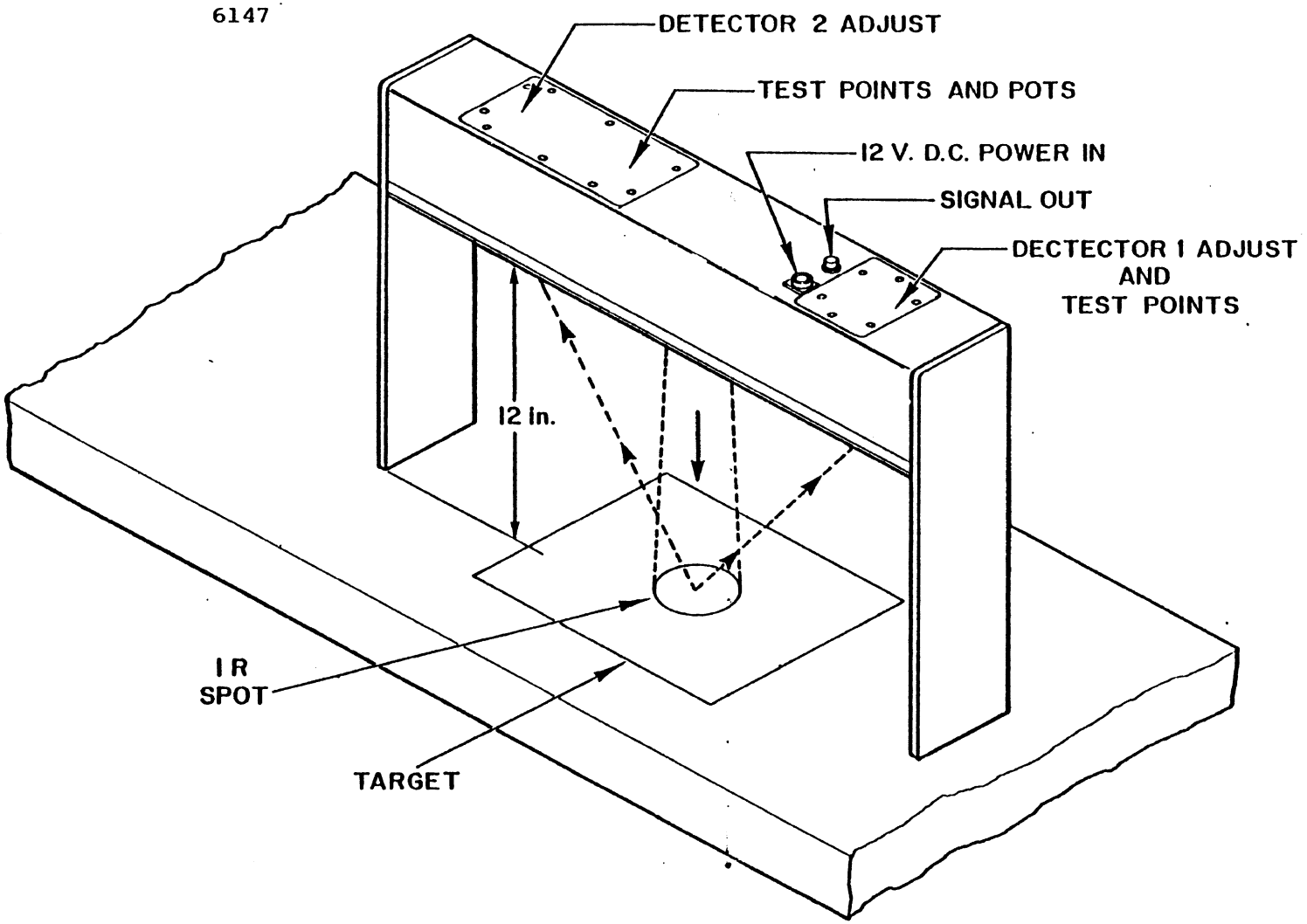


FIGURE 1. TEST SET-UP FOR ADJUSTMENT AND CALIBRATION OF INFRARED HEIGHT SENSOR

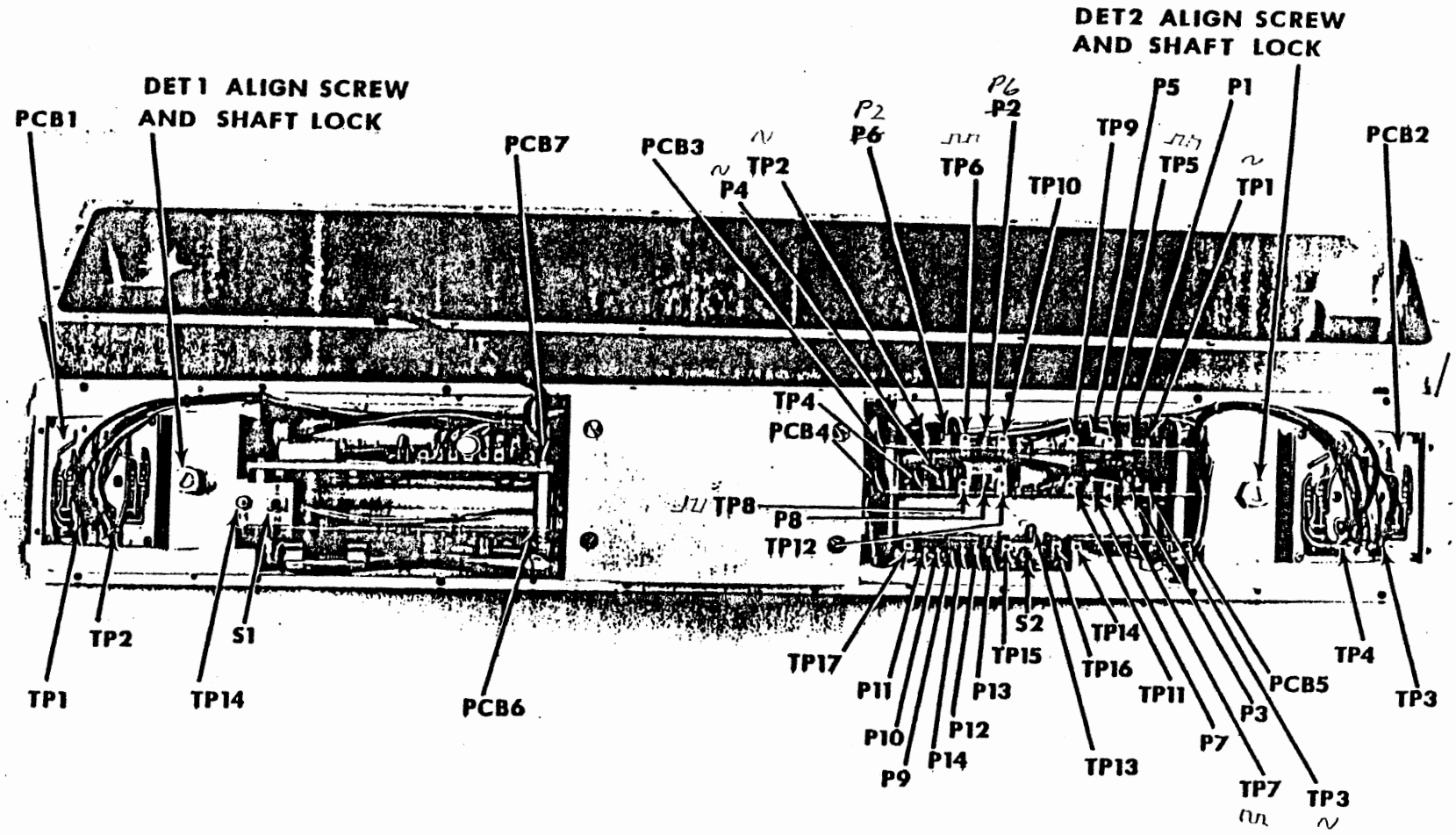


FIGURE 2. PARTS AND TEST POINT LOCATION FOR INFRARED HEIGHT SENSOR (TOP VIEW, COVER REMOVED).

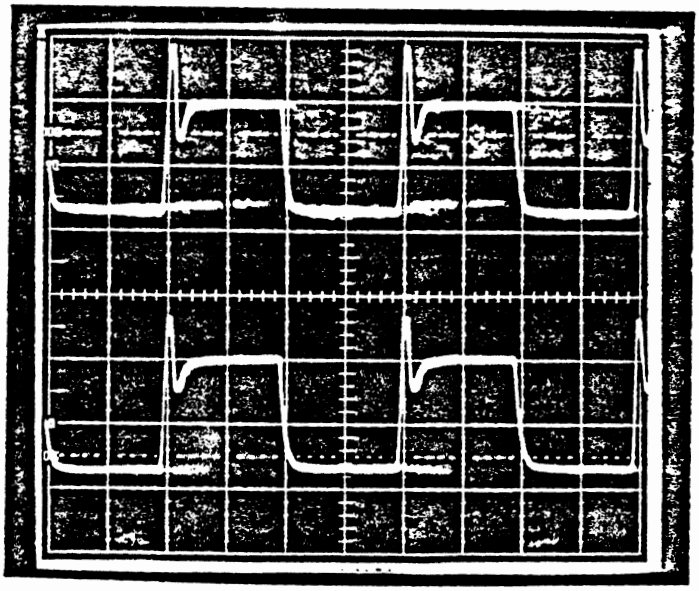

A. TP1 and TP2

6148

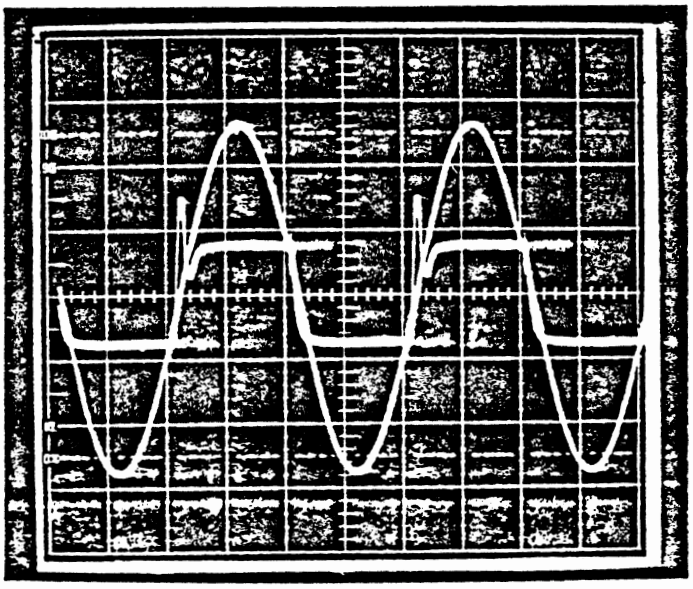

B. TP1 and TP5

FIGURE 3. OSCILLOSCOPE WAVEFORMS

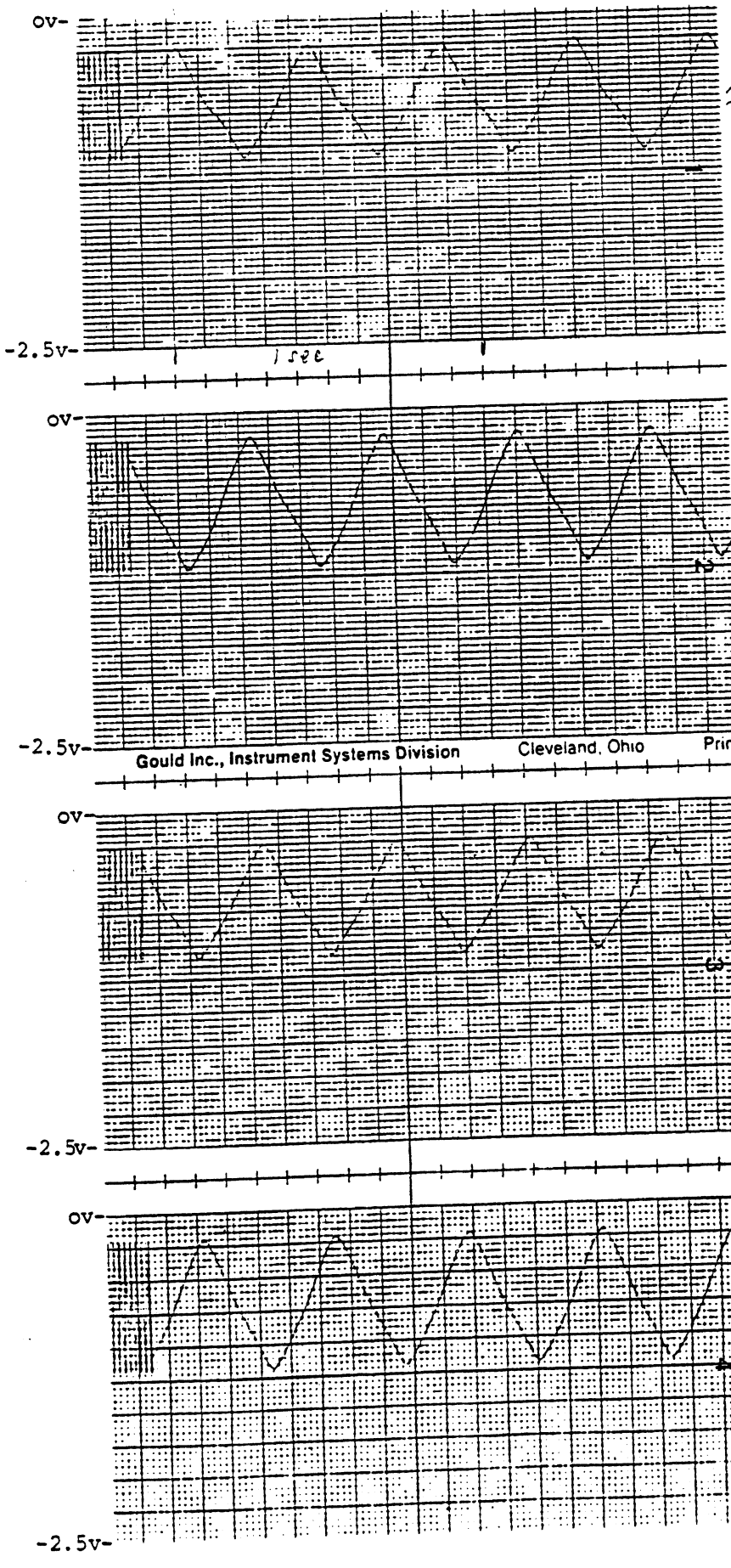


Figure 4a. Detector 1A, TP9 (-E1)
CH1
~2 Hz
Small AC component
Phase = $\phi$

Figure 4b. Detector 1B, TP10 (-E2)
CH2
Large AC Component
Phase = $\phi + \pi$

Figure 4c. Detector 2A, TP11 (-E3)
CH3
Small AC component
Phase = $\phi + \pi$

Figure 4d. Detector 2B, TP12 (-E4)
CH4
Large AC component
Phase = $\phi$

FIGURE 4. SIGNALS OBTAINED ON TEST POINTS 9, 10, 11, and 12 WHEN ROTATING PIEBALD DISK IS USED AS THE TARGET SURFACE. 50 mm/sec chart speed.

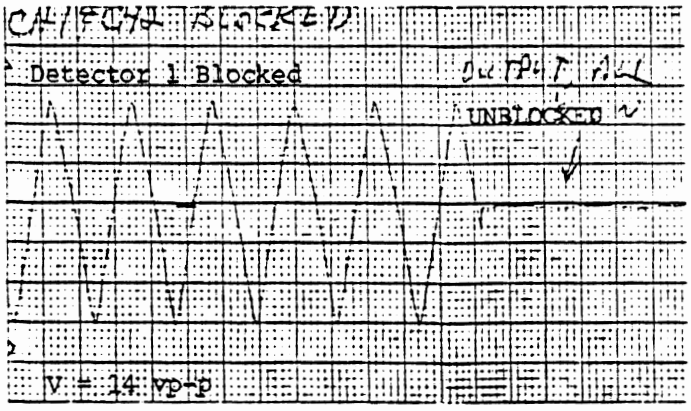


FIGURE 5a. Output signal with Detector 1 blocked 25 V.F.S. v = 14 vp-p

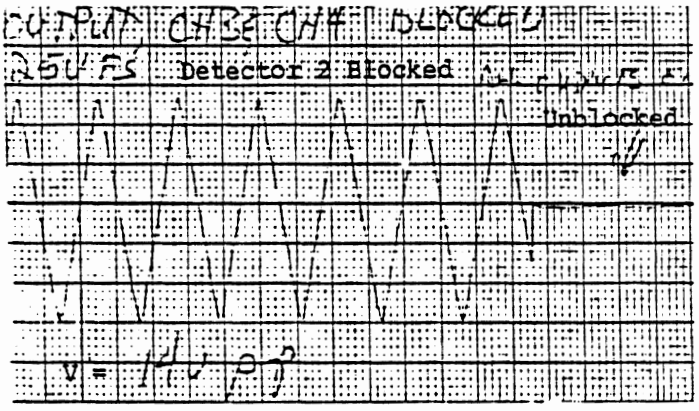


FIGURE 5b. Output signal with Detector 2 blocked 25 V.F.S. v = 14 vp-p

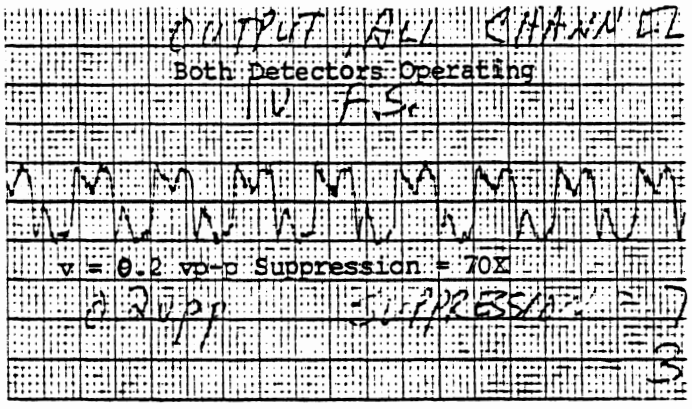


FIGURE 5c. Output signal with both Detectors Operating 1 V.F.S. v = 0.2 vp-p error reduction = 37 dB

Figure 5. HEIGHT DETECTOR OUTPUT WITH ROTATING PIEBALD DISK AS TARGET SURFACE SHOWING MEASUREMENT ERROR REDUCTION OF 37dB.

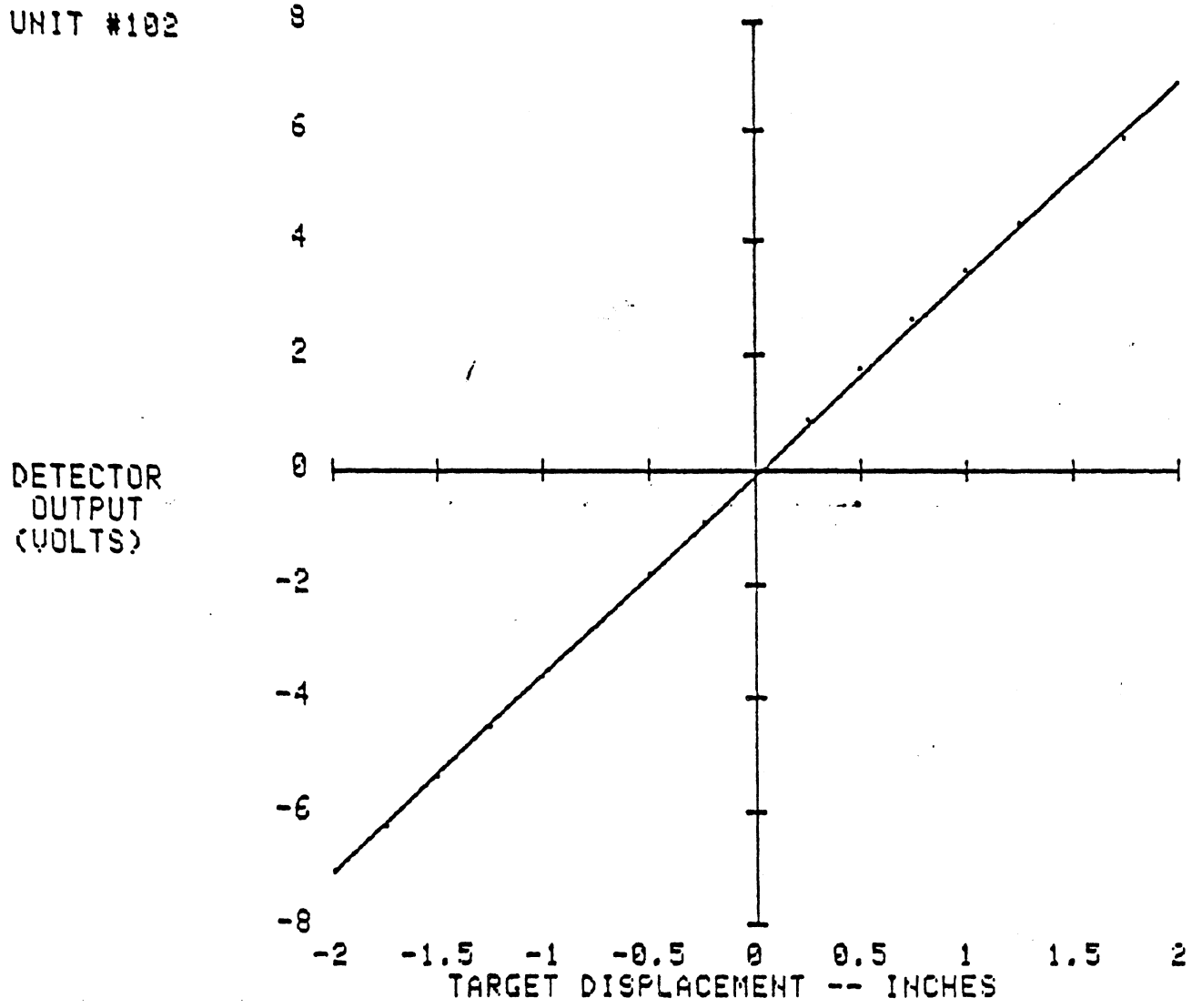


FIGURE 6. INFRARED HEIGHT SENSOR RESPONSE WITH REFERENCE SURFACE AT 14 INCHES

# 9.0 APPENDIX B

## SENSOR RECALIBRATION DATA

Initial checks of the performance of the IR sensor revealed unexpected deficiencies with regard to the effects of nonuniform surface reflectivity and dynamic response. Consequently, both to become familiar with the sensor circuitry and calibration characteristics, and to assure that the observed performance was not a result of faulty calibration and/or faulty components, an overall recalibration of the sensor was undertaken. The calibration procedure recommended by the Southwest Research Institute (Appendix A) was followed, except the "piebald disk" procedure, recommended for final adjustment trimming to minimize the sensor response to nonuniform surface reflectance, was not applied. An alternate, more precise procedure was used, and is described below. Only minor adjustments were required to obtain the signal waveforms and voltages specified in the calibration procedure, indicating that the original calibration was accurately performed "by the book."

This appendix includes a number of observations concerning details of the sensor operation, and sample data, which may prove helpful to anyone using or investigating the IR sensor. Measurements made while performing the recalibration of the sensor are presented. Data showing unequal difference amplifier input gains are tabulated and the effect on sensor performance is discussed. This same data show that the photocell signals are the source of the change in sensor output for changes in surface reflectivity (with the AGC on and off). Data are tabulated showing the improvement achieved in the tracking between the photocell signals, when a new procedure was used to trim the sensor adjustments for optimum cancellation of surface reflection changes.

**Recalibration.**

Recalibration of the sensor was performed with the bottom reference surface of the sensor case 14 inches away from the white surface on the drum roller (the drum roller test surface is described in the report). Before

recalibration, the D.C. voltages at the four gain adjust test points, TP9, TP10, TP11,and TP12, ranged from -0.70 volts to -0.75 volts, with the sensor viewing the white paint. The calibration procedure specifies each of these voltages to be equal to -1.25 volts (AGC off), with a piece of white bond paper as the target at a 14 inches distance. A piece of white bond paper was found to produce about 1.1 volts, thus with the white paint target the voltages were each set equal to 0.800 volts. Final adjustment of the DC gain controls were made to obtain these values after making minor adjustments of the photocell alignment screws and of the phase trim of the bandpass amplifiers to obtain the waveforms recommended in the calibration procedure.

Only small adjustments of the trim pots were required to trim the sum and difference amplifier offsets and the analog divider circuit to the specified values. The following offset values were obtained:

| | |
|---|---|
| Difference amplifier offset: | 0.001 volt |
| Sum amplifier offset: | 0.002 volt |
| Analog divider offset: | 0.000 volt |
| Sensor output offset: | 0.010 volt |

Note that no provision is made in the circuit for the adjustment of the sensor output offset. About two weeks later the offsets were within plus or minus 0.002 volts of these values, indicating good drift performance in a laboratory environment.

When the D.C. photocell channel signals were reapplied to the circuit after making the offset adjustments, an offset of 0.189 volts (0.054 inch) was present on the sensor output. Considering that the four inputs to the sum and difference amplifiers were equal to within 0.002 volts, and that the calibration offsets given above were all less than 0.010 volt, this offset is larger than expected. When the dark-gray surface was moved under the sensor, the offset changed by 0.206 volts, from 0.189 to 0.395 volts. This is about the same change in the sensor output observed in the oscillograph in Figure 9 (see report) when the dark-gray to white surface was passed under the sensor at the reference height of 14 inches. The data presented in Table B1 help explain these observations.

**Measured Data and Some Observations.**

Table B1 contains both measured and calculated values. The measured values are: the four photocell channel voltages ($E_1$, $E_2$, $E_3$, and $E_4$) measured at the input to the difference and sum amplifiers (TP9, TP10, TP11, and TP12); the difference and sum amplifier outputs (TP13 and TP14); the analog divider output (TP17); and the sensor output. The measurements were made with the AGC on and off, with the sensor viewing the white, the dark-gray, and the bare steel surfaces of the drum roller from the reference height of 14 inches. While the measurements were taken, the sensor was left in one position and the drum was turned to bring the desired section of the test surface into the IR spot. With this procedure the change in the distance from the sensor to the drum surface during the measurement period was equal to the runout of the drum (less than 0.003 inch).

**Observations on the Data.** The data in Table B1 show the following:

1. The approximate reflectance ratio of the white to the dark-gray surfaces is 8:1. The ratio is found from the measured photocell voltages for the white and dark-gray surfaces with the AGC off.

2. Statically, the AGC reduces the white to dark-gray reflectance ratio to an effective value of about 1.8:1. This ratio is found from the measured photocell voltages with the AGC on.

3. Turning the AGC on results in a small decrease in the four photocell channel outputs on the white surface, but they remain equal and the sensor output does not change.

4. Turning the AGC on results in a large increase in the four photocell channel outputs on the dark-gray surface and a small change on the sensor output.

Table B1

Measured and Calculated Sensor Signals.

| Surface: | white | | dark gray | | steel | |
|---|---|---|---|---|---|---|
| AGC: | ON | OFF | ON | OFF | ON | OFF |
| Signal | | | | | | |
| | Measured Values: | | | | | |
| cell 1 | .742 | .798 | .409 | .101 | .622 | .862 |
| cell 2 | .744 | .799 | .431 | .106 | .801 | 1.105 |
| cell 3 | .743 | .798 | .420 | .104 | .674 | .926 |
| cell 4 | .744 | .802 | .431 | .109 | .944 | 1.307 |
| Difference | -.071 | -.076 | -.082 | -.022 | -.528 | -.720 |
| Sum | 3.040 | 3.250 | 1.750 | .458 | 3.100 | 4.270 |
| Div. Out (A) (10xDiff/Sum) | -.227 | -.227 | -.452 | -.460 | -1.682 | -1.683 |
| Output | .189 | .189 | .385 | .395 | 1.457 | 1.458 |
| | Calculated Values. Diff., Sum, and Divider Outputs, With Gains = 1.000 | | | | | |
| Difference | -.003 | -.005 | -.033 | -.010 | -.449 | -.624 |
| Sum | 2.973 | 3.197 | 1.691 | .420 | 3.041 | 4.200 |
| Div. out (B) | -.010 | -.015 | -.195 | -.238 | -1.476 | -1.486 |
| Error (B-A) | .217 | .211 | .257 | .222 | .226 | .197 |
| | Calculated Values. Diff., Sum, and Divider Outputs, With Actual Gains | | | | | |
| Difference | -.054 | -.060 | -.063 | -.017 | -.509 | -.707 |
| Sum | 3.030 | 3.258 | 1.723 | .432 | 3.100 | 4.281 |
| Div. out (C) | -.178 | -.184 | -.363 | -.428 | -1.642 | -1.651 |
| Error (C-A) | .039 | .043 | .089 | .032 | .040 | .032 |

5. The four photocell outputs were set equal on the white surface in the calibration procedure. When the dark-gray surface is moved under the sensor the four outputs do not remain equal, causing the output to change by 0.196 volts with the AGC on and by 0.206 volts with the AGC off. The maximum difference between any two photocell outputs is about 5 percent. This indicates a nonlinearity, either in the photocells or in the circuits following the photocells.

6. Large differences occur between the photocell outputs for the steel surface, causing a large output error. This apparently is a result of nonuniform directional reflectivity of the steel surface resulting from minute grooves left by the cutting tool when the drum was machined.

7. The gain of the output amplifier is about -0.85 (ratio of the sensor output to the divider output).

**Sum-Difference-Divider Circuit.** The first set of calculated values in Table B1 are a check on the performance of the sum, difference, and analog divider circuits. These values were calculated from the measured values of the four photocell channel outputs, assumming a gain of one in the sum and difference amplifiers to each of the four inputs. Comparison of the measured and calculated values show small but significant differences. Errors on the difference amplifier outputs are larger than on the sum amplifier outputs. The row marked Error(B-A) in the Table is the difference between the calculated divider ouput and the measured divider output. This error is on the order of 0.220 volts across the board. These results suggested that the gains of the sum and difference amplifiers are not equal to one for each of the four input signals from the photocells. Therefore, the gains of the amplifiers to each of the inputs were measured. The results are tabulated in Table B2. The sum amplifier gains differ by about 0.1 percent, however the difference amplifier gains to the channel 2 and channel 4 inputs are about 3.3 percent larger than the gains to the channel 1 and channel 3 inputs.

## Table B2

**Measured Sum and Difference Amplifier Gains**

| Channel | Sum amp. Gains | Difference Amp. Gains |
|---|---|---|
| 1 | 1.019 | 0.999 |
| 2 | 1.020 | 1.034 |
| 3 | 1.019 | 1.002 |
| 4 | 1.020 | 1.036 |

The second set of calculated values of the sum, difference, and analog divider outputs, listed in Table B1, were calculated using the measured gain values from Table B2. Comparing these calculated values with the measured values, we see that using the measured gain values reduces the errors. The last row in Table B1, marked Error(C-A), is the difference between the calculated divider output (using the measured gains in the calculations) and the measured divider output. The error has been reduced from a nominal value of 0.220 volts, when a gain of 1.00 was used in the calculations, to a nominal value of 0.04 volts by using the measured gain values in the calculations, showing that the offset observed on the sensor output upon completing the calibration procedure is primarily due to the unequal gains to the four inputs to the difference amplifier.

Gain errors in the difference amplifier are more critical than in the sum amplifier because they affect both the offset and overall gain of the sensor, whereas gain errors in the sum amplifier affect only the overall gain. The effect of the sum and difference amplifier gain errors on the sensor performance can be evaluated using the equation defining the sensor output, equation (6), developed in the analysis section of this report. To do this, each of the reflection coefficients ($R_1$ through $R_4$) in the numerator of equation (6) is multiplied by the corresponding gains of the difference amplifier, and each of the reflection coefficients in the denominator is multiplied by the corresponding gains of the sum amplifier. The result is a curve similar to those plotted in Figure 4 of this report. When equation (6) is evaluated in this way, assumming equal reflection coefficients ($R_1=R_2=R_3=R_4$) and using the sum and difference amplifier gains listed in

Table B2, the curve obtained shows an output (offset) of 0.016 for zero input (X=0). Except for this small offset, unequal difference amplifier gains on the order 3 percent do not have a significant effect on the operation of the sensor.

**Fine Tuning The Color Cancellation.**

**Color Cancellation Theory** The output of the IR sensor was defined in equation (1) of this report, that is

$$E = G\ (E_1-E_2+E_3-E_4)\ /\ (E_1+E_2+E_3+E_4).$$

where $E_1$ through $E_4$ are the photocell outputs, after demodulation, amplification, and filtering, appearing at the inputs to a perfect sum, difference, and divider circuit. Our analysis of the IR sensor has shown that perfect color cancellation can be obtained only with the sensor at its reference height (where the IR spot image is exactly centered on each photocell pair). Also, the spot image must have geometric symmetry about the center line (or junction) of the two photocells in each pair, and the system must be linear. For these conditions, a color (surface reflectance) change passing under the sensor does not cause an output error. Even though all four photocell outputs change, $E_1$ tracks $E_4$ ($E_1$=$E_4$) and $E_2$ tracks $E_3$ ($E_2$=$E_3$) so that the net output remains zero. Unfortunately, perfect tracking of these signals is not obtained in practice, and the output does change with color, even at the reference height. The main causes of imperfect signal tracking appear to be photocell nonlinearity and image spot asymmetry. Analysis and tests of the IR sensor have shown that the output errors due to color change obtained when the sensor is displaced from its reference height are large compared to those observed at the reference height. That is, errors at the reference height are for the "best case." Therefore, improved color cancellation at the reference height will still leave large errors at other heights.

**Piebald Disk Method** Southwest Research recommends a procedure to optimize color cancellation using a rotating piebald disk, a disk with one half dark and one half light. The disk is placed at the fourteen inches zero

reference distance with the dark-light line on the disk perfectly centered on the IR spot in both the "x and y directions." The two photocell alignment screws are adjusted to obtain quadrature phasing of the four photocell signals (thus centering the spot images on the photocell pairs), and the gains of the four photocell channels are tweeked to minimize the peak-to-peak signal variation observed at the sensor output, hopefully while maintaining the required equality of channel gains required for optimum sensor linearity vs displacement from the reference height. Consideration of equation (6), restated above, shows that minimum variations on the sensor output can be obtained for these test conditions even with significant gain differences between the pairs of channels 1,2 and 3,4. A strip chart recorder is recommended for observing the signals while making the adjustments. This approach has several conceptual flaws: 1) it optimizes the cancellation at the reference height at the possible expense of other measures; 2) the resolution of the strip chart recorder display is inadequate to observe the signals with the precision required; and 3) it is difficult to center the disk precisely at the center of the IR spot. The latter difficulty arises because: 1) the spot does not have sharply defined edges; and 2) the IR viewer does not provide a sharp image. Centering the spot within five percent accuracy is doubtful. If the disk is not centered on the IR spot, the optimum color cancellation will be obtained when the spot image is slightly off center on each of the photocell pairs, reducing the linear displacement range and symmetry of the sensor output.

**A New Method** A different procedure was tried for optimizing the color cancellation with the sensor at the reference height, which yielded some illuminating results. The dark-gray/white test surface that was used for the quasi-static tests of the sensor response to color changes - and described in the report - was placed on the mill table fourteen inches under the sensor with the IR spot on the white surface. After calibrating the sensor on this white surface following the recommended procedures, the surface was moved horizontally, bringing the dark-gray surface into the IR spot, with the edge of the color change moving perpendicular to the long axis of the sensor as, depicted in Figure 5c in the report. This direction of travel produces the largest changes in the "effective" average surface reflectivity as the color change moves across the IR spot. With the AGC turned off, the outputs of the

four photocells ($E_1$ through $E_4$) were measured at the test points at the input to the sum and difference amplifiers, and recorded for incremental horizontal moves of the target surface. The measured data, along with the calculated differences or tracking errors between $E_1$ and $E_4$, and between $E_2$ and $E_3$, are tabulated in Table B3. Applying the scale factors implemented in the actual sensor, the sensor output was calculatedfor each set of the photocell output values. The calcuated sensor output is also listed in Table B3.

The maximum value of the difference ($E_1$-$E_4$) is 0.070 volts and of ($E_2$-$E_3$) is 0.066 volts. These differences are positive over the whole range, with the exception of the first and last data points for $E_2$ and $E_3$. Consequently, adjusting the alignment of either photocell pair in the direction to decrease the tracking error between one set of photocells would increase the tracking error between the other set. For example, adjustment of the alignment screw controlling the photocell pair 1 and 2 to decrease the tracking error ($E_2$-$E_3$) would increase the tracking error ($E_1$-$E_4$). This indicates that the sensor height, that is the reference height, must be changed in order to obtain closer tracking. An increase in the reference height was found to be required. The sensor was set to a new reference height of fourteen and one eighth inches, where it was recalibrated on the white surface at this height. The tracking data obtained at this reference height are tabulated in Table B4. The maximum tracking error ($E_1$-$E_4$) is reduced to -0.016 volts and the maximum tracking error ($E_2$-$E_3$) is reduced to 0.021 volts. Positive and negative values appear on both tracking errors indicating the adjustment is near optimum. Comparing the calculated sensor outputs in Tables B3 and B4, the peak-to-peak output variation was reduced from 0.719 inches to 0.292 inches. With more tweeking some additional improvement might be obtained.

The data in Tables B3 and B4 reveal another effect that has a small influence on the degree of color cancellation at the reference height. Ideally, the output of photocells 2 and 3 would not start to change until the edge of the color stripe on the surface was half way across the IR spot. Yet, small changes are seen as soon as the color stripe enters the edge of the IR spot. This is probably due to some scattering of the light by the window and lens in front of the photocells.

Table B3

Photocell Output Tracking and Calculated Divider Output Before Fine Adjustment

| | | Voltage | | | | |
|---|---|---|---|---|---|---|
| E1 | Diff. (1-4) | E4 | E2 | Diff. (2-3) | E3 | Calculated Divider Output.in. |
| .789 | 0 | .789 | .784 | -.007 | .791 | .022 |
| .701 | .033 | .668 | .796 | 0 | .796 | .111 |
| .600 | .051 | .549 | .798 | .009 | .791 | .161 |
| .501 | .061 | .440 | .797 | .010 | .787 | .202 |
| .400 | .068 | .332 | .794 | .013 | .781 | .238 |
| .300 | .070 | .230 | .787 | .016 | .771 | .259 |
| .200 | .052 | .148 | .762 | .037 | .725 | .082 |
| .149 | .021 | .128 | .700 | .064 | .636 | -.267 |
| .128 | .008 | .120 | .600 | .066 | .534 | -.420 |
| .120 | .005 | .115 | .500 | .059 | .441 | -.459 |
| .115 | .003 | .112 | .400 | .048 | .352 | -.460 |
| .111 | .002 | .109 | .300 | .033 | .267 | -.394 |
| .108 | 0 | .108 | .200 | .014 | .186 | -.233 |
| .105 | 0 | .105 | .127 | -.003 | .130 | .064 |
| | Max. Diff. | | | Max. Diff. | | Pk to Pk Error |
| | .070 | | | .066 | | .719 |

Table B4

Photocell Output-Tracking and Calculated Divider Output After Fine Adjustment

| | | Voltage | | | | |
|---|---|---|---|---|---|---|
| E1 | Diff. (1-4) | E4 | E2 | Diff. (2-3) | E3 | Calculated Divider Output.in. |
| .801 | .001 | .800 | .799 | -.001 | .800 | .006 |
| .700 | .013 | .687 | .812 | .009 | .803 | .013 |
| .600 | .010 | .590 | .812 | .013 | .799 | -.011 |
| .500 | .003 | .497 | .811 | .013 | .794 | -.054 |
| .400 | -.006 | .406 | .809 | .021 | .788 | -.112 |
| .300 | -.016 | .316 | .802 | .020 | .782 | -.164 |
| .200 | -.016 | .216 | .774 | .004 | .770 | -.102 |
| .148 | .002 | .146 | .700 | -.020 | .720 | .128 |
| .130 | .004 | .126 | .600 | -.010 | .610 | .095 |
| .121 | .002 | .119 | .500 | -.001 | .501 | .024 |
| .116 | .001 | .115 | .400 | .003 | .397 | -.019 |
| .112 | 0 | .112. | .300 | .004 | .296 | -.049 |
| .109 | 0 | .119 | .200 | 0 | .200 | -.159 |
| .105 | -.002 | .107 | .127 | -.006 | .133 | .085 |
| | Max. Diff. | | | Max. Diff. | | Pk to Pk Error |
| | -.016 | | | .021 | | .292 |